
Supplementary information

**A high-performance neuroprosthesis for
speech decoding and avatar control**

In the format provided by the
authors and unedited

1

A high-performance neuroprosthesis for speech decoding and avatar control

2

3

Supplementary Information

4 Contents

5	List of investigators	5
6	Supplementary notes	6
7	Note S1. The participant’s residual articulatory capacity	6
8	Note S2. The participant’s assistive-communication device	7
9	Supplementary methods	9
10	Method S1. Text corpora	9
11	Text test set and data organization	9
12	Creation of the test dataset for speech-synthesis and avatar evaluations	9
13	Method S2. Text decoding	10
14	RNN model architecture	10
15	Connectionist temporal classification (CTC) loss	11
16	Data augmentations	12
17	Optimization	12
18	CTC beam search	12
19	Model evaluation and early stopping	13
20	Hyperparameter optimization for the 1024-word-General sentence set	13
21	Real-time implementation details for the 1024-word-General sentence set	13
22	Differences for the 50-phrase-AAC sentence set and the 529-phrase-AAC	
23	sentence set	14
24	Simulated evaluation of performance on the 50-phrase-AAC sentence set and	
25	the 529-phrase-AAC sentence set	15
26	Freeform Evaluation	15
27	Method S3. Decoding NATO code words and hand-motor movements	17
28	Data preparation	17
29	RNN architecture	17
30	Data augmentations	17
31	Optimization	17
32	Model evaluation and early stopping	18
33	Model Ensembling	18
34	Method S4. Synthesis	19
35	Decoding of discrete speech units	19
36	HuBERT unit-to-speech vocoder	19
37	Model architecture	19
38	Training and optimization	19
39	CTC decoding	20
40	Hyperparameter search	20
41	Perceptual assessment	20
42	Method S5. Avatar	21
43	Virtual environment and avatar animation system	21
44	Continuous articulatory gesture decoding: VQ-VAE	21
45	CTC decoding	22

46	Evaluation	22
47	Expression Decoding	24
48	Articulatory-movement decoding	24
49	Avatar implementation during articulatory-movement and expression decoding	24
50	Supplementary figures	26
51	Figure S1. Examples of directly decoded avatar articulatory gestures	26
52	Figure S2. Correlations of directly decoded avatar articulatory gestures with	
53	reference articulatory gestures	27
54	Figure S3. Correlations between avatar articulatory gestures with reference	
55	articulatory gestures using the acoustic approach	28
56	Figure S4. Perceptual accuracy for the avatar using the acoustic approach	29
57	Figure S5. Correlations of facial landmarks using the acoustic approach for avatar	
58	decoding the 1024-word-General sentence set	30
59	Figure S6. Classification of emotional expressions	31
60	Figure S7. Cross-phone place-of-articulation encoding	32
61	Figure S8. Spatial distribution of electrode tuning to articulatory features	33
62	Figure S9. Attempted finger flexion and speech are largely encoded orthogonally .	34
63	Figure S10. Effects of limiting electrode density on decoding	35
64	Figure S11. Phone confusion matrices during text decoding	38
65	Figure S12. Decoding contributions of articulatory encoding electrodes	39
66	Figure S13. Mean contribution of electrode groups, controlled for number of electrodes	40
67	Figure S14. Region-exclusion analysis for NATO code words	41
68	Figure S15. Timing comparison between precentral and postcentral gyri	42
69	Figure S16. Relationship between temporal lobe decoding contributions and auditory	
70	responses	43
71	Figure S17. Visual-speech recognition for participant vs. able speakers	44
72	Figure S18. Virtual environment for avatar decoding	45
73	Figure S19. Example of dlib facial-landmark detection	46
74	Figure S20. Distribution of phone-encoding r-values across electrodes	47
75	Supplementary tables	48
76	Table S1. Participant’s personalized voice MCD comparisons	48
77	Table S2. Illustrative speech-synthesis examples	49
78	Table S3. Comparisons for dlib traces with the direct approach	50
79	Table S4. Comparisons for articulatory gesture decoding using the direct-decoding	
80	approach	51
81	Table S5. Comparisons for acoustic approach to avatar animation	52
82	Table S6. Comparisons for dlib traces with the acoustic approach	53
83	Table S7. Exclusion comparisons between anatomical regions	54
84	Table S8. Exclusion comparisons between electrode densities	56
85	Table S9. User experience survey	57
86	Table S10. Text RNN neural-decoding model hyperparameter values	58
87	Table S11. NATO code word and hand-motor movement decoder hyperparameters	59
88	Table S12. Speech synthesis RNN neural-decoding model hyperparameters	60

89	Table S13. Articulatory gesture descriptions	61
90	Table S14. Avatar CTC decoding hyperparameters	62
91	Supplementary references	63

92 **List of investigators**

93 **List of investigators (authors)**

- 94 1. Sean L. Metzger*
- 95 2. Kaylo T. Littlejohn*
- 96 3. Alexander Silva*
- 97 4. David A. Moses*
- 98 5. Margaret P. Seaton*
- 99 6. Ran Wang
- 100 7. Maximilian E. Dougherty
- 101 8. Jessie R. Liu
- 102 9. Peter Wu
- 103 10. Michael A. Berger
- 104 11. Inga Zhuravleva
- 105 12. Adelyn Tu-Chan
- 106 13. Karunesh Ganguly
- 107 14. Gopala K. Anumanchipalli
- 108 15. Edward F. Chang

109 *These five authors contributed equally

110 **Supplementary notes**

111 **Note S1. The participant's residual articulatory capacity**

112 During clinical-trial enrollment, the participant underwent testing with a speech-language
113 pathologist (SLP). This is briefly described in the Methods (Participant) section. The SLP
114 determined that our participant's inability to speak is due both to her articulatory weakness
115 and inability to sustain sufficient airflow. Her inability to sustain sufficient airflow is due to
116 respiratory weakness as well as inability to restrict and manipulate airflow through her vocal
117 folds, lips and tongue. The SLP also determined that she is unable to produce adequate
118 pressure to produce plosives, fricatives, and affricates. In a voicing assessment, she shows
119 limited laryngeal control, with effortful, monotonic, and elevated vocalizations. Together,
120 these deficits result in uncoordinated, unintelligible speech.

122 **Note S2. The participant’s assistive-communication device**

123 **Description of the assistive-communication device**

124 The participant’s primary mode of communication is a commercially available assistive-
125 communication interface (Tobii Dynavox). This setup consists of a computer, monitor, and
126 camera on a rolling stand as well as special glasses that the participant wears during use.
127 The glasses have a reflective circle in the center which enables the camera to track her head
128 movements. These movements are used to control a cursor in a two-dimensional visual space
129 containing letters (laid out like a keyboard), punctuation, a Return key, and other items. To
130 select (click on) an item, the participant “dwells” on an item (that is, maintains the cursor
131 position over the item) for a brief period of time (approximately 1 second). Through this
132 cursor-control interface, the participant is able to spell out intended messages.

133 In a more advanced mode with the same interface, the device suggests autocomplete
134 options (as additional selectable items) using predictive-text technology. This feature can
135 speed up communication rates by using natural-language modeling to suggest probable
136 proceeding text items on a word and character level. For example, if the participant had
137 typed “Hel”, a “Hello” item might appear on the screen as a selection option. As another
138 example, if the participant had typed “Good”, a “ morning” item might appear as an option.
139 In this mode, the participant can also select an item that will synthesize the typed text string
140 into an audible speech waveform using a voice of her choosing. The participant primarily
141 uses this mode in her daily life.

142 **Typing-rate assessment: Task design**

143 To compare to the decoding rates achieved with our neural-decoding system, we measured
144 the participant’s typical typing rate using her assistive-communication device. In each trial
145 of this task, one of the researchers stated a sentence aloud, and the participant typed out
146 that sentence using her typing interface. We computed the elapsed time between her first
147 and final selections, excluding any time spent capitalizing the first letter (if she elected to do
148 so) and selecting any final punctuation character (if she included one). Using this elapsed
149 time along with the number of words and characters (excluding final punctuation characters)
150 in the stated target sentence, we measured her typing rate in each trial in units of words per
151 minute and characters per minute.

152 The participant performed this task twice: once in which she had to manually enter
153 each letter without access to autocomplete options and once in which she had access to the
154 autocomplete options.

155 We randomly selected 8 sentences from the 1024-word-General sentence set to use in
156 this task:

- 157 1. It is for me too.
- 158 2. How am I supposed to get away?
- 159 3. Now, where would I be?

- 160 4. It looks wonderful and so do you.
161 5. This could be a trap.
162 6. How do you mean that?
163 7. What if I said goodbye?
164 8. I need to sit down.

165 The comma in following “Now” in the third sentence is included when counting the number
166 of characters in the target sentence; all other punctuation is excluded.

167 **Typing-rate assessment: Results**

168 The participant’s typed sentence matched the stated sentence in each trial. If she made an
169 error, she used backspace to correct the error before proceeding. When typing without access
170 to autocomplete options, she exhibited a typing rate of 8.61 ± 1.08 words per minute and
171 34.1 ± 1.87 characters per minute (given as mean \pm standard deviation across the 8 sentence
172 trials). When typing with access to autocomplete options, she exhibited a typing rate of
173 14.2 ± 3.94 words per minute and 56.4 ± 15.0 characters per minute.

174 **Supplementary methods**

175 **Method S1. Text corpora**

176 **Text test set and data organization**

177 To create the test sentences for the text decoder, we randomly selected 249 sentences from
178 the entire corpus. By design, these sentences were not used at any point in training any
179 neural decoders, so at test time, models had to generalize to these unseen sentences.

180 To promote coverage of all words in the 1024-word vocabulary, including infrequent
181 words, we arranged the corpus to have any sentence containing any word with fewer than 6
182 repetitions in the training data to fall within the first half of the training data, such that all
183 infrequent words had already appeared early within data collection. This helped us monitor
184 offline model performance on all words in the vocabulary early on during data collection.

185 After collecting the real-time testing data, we identified that due to an error, for one of
186 the 250 sentences originally in the test set for text decoding, the participant had attempted
187 to say the same sentence for one trial in the training set. To keep our results with the
188 1024-word-General set a measure of performance on previously unseen sentences, we decided
189 to exclude this trial and report performance on the remaining 249 sentences that were not
190 used during model training. Thus, that sentence was excluded from evaluations [values were
191 set to nan and ignored] during its corresponding pseudo-block, leading to one pseudo-block
192 with 9 sentences rather than 10.

193 **Creation of the test dataset for speech-synthesis and avatar evaluations**

194 For synthesis and avatar models, we randomly sampled 200 sentences that had not been used
195 during training of any model and that were not in the test sentences for the text decoder.

196 **Method S2. Text decoding**

197 Here, we describe the model training and procedures in detail, for the RNN neural-decoding
198 model used with the `1024-word-General` sentence set The models used with the `50-phrase-`
199 `AAC` and `529-phrase-AAC` sentence sets are further detailed later but contain only minor
200 modifications.

201 **Data preparation**

202 For decoding, we used a window of neural activity, consisting of the high-gamma and
203 low-frequency signals from all electrodes. The details for extraction of high-gamma and
204 low-frequency signals were detailed extensively in previous work [1]. Then, we normalized
205 the ℓ_2 -norm of each channel for the high-gamma and low-frequency signals to be 1 across
206 all time-steps for each channel. The window of neural features was larger than the windows
207 seen by the RNN model. We used temporal-jittering to pull smaller windows from larger
208 trial-relevant windows. For the `1024-word-General` sentence set, we used a window of neural
209 activity from -1 to 8 seconds relative to the go-cue for training, with data augmentation
210 that randomly selected an 8 second window of neural activity that started between .75 and
211 .25 seconds prior to the go cue to make the RNN model more robust to variability in the
212 timing of the participant’s productions relative to the go-cue as in previous work [1, 2]. Of
213 the 9,512 trials collected prior to real-time testing with the `1024-word-General` sentence
214 set, we used 95% for model training,

215 We used the `g2p-en` python package [3] to extract the phonetic pronunciation for each
216 word in the target sentence. Spaces were replaced with a silence token. To account for silence
217 at the start and end of each sentence, we prepended and appended the silence token at the
218 start and end of the sentence. We reserved the code 0 for the blank token traditionally used
219 with the CTC loss [4] then one-hot encoded all the phonemes and the silence token.

220 During training of the RNN models used in real-time for the `1024-word-General` sentence
221 set, we randomly selected 95% of the data to use as training set, and 5% as the development
222 set, to use as a held-out set to estimate model performance on unseen data. We used
223 this development set for hyperparameter optimization as well. The data used for real-time
224 demonstrations were recorded after hyperparameter optimization for all models. For the
225 development set used during training for early stopping and evaluation, the model used a
226 fixed window of neural activity from 0.5 seconds prior to the go-cue to 7.5 seconds after.

227 **Modeling**

228 **RNN model architecture**

229 The RNN consisted of a 1-dimensional convolutional layer, followed by three layers of
230 bidirectional gated-recurrent units (GRUs), which were followed by a linear readout layer.
231 The convolutional layer processes and downsamples the input signals, and finds combinations
232 of signals that form meaningful representations. The GRUs then further process these
233 representations, incorporating temporal structure across the neural time series. We used
234 GRUs since they have been shown to outperform other recurrent architectures on sequence
235 tasks [5]. To improve accuracy, bidirectional gated-recurrent units were used. We used

236 dropout layers during training after the convolutional layer, as well as between the GRU
 237 layers. We used a dropout rate which was found via manual hyperparameter search (see
 238 Table S10). The hidden state of the final gated recurrent unit was then passed through a
 239 linear layer followed by a softmax activation to approximate the probability over the 39
 240 phonemes we used, plus the silence phone and the blank token used for CTC decoding [4].

241 The full set of hyperparameters used for decoding can be found in Table S10.

242 Connectionist temporal classification (CTC) loss

243 Given a trial of neural data x_i and the corresponding ground truth sequence of phones y_i , we
 244 want to maximize the probability of the ground truth sequence of phones y_i , given the neural
 245 activity x_i , $p(y_i|x_i)$.

246 Because alignment between x_i and y_i is unknown, the connectionist temporal classification
 247 (CTC) objective aims to maximize the probability of y_i over all valid alignments that
 248 produce y_i . For example, "was", with pronunciation $[w, aa, z]$ can be produced from
 249 the following valid alignments with four timesteps by collapsing over repeated phones:
 250 $[w, w, aa, z]$, $[w, aa, aa, z]$, $[w, aa, z, z]$. To decode silence and word boundaries, we also include
 251 the silence phone \emptyset as a target during training. To allow for the decoding of silence within
 252 words that does not necessarily result in a word boundary, we also introduced the flexible blank
 253 token ϵ as a target, which is commonly used in CTC decoding [4]. The blank token can be
 254 ignored in the decoded output, hence e.g. $[\epsilon, w, aa, zz]$, $[w, \epsilon, aa, zz]$, $[w, aa, \epsilon, zz]$, $[w, aa, zz, \epsilon]$,
 255 are also valid alignments with four timesteps for $[w, aa, z]$.

256 The blank token can also be used to decode repeated tokens - e.g. if one was decoding
 257 sequences of letters instead of sequences of phones, collapsing over repeated letters would
 258 make it impossible to decode repeated letters, like the ls in 'hello'. Hence, decoding the blank
 259 token between the two instances of the letter l, then replacing it with the empty string, would
 260 enable the word to be decoded.

261 Let us denote the phone at each timestep t in each alignment a as a_t . Hence a_1 for the
 262 valid alignments for "was" in this case is w in all cases except if the alignment is $[\epsilon, w, aa, zz]$.
 263 Thus, the CTC objective for the i -th trial of neural data x_i and the corresponding label y_i ,
 264 where y_i is the ground truth sequence of phones can be expressed as follows:

$$p(y_i|x_i) = \sum_{\mathcal{A} \in \mathcal{A}_{x_i, y_i}} \prod_{t=1}^T p_t(a_t|X)$$

265 .

266 Here \mathcal{A}_{x_i, y_i} represents the set of all valid alignments with length equivalent to the length
 267 of x_i that could produce y_i . During the loss calculation, the RNN is used to estimate the
 268 per time-step probability $p_t(a_t|X)$. In practice, we optimize our RNN model's parameters to
 269 minimize the negative log likelihood over all the samples - $\sum_i \log p(y_i|x_i)$, which is equivalent
 270 to maximizing the probability of the training labels y_i given the neural data x_i , $\prod_i p(y_i|x_i)$.
 271 We used PyTorch's `CTCLoss` function to efficiently calculate this loss.

272 Data augmentations

273 For the 1024-word-General sentence set set, in order to improve the RNN model performance
274 on unseen data and make the RNN model robust to variability in the neural signals, as in
275 previous work [1], we used the following set of data augmentations:

- 276 • Temporal jittering: shift the neural features by a time shift τ , so that the for a sample
277 x_i , $x_i(t) = x_i(t - \tau)$, where $\tau \sim \mathcal{U}(-j, j)$, where j is a hyperparameter, and \mathcal{U} is the
278 uniform distribution.
- 279 • Temporal masking, where we randomly set some neural timepoints of the neural features
280 to 0, yielding $x_i[t_0 : t_1] = (1 - \delta_p)$, $t_1 = t_0 + s$, $s \sim \mathcal{U}(0, b)$. Here t_0 is a randomly drawn
281 time point within x_i and p is the probability of δ_p being one, and subsequently the time
282 points being set to 0. Both b and p are hyperparameters.
- 283 • Additive noise: adding a matrix of random gaussian noise to the neural features, st
284 $x_i = x_i + \mathcal{N}(0, \sigma_n^2)$. Here σ_n^2 is a hyperparameter.
- 285 • Channel-wise noise: Offset each channel by a single value randomly sampled from
286 a gaussian for each channel, therefore: $x_i[:, c] = x_i + \mathcal{N}(0, \sigma_{ch}^2)$, here σ_{ch} is a
287 hyperparameter shared across all features.
- 288 • Scaling augmentation: Scale the magnitude of the neural features, such that $x_i = \alpha x_i$,
289 with $\alpha \sim \mathcal{U}[\alpha_{min}, \alpha_{max}]$. Here α_{min} and α_{max} are both hyperparameters

290 For all hyperparameters, we used hyperparameters that were previously found to be
291 effective [1], save the hyperparameter for j , which we found via manual tuning.

292 Optimization

293 To train our RNN model for the 1024-word-General sentence set, we used the AdamW
294 optimizer [6] to perform stochastic batch gradient descent. Briefly, AdamW implements
295 decoupled weight decay for model parameter regularization with the Adam adaptive gradient
296 algorithm. We used a weight decay value $\lambda = 1e - 5$ with a learning rate of $1e - 3$. We used
297 the default parameters for $\beta_1 = 0.9$, $\beta_2 = 0.999$, $\varepsilon = 1e - 8$. We used a batch size of 64. We
298 clipped the gradient for each batch to have a total ℓ_2 -norm of $\lambda_{grad} = 1e - 4$.

299 CTC beam search

During inference, we evaluated our RNN model on the word error rate (WER) metric,
commonly used to evaluate automatic speech recognition systems and speech and text brain-
computer interfaces. This required transforming the RNN outputs, given by $p_t(a_t|x_i)$, (where
 a_t represents the probability of a at time t , where a can be any phone, the silence phone \emptyset , or
the blank token ϵ used in CTC decoding), into text. To do this, we sought the transcription
 W_i for trial i which maximizes the probability:

$$p_{RNN}(W_i|x_i)p_{lm}(W_i)$$

300 .

301 Here $p_{RNN}(W_i|x_i)$ denotes the probability of possible alignments of phones that result in
302 transcription W_i under the RNN, given the neural data for trial i , x_i . $p_{lm}(W_i)$ denotes the
303 probability under a language model prior of the transcription W_i .

304 To account for the fact that language models rate sentences as being less likely as words
305 are added, we include a word insertion penalty or bonus, giving

$$p_{RNN}(W_i|x_i)p_{lm}(W_i)^\alpha|W_i|^\beta \tag{S1}$$

306 Here, $|W|$ denotes the number of words in W_i , and α and β are hyperparameters for
307 weighting the language model and number of words.

308 We find the W_i that optimizes equation S1 via a CTC beam-search algorithm, using
309 `torchaudio`'s CTC decode function [7]. The beam-search works by keeping a set of at most
310 B candidate sentences at each timepoint, where B is a hyperparameter. It then adds each
311 phone (or the silence or blank token) to the candidate sentence, and re-evaluates the resulting
312 candidate sentence after the addition using equation S1. Then, only the B most probable
313 sentences are kept. The algorithm repeats until all timesteps have been processed.

314 For the `1024-word-General` sentence set, during RNN model training, models were
315 evaluated using $\alpha = 4$, $\beta = -.26$ and $B = 100$. We used an n -gram language model [8]
316 trained with $n = 5$ using `kenlm` that was trained on all 18,284 sentences generated for the
317 conversational set prior to pruning sentences.

318 For final evaluations with the `1024-word-General` sentence set we performed a small
319 hyperparameter search to evaluate optimal hyperparameters for the language model prior to
320 decoding, and used $\alpha = 4.5$, $\beta = -.26$, and a beam-width of $B = 3e3$.

321 **Model evaluation and early stopping**

322 For all RNN models, starting with the first epoch, we kept track of the RNN model's WER
323 on a set of held out data every 3 epochs. While we evaluated loss at each epoch, to save time,
324 WER was only evaluated every 3rd epoch. If the WER improved, then we saved the current
325 RNN model's weights. If the WER did not improve for 20 evaluations (corresponding to 20
326 evaluations over 60 epochs), then training was ended.

327 **Hyperparameter optimization for the 1024-word-General sentence set**

328 Due to limited time, hyperparameters were largely hand tuned as data collection occurred.

329 We first selected hyperparameters for the RNN neural-decoding model using by evaluating
330 its performance with fixed CTC beam search hyperparameters. Then, once the best model
331 with the fixed hyperparameters had been selected, we selected hyperparameters for the CTC
332 beam search using just that model and its predictions on the development set.

333 We chose the number of samples used for early stopping to be 8 based on offline evaluation
334 of two blocks collected prior to any real-time test blocks.

335 **Real-time implementation details for the 1024-word-General sentence set**

336 To improve decoding rates, we reasoned that the decoding model should predict a sentence as
337 soon as the participant stopped attempting to say it, rather than waiting for a fixed window

338 which could be composed of much silence for shorter utterances. Hence, starting 1.9 seconds
339 after the go-cue and every 800ms thereafter, we ran the RNN on all the neural data available.
340 We then evaluated if the probability of the silence or blank token in the final 8 model outputs
341 (corresponding to 960ms of neural data) was on average greater than 0.8875. If this threshold
342 was exceeded, then trial ended, the beam-search was run over the model’s predictions at
343 each timestep, and the most likely resulting sentence was kept as the final prediction. In the
344 case that the model was fed over 8 seconds of neural data, then the trial was automatically
345 ended. However, this only occurred for 2 of the 249 real-time test trials, demonstrating the
346 effectiveness of our early stopping strategy.

347 During real-time testing, due to an error we used a lexicon that was missing two words
348 (the final two lines of the lexicon containing pronunciations for the words “pen” and “self”
349 were not present). However, we confirmed that for all trials, the prediction obtained online
350 with this 1,022 word lexicon perfectly matched the prediction of an offline simulation where
351 we used the full 1,024 word lexicon.

352 **Differences for the 50-phrase-AAC sentence set and the 529-phrase-AAC sentence** 353 **set**

354 Here we denote any differences (or lack thereof) in model training used for **50-phrase-AAC** and
355 the **529-phrase-AAC** sentence sets. Most differences are because the models were developed
356 prior to the **1024-word-General** RNN model. We denote any differences below.

357 • **Data preparation:** A unique model was trained for each dataset. Because of the rate
358 of attempted speech during collection of the **1024-word-General** sentence set vs. the
359 AAC sets differed, we found that using data across these datasets was not helpful for
360 improving performance. However, within the AAC sets, some usage of the **50-phrase-**
361 **AAC** sentence set data was helpful for the **529-phrase-AAC** sentence set (further details
362 below). Because the **50-phrase-AAC** sentence set has a small number of sentences, we
363 did not use additional data from the **529-phrase-AAC** sentence set, as learning that
364 sentences fall within the **50-phrase-AAC** sentence set is beneficial in this context.

365 – For the **1024-word-General** sentence set: We only used data from the **1024-word-**
366 **General** sentence set during training and initialized model weights randomly.

367 – For the **50-phrase-AAC** sentence set: We only used data from the **50-phrase-AAC**
368 sentence set and initialized model weights randomly.

369 – For the **529-phrase-AAC** sentence set: We initialized the model using the **50-**
370 **phrase-AAC** sentence set model weights. We also used the most recent 500 samples
371 from the **50-phrase-AAC** sentence set to supplement the **529-phrase-AAC** samples
372 used during training.

373 • **CTC loss:** The same loss was used.

374 • **Model architecture:** The same underlying architecture was used, just with different
375 hyperparameters, which were also found via hand-tuning on evaluation data prior to
376 when the evaluation blocks were collected. The full set of hyperparameters are detailed
377 in Supplementary Table S10.

- Data augmentation: No data augmentations were used during training of the RNN models used with `50-phrase-AAC` and `529-phrase-AAC` sentence sets.
- Optimization: For the AAC sentence sets, we used the Adam Optimizer [9] with a learning rate of $1e-3$, and $\beta_1 = 0.9, \beta_2 = 0.999$. We clipped model gradients to have a norm of 1 across the batch, and used a batch size of 32.
- CTC Beam search and hyperparameters: For the `50-phrase-AAC` sentence set, we used $\alpha = 3.23, \beta = -.26$ and $B = 100$ as beam search hyperparameters during training and offline evaluation. For the `529-phrase-AAC` sentence set, we used $\alpha = 4, \beta = -.26$ and $B = 3000$. For each set, we used a custom n -gram language model with $n = 5$ that was trained on all sentences within each restricted set using `kenlm`. Beam-search hyperparameters were hand-tuned on held-out data from days prior to evaluation.
- Other: Due to limitations in the amount of data, we found it beneficial to initialize our `529-phrase-AAC` model with the model trained on the full set of the `50-phrase-AAC` sentence set, and we also used an additional 500 samples from the `50-phrase-AAC` sentence set during training. Hence, we optimized model parameters for the `529-phrase-AAC` sentence set after a model had been trained on the `50-phrase-AAC` sentence set.

Simulated evaluation of performance on the `50-phrase-AAC` sentence set and the `529-phrase-AAC` sentence set

We used the same blocks used for evaluation of the synthesis models to evaluate text decoding performance on the `50-phrase-AAC` sentence set and the `529-phrase-AAC` sentence set.

For the `529-phrase-AAC` sentence set and the `50-phrase-AAC` sentence set only we found the model tended to hold its last prediction and consistently output it within the last 3 samples, which is prone to happen given the CTC-loss trains the bidirectional network to output any valid sequence of phones regardless of its timing. We found this did not occur with the `1024-word-General` sentence set set however, likely since there were more distinct periods of silence in the middle of the sentence productions that encouraged the model to predict silence with more temporal precision. Hence, we checked if a model had predicted silence or the blank token with a probability $> 88.75\%$ in the 8 samples prior to the last 3 samples. We decided to use the delay of 3 samples using a held out block recorded after all train and evaluation blocks were recorded.

In our offline scenario, we first checked if the model had completed its prediction 2.2 seconds after the go-cue, and then every 350 ms after that, or until 5.5 seconds had elapsed since the go cue. Once this occurred, we ran the beam-search and kept the most likely prediction as the final sentence.

Freeform Evaluation

For day-to-day usage, a speech BCI should be capable of being engaged volitionally by the user and generating outputs in a freeform (unprompted) fashion based on the user’s intention.

To this end, we used a speech-detection model, similar to versions we have used in our previous work [1, 2], which detected when the participant was attempting to speak directly from neural features alone in real time.

418 Specifically, the speech detection model was trained to predict 3 states (silence, speech
419 preparation, and attempted speech) using both low frequency and high gamma neural features
420 (for a total of 506 features) at 200 Hz from the 1024-word-General sentence set. Similar
421 to previous work, the speech detection model was an RNN composed of 3 long short-term
422 memory layers (with 128, 96, and 16 nodes), followed by a single fully connected layer to
423 project latent states to the 3 classes. The model was trained with 50% dropout, early stopping,
424 and the Adam optimizer with a learning rate of 0.001, and as in previous work, we used
425 truncated backpropagation through time and evaluated the loss at each training step and
426 epoch using cross-entropy [1, 2].

427 For the training data, we labeled time points as one of the 3 states according to predefined
428 windows. The time between the presentation of the phrase and the go-cue was labeled as
429 speech preparation. Because the phrases presented in each trial were of varying lengths, we
430 defined a variable sized window aligned to the go-cue to be labeled as attempted speech. This
431 window was defined as 85% of the duration from the go-cue to the end of the trial. That is,
432 if the phrase was on the screen for 1 second after the go-cue, then time points between the
433 go-cue and 0.85 seconds after the go-cue would be labeled as attempted speech. Time points
434 from the end of the variably defined window to the end of the trial (in the last example,
435 this would be the 0.15 remaining seconds) were discarded from training as it was ambiguous
436 whether these would be silence or whether the participant would still be attempting speech.
437 All other time points were labeled as silence.

438 As in previous work, we took only the predicted probability of attempted speech and
439 processed this to generate discretely predicted events [2]. In brief, this process involves
440 smoothing the probabilities, setting a probability threshold, and debouncing with a time
441 threshold. For real-time testing, we used a smoothing factor of 50 time points (i.e. 0.25
442 seconds), a probability threshold of 0.5, and a time threshold of 100 time points (i.e. 0.5
443 seconds).

444 We then used the model alongside our text decoder as the participant engaged in a
445 freeform task in which she attempted to say whatever she wanted. Instead of aligning the
446 neural data sent to the text decoder in real time based on the go cue, we instead used the
447 detected speech-onset time. Because the participant was allowed to attempt to say whatever
448 she wanted (in an unprompted fashion), it was not practical to determine (for example, post
449 hoc with her assistive-communication device) exactly what sentences she was attempting to
450 say as this would take a prohibitively long time, which is why our evaluation in this setting
451 is limited. Instead, we instructed her to make eye contact with a researcher if the sentence
452 was perfectly decoded and to continue looking forward otherwise. We collected one block of
453 this freeform task, and in this block the participant indicated that 10 out of 20 attempted
454 sentences were perfectly decoded. This matches performance observed during our real-time
455 testing with the 1024-word-General set, in which the text decoder perfectly decoded 111
456 out of 249 prompted sentences (keep in mind that being off by one word, or even one letter,
457 results in the entire sentence being deemed incorrect; this is a harsher metric than word error
458 rate). We compared if the rate of correct trials using the freeform setup was different than
459 the rate of correct trials using the go-cue and we found no significant difference (p=.641,
460 two-sided t-test, $t=-0.467$, $n_1 = 249$, $n_2 = 20$) We have added a video of a segment of this
461 task as Supplementary Video 3.

462 **Method S3. Decoding NATO code words and hand-motor** 463 **movements**

464 **Data preparation**

465 We used the high-gamma and low-frequency signals as described in previous work [1], streamed
466 from the real-time system at 200Hz. Then, we downsampled the neural activity by a factor
467 of 6. Then, we normalized the neural activity to have an ℓ_2 norm of 1 across all channels at
468 each timestep for each set of features.

469 We used a window of neural activity from [-2, 4] seconds relative to the go-cue during
470 training, and used temporal jittering and the data augmentations used in text decoding and
471 in our previous work [1] to make the model more robust to variation in the participant’s
472 timing.

473 We split the training data into a train set and development set by using the last 40 trials
474 of neural activity as the development set, and using the remaining data as the training set.
475 The decoding model was evaluated only on real-time data which had not yet been collected
476 when models were trained.

477 During evaluation with the development set and during real-time blocks, we used a window
478 of neural activity from [-1, 3] seconds relative to the go-cue for prediction.

479 **RNN architecture**

480 We use the same architecture described in previous work [1], which consists of a 1-D
481 convolutional layer, followed by multiple layers of bidirectional GRUs. Then, we take the last
482 hidden state of the final GRU layer, and pass it through a linear layer followed by the softmax
483 activation function, which produces the probability across the 30 targets (the 26 NATO code
484 words + 4 hand-motor targets). During training, we applied dropout [10] between each layer
485 except for between the final GRU layer and the linear layer. The full model hyperparameters,
486 including the hidden units for each layer and dropout rate are in Supplementary Table S11.
487 The hyperparameters used were the best hyperparameters from [1].

488 **Data augmentations**

489 . We use the same data augmentations and data augmentation parameters as used in previous
490 work [1]. The augmentations are described in Supplementary Method S2.

491 **Optimization**

492 To begin model training, we first loaded model weights from our previous work [1] that were
493 trained on a participant with a lower density grid, doing a task where we were decoding the
494 26 NATO code words and a single hand-motor command. Hence, we replaced the first layer
495 to accommodate for the different number of channels with our new participant’s grid, and
496 replaced the final layer to account for the increased number of classes. Then, we trained the
497 model to minimize cross-entropy loss between the models predictions and the training labels.
498 We used the Adam Optimizer to update model parameters, with a learning rate of $5e - 4$,
499 batch size of 16, and the default Adam parameters $\beta_1 = 0.9$, $\beta_2 = 0.999$, $\epsilon = 1e - 8$ [9].

500 **Model evaluation and early stopping**

501 During training, we kept track of the model with the best accuracy on the held out development
502 set and saved the model with the best accuracy. If accuracy did not improve for 35 epochs,
503 then model training ended, and that model was used as the final model.

504 **Model Ensembling**

505 Starting 40 days after implantation, we began using model ensembling as in previous work
506 [1] to improve model predictions. Prior to this date, we only used one models predictions
507 during real-time decoding. This meant we ran our training procedure 10 times to optimize
508 models with 10 different random initializations. This yielded an ensemble of 10 models we
509 used during real-time prediction, where we averaged the probability of the 10 models to get
510 the final probability across the 30 classes.

511 **Method S4. Synthesis**

512 **Modeling**

513 **Decoding of discrete speech units**

514 As described in the main text, we generated a sequence of discrete speech units for each
515 utterance by passing a basis waveform through a pre-trained HuBERT model [11]. We then
516 use high-gamma and low frequency features from neural data to decode a sequence of discrete
517 speech units sampled at 50 Hz.

518 **HuBERT unit-to-speech vocoder**

519 We apply a two-step process to synthesize speech from decoded sequences of discrete speech
520 units. We adapted the discrete-unit synthesizer introduced in Generative Spoken Language
521 Model (GSLM) [12]. The synthesizer first applies a Tacotron2 model that generates a
522 mel-spectrogram from a sequence of discrete speech units. This is then followed by a
523 WaveGlow vocoder that outputs a speech waveform from the mel-spectrogram. We obtained
524 the pre-trained HuBERT, Tacotron2, and WaveGlow models from fairseq [13]. These can
525 be obtained using the following link: [https://dl.fbaipublicfiles.com/textless_nlp/
526 gslm/hubert/tts_km100/tts_checkpoint_best.pt](https://dl.fbaipublicfiles.com/textless_nlp/gslm/hubert/tts_km100/tts_checkpoint_best.pt)

527 **Model architecture**

528 We trained a neural network to predict sequences of discrete speech units from neural activity.
529 This neural network consists of a 1-D convolutional layer followed by a 3-layer bidirectional
530 gated-recurrent units (GRUs). The hidden state of the final GRU is then passed into a 1D
531 transpose convolutional layer, which upsamples the hidden representation back to a 50 Hz
532 sampling rate. The output feature dimension of the transpose convolutional layer is 101,
533 which corresponds to the logits of the 100 HuBERT units and an additional blank token
534 needed for CTC decoding. Hyperparameters of the network are listed in Table S12.

535 **Training and optimization**

536 As for text decoding, we trained the synthesizing network with a fixed duration window of
537 neural activity. For decoding with the **529-phrase-AAC** and **50-phrase-AAC** sets, we used a
538 window of -0.5 to 4.62 seconds relative to the go cue. For the **1024-word-General** sentence
539 set we used a longer window of 0 to 7.5 seconds relative to the go cue. During training, we
540 used the CTC loss to train the neural network. We applied SpecAugment during training as
541 a data augmentation for the ECoG data.

542 We trained the decoder with the Adam optimizer [9]. We used an initial learning rate of
543 $1e - 4$ and used a multistep learning rate scheduler with a γ of 0.5 and milestones at 40000,
544 80000, 120000, and 1600000 iterations. We used $\beta_1 = 0.5, \beta_2 = 0.9$ as hyperparameters. We
545 used a batch size of 64 for **529-phrase-AAC** and **1024-word-General** sets and batch size of
546 16 for **50-phrase-AAC** set.

547 **CTC decoding**

548 After obtaining the output logits from the neural decoding model, we applied the greedy
549 CTC-decoding algorithm to determine the final decoded discrete speech units. We first
550 computed the speech unit with the highest probability at each timepoint. Consecutively
551 repeating tokens were collapsed into one token and then blank tokens were removed, producing
552 the final decoded sequence of speech units.

553 **Hyperparameter search**

554 We manually searched for hyperparameters, including the number of hidden units in the
555 model, dropout rate, number of layers, kernel size, feature dimension, and stride size. We
556 chose hyperparameters based on the decoded unit error rate for the held-out development set.

557 **Perceptual assessment**

558 We designed perceptual assessments using a crowd-sourcing platform (Amazon Mechanical
559 Turk), where each trial from each synthesis test set was assessed by 12 workers (except for
560 3 of the 500 trials, in which only 11 workers completed their evaluations). Each evaluation
561 consisted of playback of the decoded waveform and workers were then asked to transcribe
562 what they heard. The precise instructions were as follows:

563 Please listen to the audio and write down what you hear. Many of the clips may
564 be difficult to hear. If this is the case, write whatever words you are able to make
565 out, even if it does not form a complete expression. If you are not sure about a
566 word, please only include your guess in your transcription if you feel that you are
567 over 50% confident that your guess is correct. Otherwise, exclude the guess from
568 your transcription. If you cannot make out any words, leave the entry blank. You
569 may listen as many times as needed.

570 We took the median worker response accuracy as the accuracy for that trial.

571 Method S5. Avatar

572 Virtual environment and avatar animation system

573 To animate the avatar during real-time decoding, we used Speech Graphics’ ”SG Com” audio-
574 driven animation system. This system takes a waveform, applies a speech-to-gesture model
575 [14], and then animates these articulatory gestures. During audio-visual synthesis collection,
576 we took the decoded speech waveform and passed it through this system to generate the
577 avatar animation in sync with the audio waveform. We delayed the audio waveform by 200
578 ms to improve audio-visual synchronization.

579 For direct avatar decoding, SG Com provided a custom SG Com build that instead
580 takes articulatory gestures as input, allowing us to bypass the dependency on a speech-to-
581 gesture model and speech waveform and instead feed in directly decoded articulatory gestures.
582 However, speech-to-gesture component of SG Com was used to generate reference articulatory
583 gestures for targets during direct avatar decoding.

584 We designed a virtual environment using Unreal Engine 4.26 to hold the MetaHuman
585 characters (developed by Epic Games (Cary, North Carolina) for the Unreal Engine). We
586 showed our participant the full range of over 40 MetaHuman characters and let her choose
587 which one she preferred. She selected the character ”Vivian” which was used for subsequent
588 real-time experiments and offline rendering. The virtual scene consists of a simple camera,
589 a series of spotlights, the ”Vivian” MetaHuman’s character, and a black background wall,
590 see Supplementary Figure S18. Our virtual environment ran on a Microsoft Surface Book 3
591 which we connected to the participant’s monitor to display the avatar.

592 We built a custom C++ extension to stream decoded features to the avatar. This extension
593 waits to receive data (articulatory gestures or audio) from an ethernet cable connected to the
594 real-time decoding PC. We streamed articulatory gestures (used for gesture demos) or audio
595 in 10ms chunks from the real-time PC using the Transmission Control Protocol.

596 Continuous articulatory gesture decoding: VQ-VAE

597 In order to train a model to predict articulatory gestures using the CTC loss, we first
598 discretized the articulatory gestures. We did this using a VQ-VAE [15].

599 We trained the VQ-VAE to minimize the objective in [15], with $\beta = 2$, and with additional
600 weighting of $\lambda_{jaw} = 20$ on the reconstruction loss (mean-squared-error) of the jaw opening
601 gesture, and $\lambda_{visuallysalient} = 5$ on the tongue body raise, tongue advance, tongue retraction,
602 tongue tip raise, lip rounding, and lip retraction gestures, to emphasize the most visually
603 salient avatar features and jaw over other features, which effectively had a weight of 1.
604 These weights were selected by grid searching over the weights [5, 10, 20] for both λ_{jaw} and
605 $\lambda_{visuallysalient}$. We selected the parameters based on the development set correlation of the
606 reconstructed vs reference jaw and visually salient articulatory gestures.

607 The architecture of the VQ-VAE was an encoder with 3 1-D convolutional layers, filter
608 size 40, kernel size (KS) 4, stride 2. The ReLU activation followed layers 2 and 3. After
609 that, a 1-d convolutional layer with KS 1 and stride 1 was applied. We used a codebook
610 with 40 1-dimensional vectors, which we initialized with the distribution of $\frac{\mathcal{U}[-1,1]}{d_{enc}}$, where
611 d_{enc} is the dimensionality of the codebook, in this case 40. The decoder consisted of a
612 1-dimensional convolution with 40 kernels with size 1 and stride 1, followed by 3 layers of 1d

613 transpose convolutions with $\text{KS}=4$, $\text{stride}=2$, that upsampled the representations back to the
614 original sampling rate of 100 Hz. The layers had 40, 40 and 16 kernels, respectively. The
615 dimensionality of the VQ-VAEs hidden units and codebooks were found via manual tuning
616 when evaluating the reconstruction quality of the full system (VQ-VAE and CTC decoder),
617 rather than just the VQ-VAE’s reconstruction.

618 We trained the VQ-VAE using the AdamW optimizer [6], with a learning rate of $1e - 3$,
619 weight decay of $1e - 2$, $\beta_1 = 0.9$, and $\beta_2 = 0.999$. We used a batch size of 32, and clipped
620 the ℓ_2 norm of the gradient to be 1 across all samples in the batch. For training, we first
621 held out all trials used for evaluation with the `1024-word-General` sentence set from being
622 used as training or dev set data. We then selected 90% of the remaining data (any trial that
623 was not used for evaluation with the `1024-word-General` sentence set) as training data, and
624 then used 10% of the data for early stopping. We early stopped models when the test loss for
625 that epoch did not improve over the loss from the previous epoch by at least $1e - 6$, which
626 occurred for the model we used after 636 total epochs of training. The VQ-VAE parameters
627 were then frozen and were not further trained as part of the CTC decoding process.

628 CTC decoding

629 We next trained a neural network decoder to predict VQ-VAE units based on neural activity.
630 To do this, we first encoded the units as a discrete sequence, and reserved the token 0 for the
631 blank token used in CTC decoding.

632 We preprocessed our neural data identically to the preprocessing done for text decoding
633 with the `1024-word-General` sentence set.

634 We then used an architecture nearly identical to that used for text decoding, hence we
635 manually searched over a small set of hyperparameters close to those used in text decoding.
636 We used identical training procedures as used in text decoding for the `1024-word-General`
637 set, however we did not use temporal jittering during training, and instead used a fixed
638 window from $[-1, 8]$ seconds relative to the go cue for the `1024-word-General` sentence
639 set, and $[-1, 6]$ seconds relative to the go-cue for the `50-phrase-AAC` sentence set and the
640 `529-phrase-AAC` sentence set. However, all other data augmentations were used with the
641 same values as used for text decoding.

642 Evaluation

643 During offline evaluation, we used the same full windows of activity as used for training:
644 from $[-1, 8]$ seconds relative to the go cue for the `1024-word-General` sentence set dataset,
645 and $[-1, 6]$ seconds relative to the go-cue for the `50-phrase-AAC` sentence set and the `529-`
646 `phrase-AAC` sentence set. The decoder was able to output the blank token during silence,
647 thus accounting for variations in production length. We used a greedy search over the models
648 probabilities at each timestep to get the most likely series of VQ-VAE units, and collapsed
649 across repeated units. We then passed this set of units in the VQ-VAE’s decoder (which was
650 not updated as part of further training) to produce articulatory gestures.

651 To evaluate how facial features from healthy speakers compare with those decoded from
652 the avatar, we used the `dlib` software package [16] to extract 72 facial keypoints for each frame

653 in avatar-rendered and healthy speaker videos (30 frames per second) of all three sentence
654 sets.

655 For the direct-approach, we extracted these videos by running the decoded articulatory
656 gestures through the avatar animation system offline using Speech Graphics’ gesture-animation
657 system. We then concatenated all the gestures and played the concatenated gesture animation
658 while screen recording to generate the full video of all decoded trials. For the acoustic-approach,
659 we used the videos captured during real-time audio-visual synthesis. Here we cropped the
660 videos to only include the avatar portion of the screen and environment.

661 For the healthy speakers, we recruited 8 English speakers (6 female and 2 male) to record
662 themselves while speaking sentences from the **1024-word-General** sentence set. We gave
663 them labels of sentences to read and the following instructions (with edits for brevity; we
664 also provided them with a secure location to transfer their recorded data to):

- 665 • Get familiar with the labels. The first number is the block number. The second number
666 is the trial number in order. During recording, you will record one block at a time.
- 667 • Record yourself speaking the sentences using the front-facing webcam:
 - 668 1. Make sure your face is in view, at a minimum, up until the lower part of your eyes
669 and showing the full jaw, even when mouth is open. When we process the videos,
670 we will crop to the region of interest. Make sure to remove any glasses, ensure
671 camera is clear, and that you have still background.
 - 672 2. Make sure you are recording in a quiet environment. If there is talking or noise in
673 the background, please restart the block.
 - 674 3. Record each block, reading each sentence back to back in order. Pause for roughly
675 1-2 seconds in between sentences. Make sure to close mouth in between readings
676 and try to minimize head and shoulder movement (i.e. keep them in roughly the
677 same place).
 - 678 4. Save each video and upload to a secure location.

679 For the healthy speakers and acoustic approach, we segmented the videos according to a
680 manually selected acoustic onset and offset threshold and then trimmed around the video
681 using a window of $[-1, 0.3]$ seconds. For the direct approach, we segmented the videos
682 afterwards by automatically splicing the videos according to the length of the gestures, then
683 included 1.5 seconds of padding at the beginning and end of the gestures. We then used one
684 pseudoblock of data to determine closer trimming landmarks based on visual analysis of the
685 dlib trajectories. For all three approaches, gestural padding was not included in the dlib
686 analyses.

687 To extract trajectories, we used the Euclidean distance between key points rather than
688 the value of a single keypoint in order to account for head movements, scale, and rotation.
689 We evaluated the jaw movement by extracting the distance between the keypoint at the
690 bottom of the jaw and the tip of the nose (keypoints 33 and 8). Lip aperture was evaluated
691 as the distance between the keypoint at the top and bottom of lips (keypoints 51 and 63),
692 and mouth width was evaluated as the distance between the key points at either corners of
693 the mouth (key points 54 and 48). The keypoints are in Supplementary Figure S19.

694 **Expression Decoding**

695 To decode expressions we used the same model architecture as used in NATO code-word
696 classification. We made a single change to increase dropout to 0.8, to prevent over-fitting on
697 limited training data. We initialized the weights of the model, excluding the final readout
698 layer, with a pre-trained NATO code-word classification model with the same hyperparameters
699 as described in S11 (trained on NATO blocks prior to the start of expression data collection,
700 1222 samples). We used the same data augmentations described in (Text decoding: Data
701 augmentations) with parameters that were previously found to be effective [1]. The model
702 was trained using the Adam optimizer with learning rate of $5e-4$ to perform stochastic batch
703 gradient descent. A batch size of 16 was used during training, given smaller amounts of
704 training examples. We evaluated the model loss and accuracy after each training epoch. For
705 each of 15 CV folds, we reserved 10% of the training data as a validation set. We then fit 10
706 models per fold to ensemble predictions on the held out test set. We early stopped training if
707 accuracy did not improve for 20 epochs on the validation set and kept the model with best
708 accuracy on the validation set.

709 **Articulatory-movement decoding**

710 We performed a small grid-search over the hyperparameters for the number of layers used
711 in the network, the dropout rate, and the number of hidden units. We held out the final
712 40 samples collected as an evaluation set during our hyperparameter search. The set was
713 not used for model training or evaluation after hyperparameters were selected. We did a
714 grid search over the values [128, 256, 512] for the number of hidden units, [.4, .5, .6] for the
715 dropout rate, and [2, 3, 4] as the number of layers. We found the optimal values to be 512,
716 .4, and 2, respectively. We then evaluated model performance using these hyperparameters
717 across 10 held-out folds using the remaining data (800 trials).

718 We trained our neural network using the Adam optimizer with a learning rate of $1e-3$,
719 $\beta_1 = .9$, $\beta_2 = .999$, and a batch size of 32. We evaluated the model loss after each training
720 epoch. We used 10% of the data as the test set. From the remaining 90%, we used 90% of
721 the data to train the model, and then 10% of the data as an evaluation set to early-stop the
722 model. If accuracy did not improve for 20 epochs, training stopped and the model with the
723 best evaluation set accuracy was used as the final model.

724 **Avatar implementation during articulatory-movement and expression decoding**

725 Speech Graphics also provided us with target gestures for the orofacial movements and
726 expressions tasks. After classifying the most likely movement or expression, we sent to the
727 Microsoft Surface Book 3 in a streaming fashion. For each emotion, our participant chose which
728 expression she would like to express from 10 variations. The "high" expression corresponded
729 to a maximally intense expression, where as "medium" and "low" were respectively $\frac{2}{3}$ and $\frac{1}{3}$
730 the intensity of the "strong" expression.

731 **Perceptual assessment**

732 We evaluated the decoded avatar animations (for the direct approach and the acoustic
733 approach) in the absence of speech. We designed perceptual assessments using a crowd-
734 sourcing platform (Amazon Mechanical Turk). Each decoded animation was assessed by 6
735 unique evaluators. Each evaluation consisted of playback of the decoded animation (with no
736 audio) and textual presentation of the target (ground-truth) sentence and a randomly chosen
737 other sentence from the same sentence set. Workers were presented with the ground-truth
738 phrase and a randomly chosen phrase from the test set. Evaluators were instructed to identify
739 the phrase that they thought the avatar was trying to say. The precise instructions were as
740 follows:

741 This is a lip-reading task. First, please look at the two phrase options. Then
742 watch the silent video clip of the avatar. Choose the phrase closest to what you
743 were able to lip-read. You may watch the video as many times as needed. Click
744 the submit button after selection to move to the next HIT.

745 We took the median worker response accuracy as the accuracy for that trial.

746 **Supplementary figures**

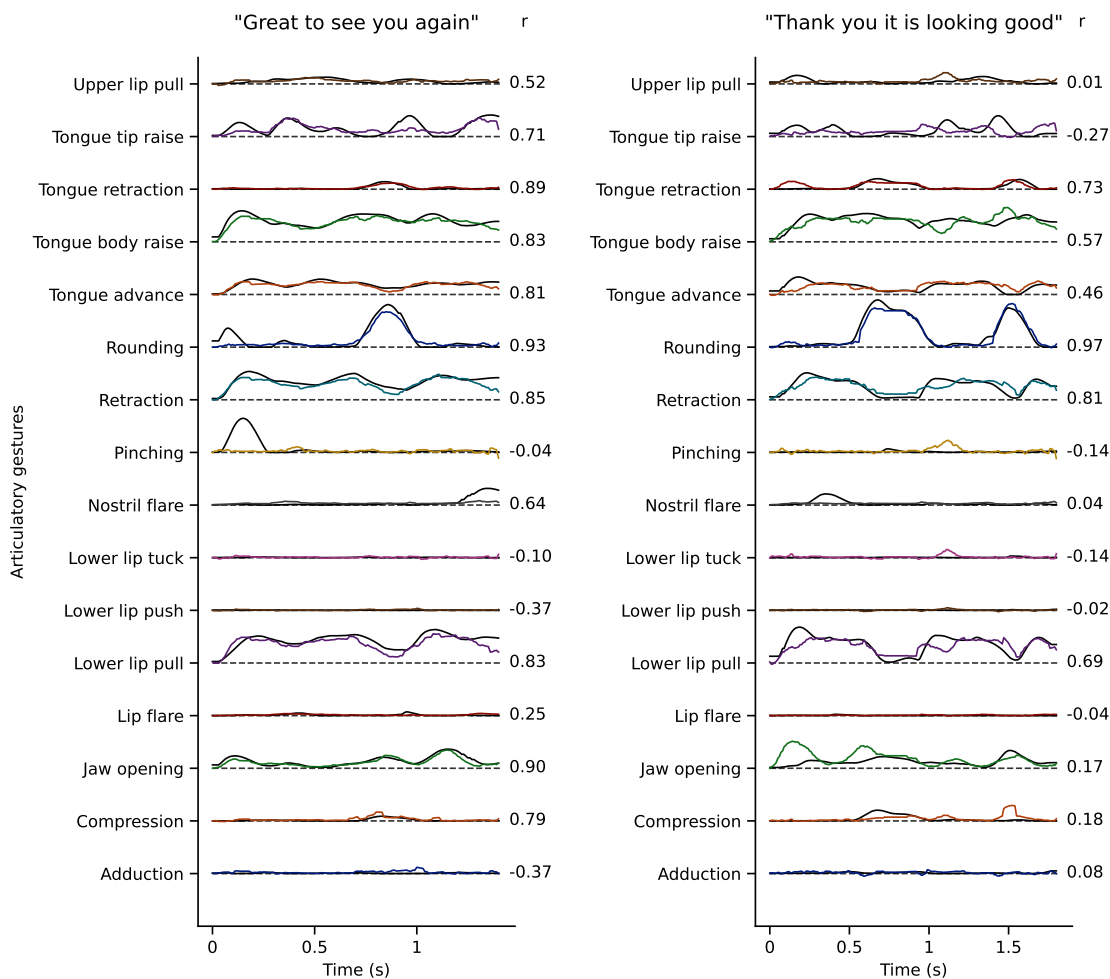


Figure S1. Examples of directly decoded avatar articulatory gestures. Examples of directly decoded articulatory gestures (colored) compared with reference articulatory gestures (black). Examples were taken from the 50-phrase-AAC sentence set. Dynamic time warping [17] was applied to align traces prior to plotting and computation of Pearson's r , which is displayed to the right of each gesture. Reference articulatory gestures were computed using the speech-to-gesture acoustic-to-articulatory inversion model from Speech Graphics' SG Com.

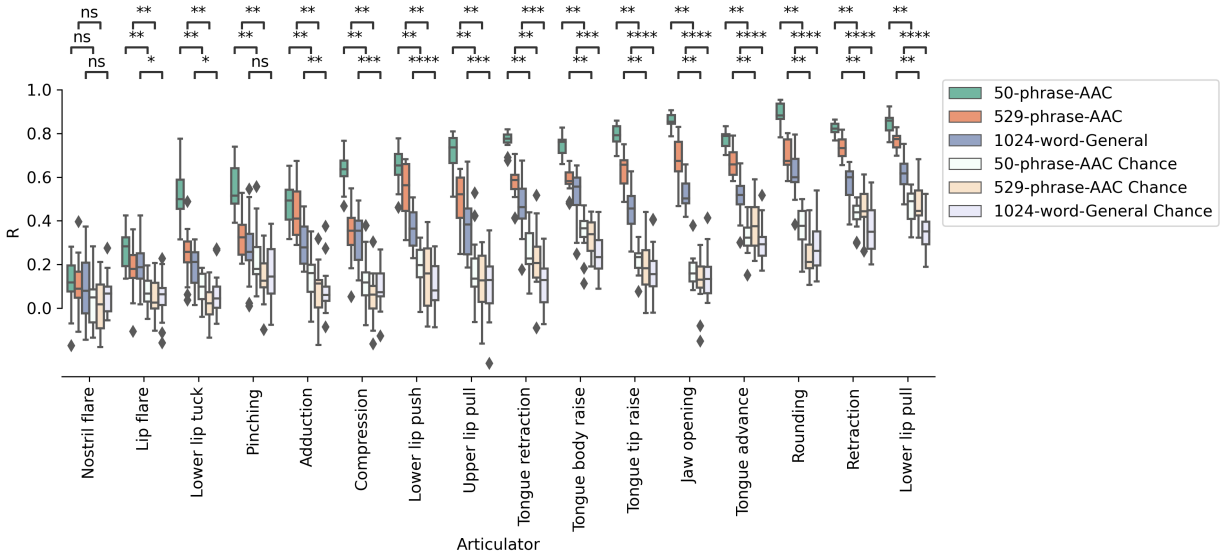


Figure S2. Correlations of directly decoded avatar articulatory gestures with reference articulatory gestures. Pearson correlation (R) of decoded articulatory gestures with reference articulatory gestures using the direct decoding approach after applying dynamic time warping using fast-dtw [17] to align the reference and decoded gestures, since the participant never heard the reference waveform used to derive reference gestures. Chance values are derived by shuffling the neural data temporally then feeding it through our decoding pipeline. The resulting traces are then warped using fast-dtw, and compared with reference traces. Correlations were significantly above chance for all comparisons except comparisons of nostril flare for all sentence sets, and pinching for the 1024-word-General sentence set, two-sided Wilcoxon Signed Rank test with 16-way Holm-Bonferroni correction across $n=20$ pseudo-blocks for the 1024-word-General sentence set, $n = 15$ pseudo-blocks for AAC sets. See Supplementary Table S4 for all p-values and statistics. **** $P < .0001$, *** $P < .001$, ** $P < .005$, * $P < .01$.

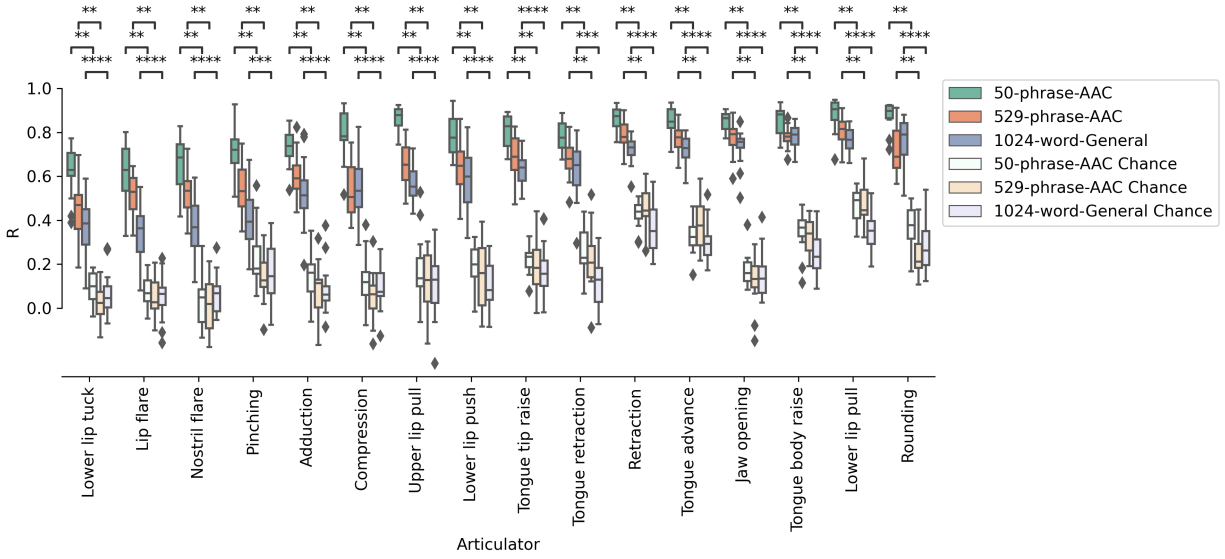


Figure S3. Correlations between avatar articulatory gestures with reference articulatory gestures using the acoustic approach. Pearson correlation (R) of decoded articulatory gestures with reference articulatory gestures during acoustic approach after applying dynamic time warping using fast-dtw [17] to align the reference and decoded gestures, since the participant never heard the reference waveform used to derive reference gestures. Chance values are derived by shuffling the neural data temporally then feeding it through our decoding pipeline. The resulting traces are then warped using fast-dtw, and compared with reference traces. Correlations were significantly above chance for all comparisons, two-sided Wilcoxon Signed Rank test with 16-way Holm-Bonferroni correction across $n=20$ pseudo-blocks for the 1024-word-General sentence set, $n = 15$ pseudo-blocks for AAC sets. See Supplementary Table S5 for all p-values and statistics. **** $P < .0001$, *** $P < .001$, ** $P < .005$, * $P < .01$.

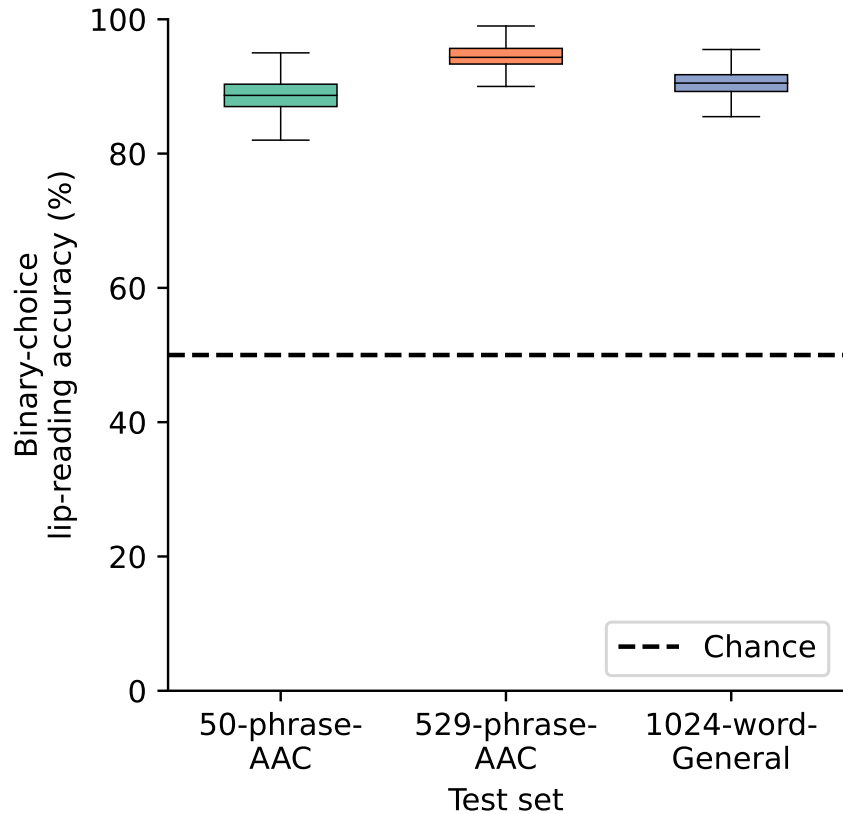


Figure S4. Perceptual accuracy for the avatar using the acoustic approach. Binary perceptual accuracy from human evaluation of silent videos extracted from the audio-visual synthesis task. We used the median bootstrapped accuracy across six evaluators to represent the final accuracy for each sentence. We obtained median accuracies of 88.7% (99% CI [81.7, 94.0]), 94.3% (99% CI [89.7, 98.3]), and 90.5% (99% CI [85.5, 95.0]) bootstrapped across 150 trials of the **50-phrase-AAC** sentence set, 150 trials of the **529-phrase-AAC** sentence set, and 200 trials of the **1024-word-General** sentence set, respectively.

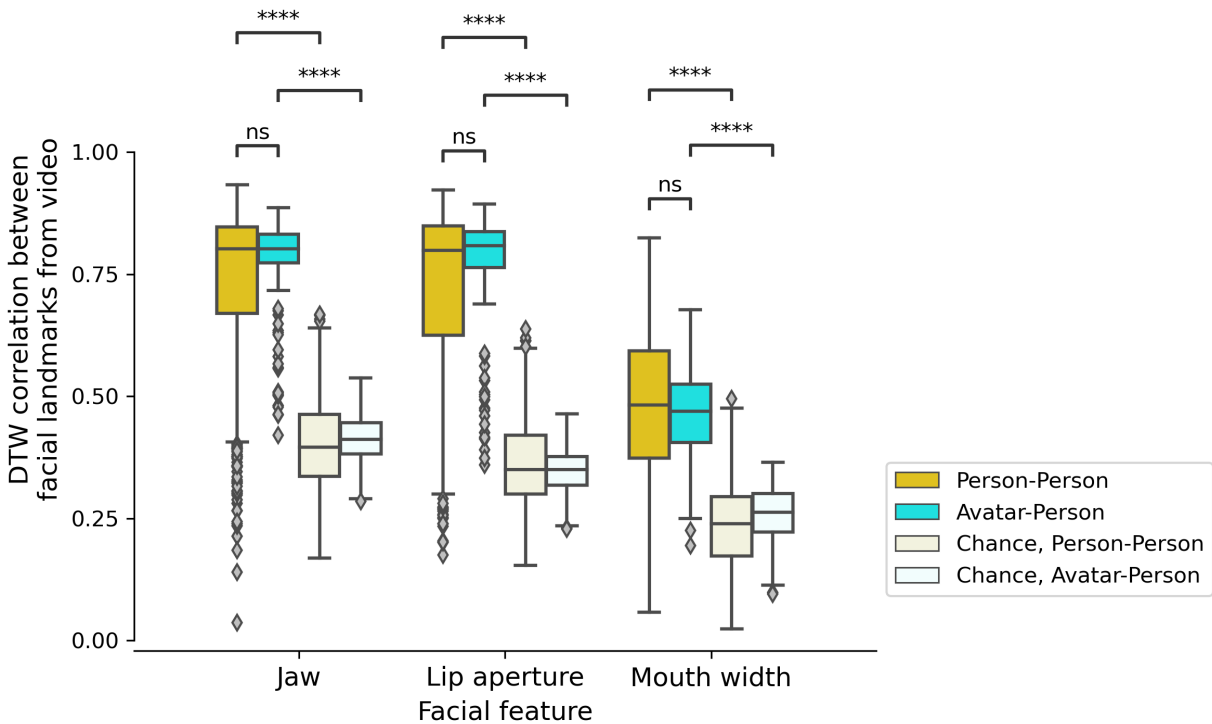


Figure S5. Correlations of facial landmarks using the acoustic approach for avatar decoding the 1024-word-General sentence set. Correlations of facial landmark trajectories (extracted using dlib) within healthy speakers and between healthy speakers and the avatar. The avatar was animated using real-time testing blocks for audio-visual synthesis where the decoded acoustic waveform was used with the acoustic speech-to-gesture approach for animation. 8 healthy speakers spoke the same sentences. Correlations were measured using the pearson correlation after applying dynamic time warping. We observed similar results as for direct decoding with the 1024-word-General sentence set (Main text, Fig 4c), where correlations between the avatar and a healthy speaker were comparable to correlations between two healthy speakers. Mean correlations were .801 (99% CI [.789, .814]), .808 (99% CI [.793, .815]), and .469 (99% CI [.443, .494]) for jaw, lip aperture, and mouth width, respectively. These results were significantly better than chance (see Supplementary Table S6 for statistics and p-values). Interestingly, the correlations between person-person and avatar-person were not significantly different with this approach, demonstrating a promising path to avatar animation, but more limited than directly decoding articulatory representations.

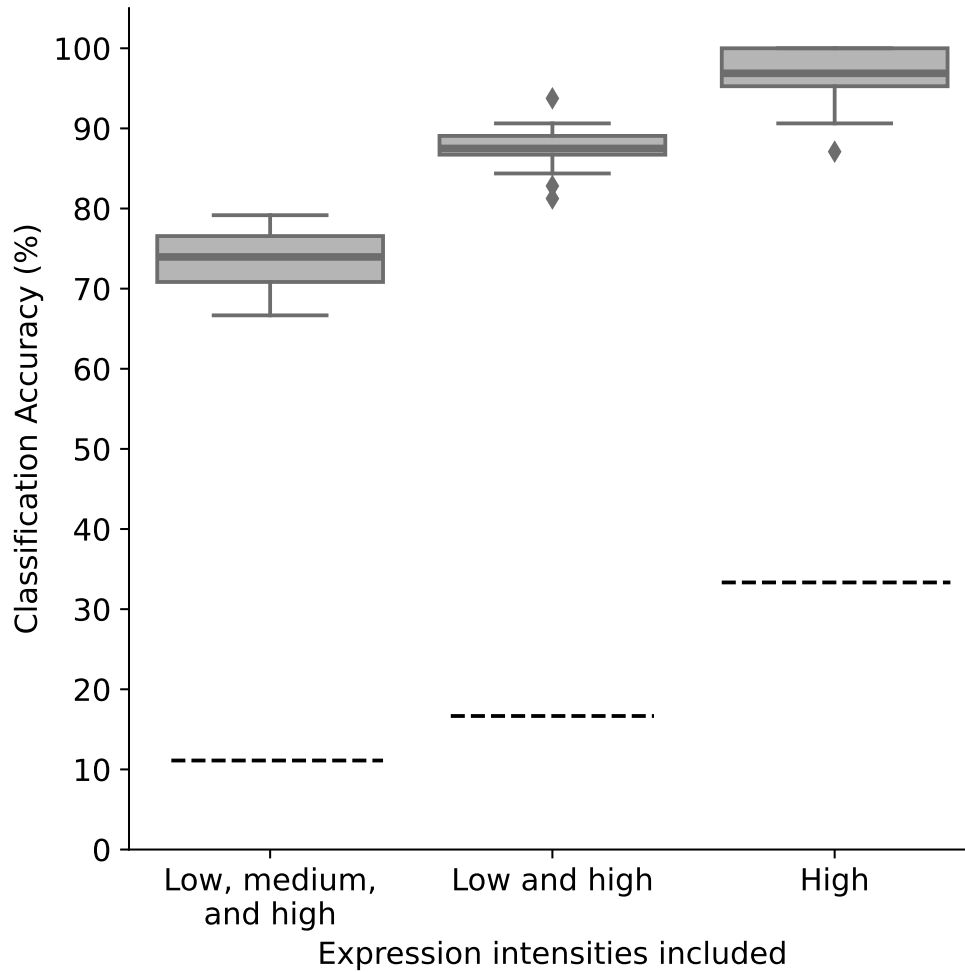


Figure S6. Classification of emotional expressions. 15-fold cross validation classification accuracy for emotional expressions across different subsets of intensities in the emotional-expression task. Chance for each paradigm is indicated by the dashed black line. Box plots consist of (n=15) accuracies for cross validation folds. Median cross-validation fold accuracy was 74.0% (99% CI [70.8, 77.1]) for all low, medium, and high intensity expressions, 87.5% (99% CI [84.4, 89.1]) for all low and high intensity expressions, and 96.9% (99% CI [93.8,100]) for all high intensity expressions.

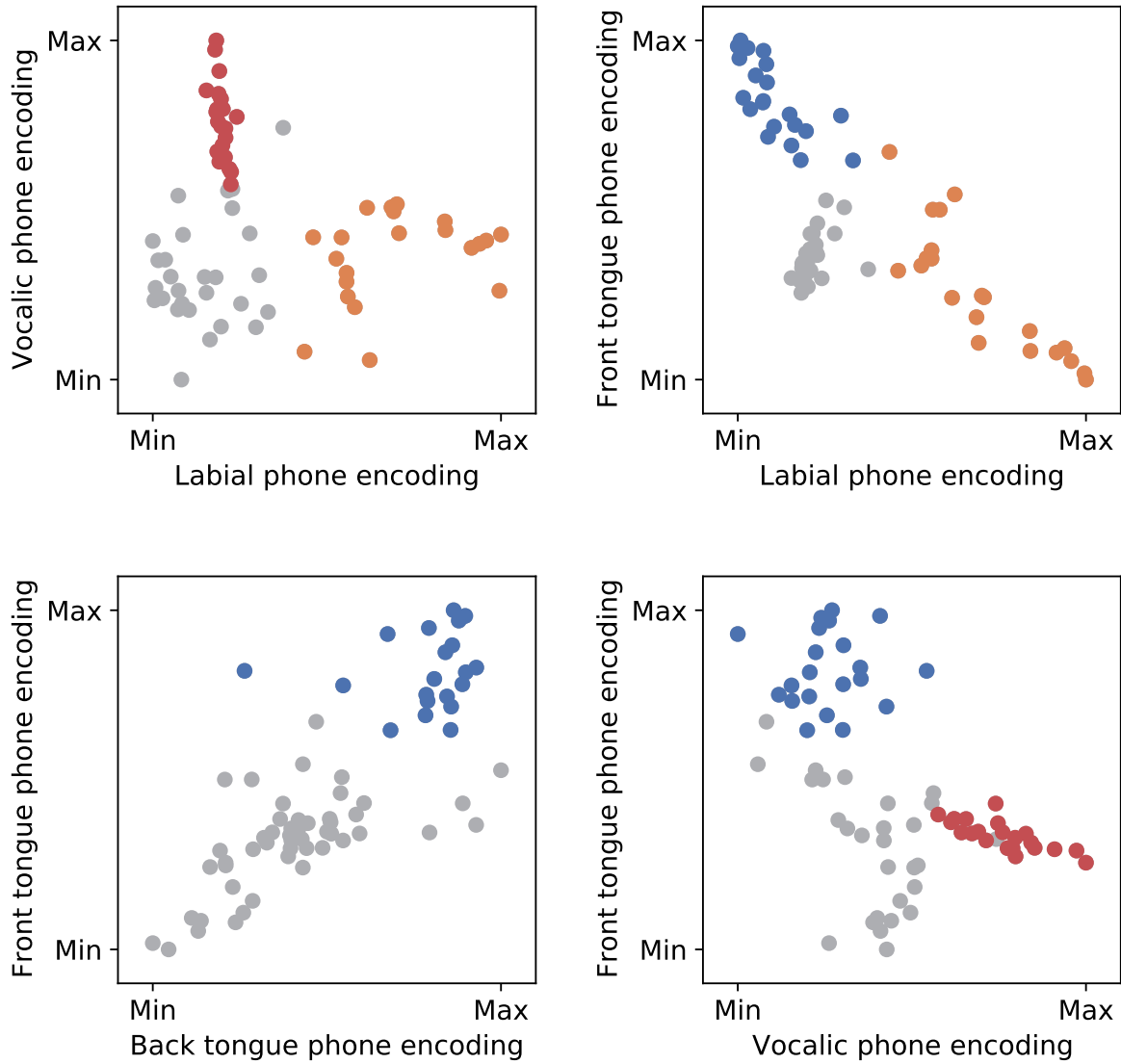


Figure S7. Cross-phone place-of-articulation encoding. For each electrode included in Fig. 5 we visualized the relationship between encoding of phone place of articulation (POA) categories. The electrode color represents the top 30% of encoding electrodes for a given POA (as in Fig. 5).

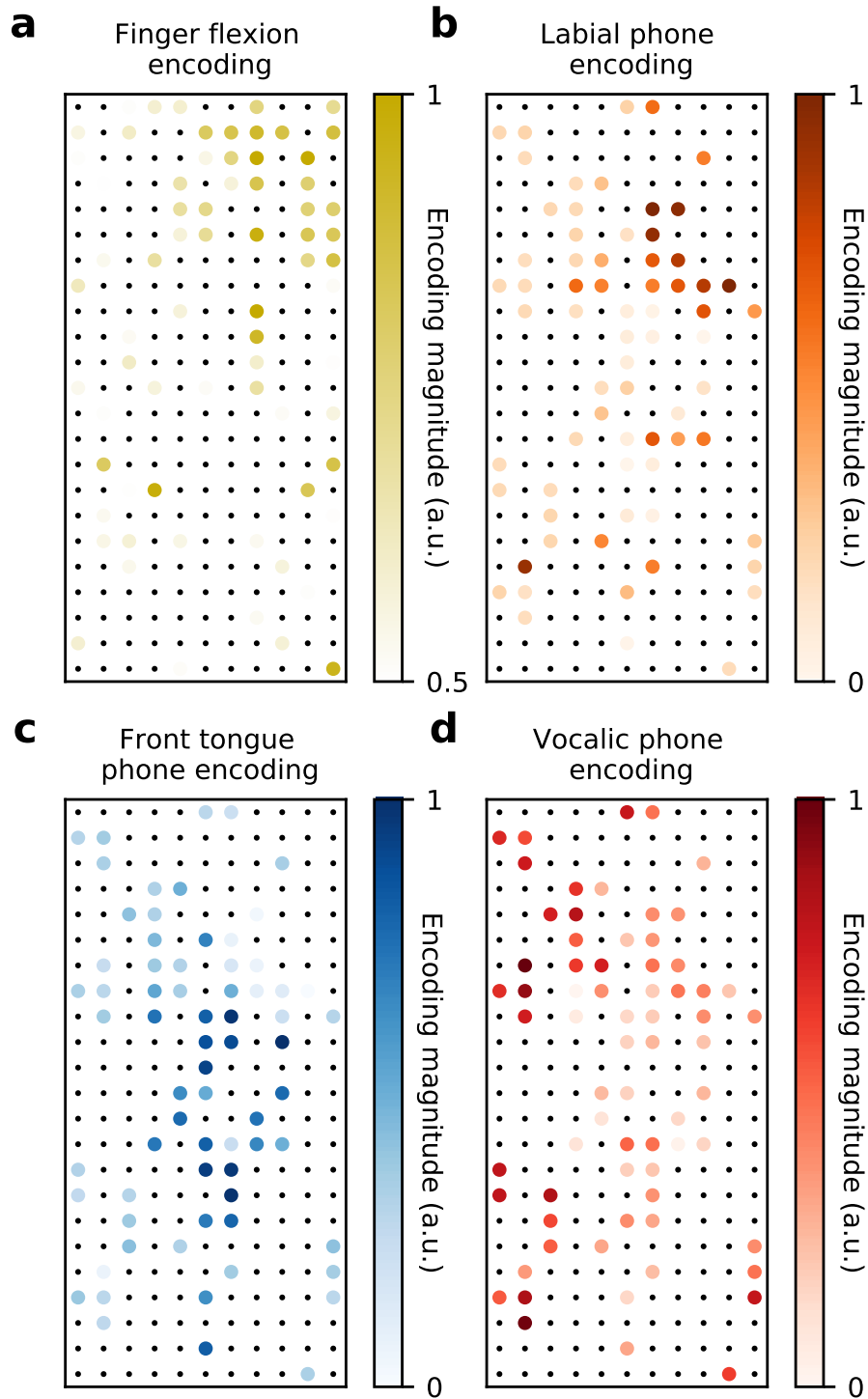


Figure S8. Spatial distribution of electrode tuning to articulatory features. Shown are normalized [0-1] encoding weights across electrodes for (a) hand finger flexion, (b) labial phones, (c) front tongue phones, and (d) vocalic phones. For b-d data is shown for all speech responsive electrodes with encoding $r > 0.2$. For (a) data is shown for the top 50% of finger-flexion encoding electrodes.

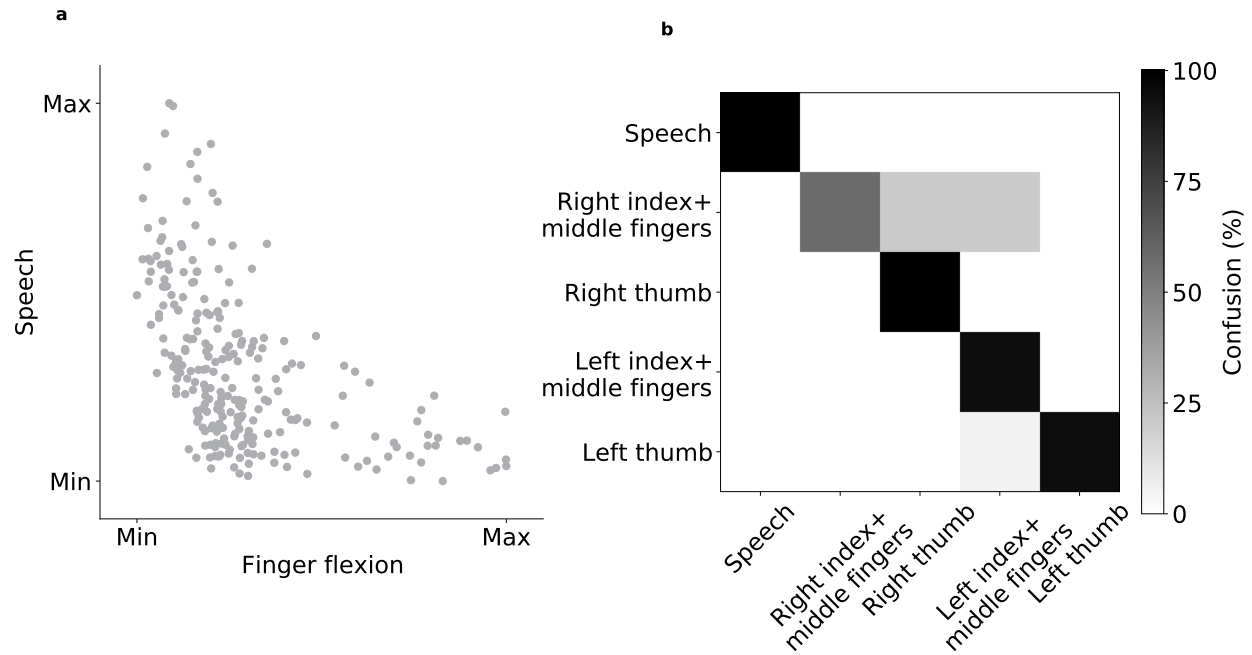


Figure S9. Attempted finger flexion and speech are largely encoded orthogonally. a. For each electrode, the normalized [0,1] encoding in response to attempted production of NATO code-words is plotted against attempted finger flexion in the NATO-motor task. **b.** Confusion matrix from the NATO-motor task, showing minimal confusion between hand and speech targets.

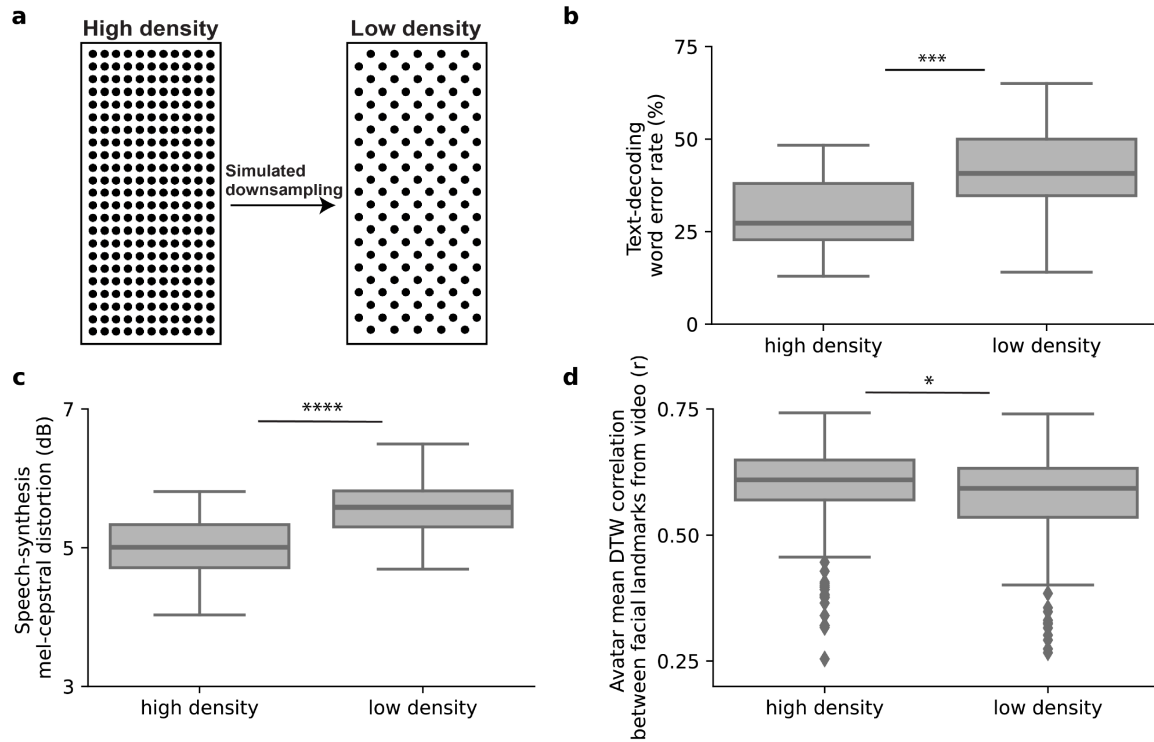


Figure S10. Effects of limiting electrode density on decoding . (a) Visualization of the checkerboard-downsampling procedure used to simulate a low-density electrocortigraphy array with 127 electrodes (4.24 mm spacing) instead of 253 (3 mm spacing). (b-d), Effect of modulating electrode density on text-decoding word error rates (b), speech-synthesis mel-cepstral distortion (c), and avatar direct-decoding correlation (average DTW correlation of jaw, lip, and mouth-width landmarks between the avatar and healthy speakers) (d). * $P < 0.01$, ** $P < 0.005$, *** $P < 0.001$, **** $P < 0.0001$, two-sided Wilcoxon signed-rank test with 3-way Holm-Bonferroni correction (full comparisons for b-d are given in Table S11). Distributions are over 25 pseudo-blocks for text decoding, 20 pseudo-blocks for speech synthesis, and $n=152$ avatar comparisons (19 pseudo-blocks for 8 healthy speakers) for avatar direct-decoding on the 1024-word-General set.

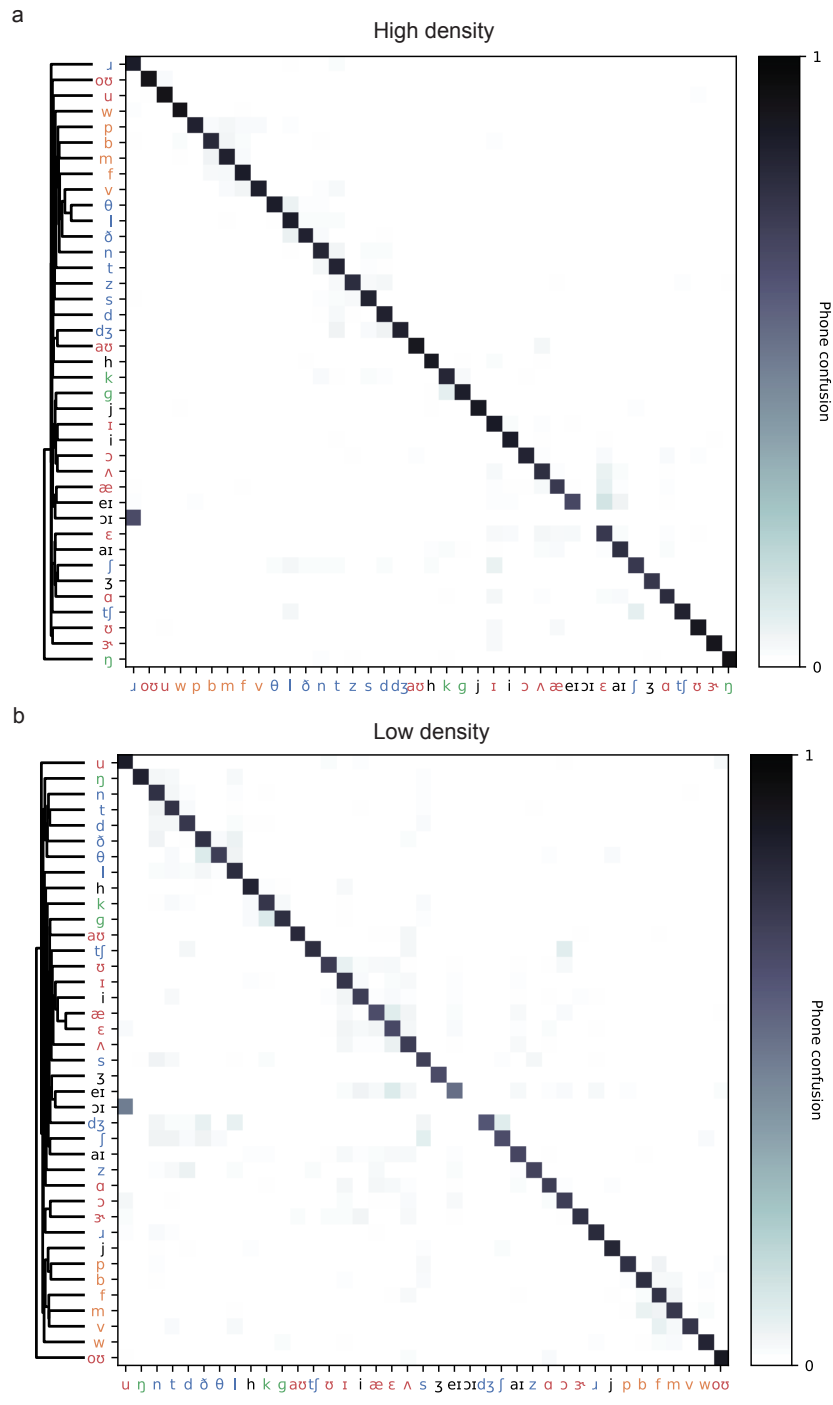


Figure S11. Phone confusion matrices during text decoding. Phone confusion matrices computed using substitutions in edit distance for the 1024-word-General text evaluation set. Phones are colored by place of articulation (POA) features (as in Fig. 5). Hierarchical clustering was performed using Ward’s method. Confusion matrices provided for (a) full model and (b) low-density simulation. Although confusion is higher in the low-density case (which is expected), clustering by POA persists.

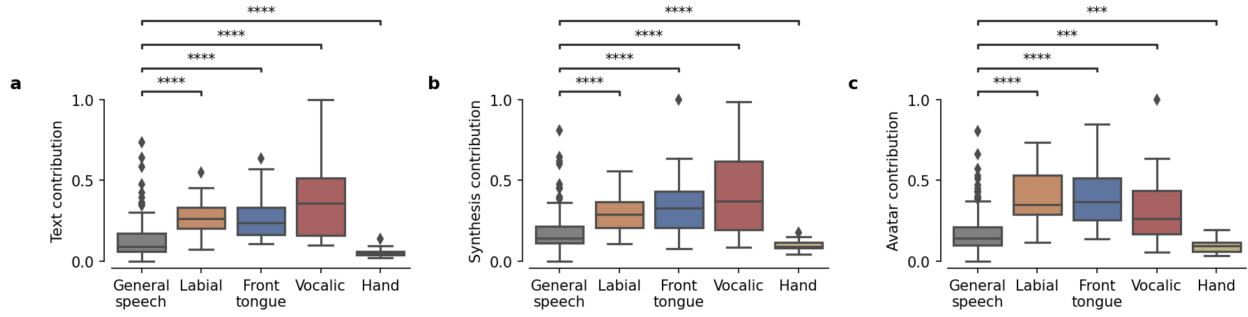


Figure S12. Decoding contributions of articulatory encoding electrodes. Electrode contributions, computed the same as in Fig. 6, for each of the articulatory encoding groups shown in Fig. 5. General-speech refers to electrodes that did not fall within the top 30% of an articulatory encoding group. Contributions for (a) text-decoding, (b) speech-synthesis, and (c) direct avatar decoding are provided. Statistical tests were performed between General-speech electrodes and each articulatory group. **** $P < 0.0001$ and *** $P < 0.001$, Two sided Mann-Whitney U-test with 4-way Holm-Bonferroni correction for multiple comparisons.

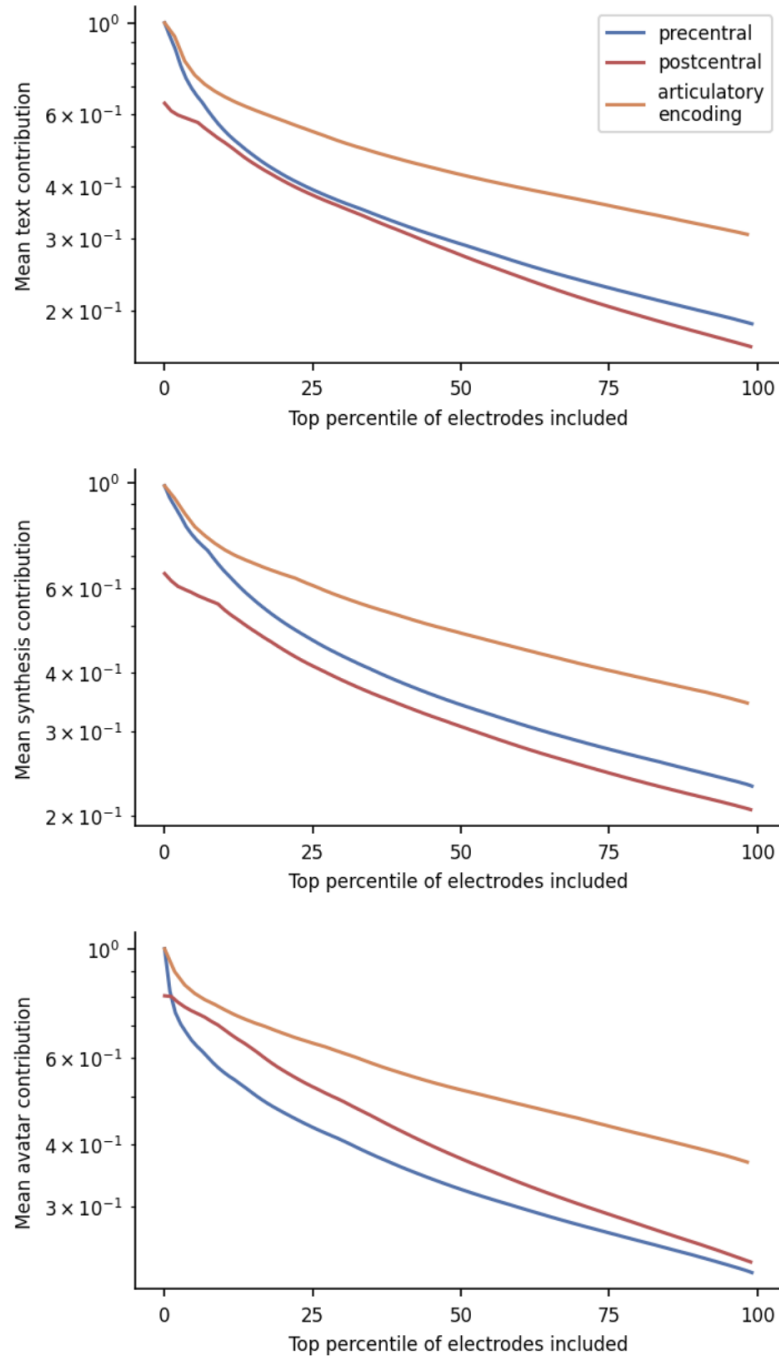


Figure S13. Mean contribution of electrode groups, controlled for number of electrodes.

The mean electrode contribution, computed the same as in Fig. 6, is quantified as a function of top percentile of electrodes included in the precentral gyrus, postcentral gyrus, and articulatory encoding electrodes from Fig. 5f (not including the hand). Across text-decoding (top), speech-synthesis (middle), and avatar direct-decoding (bottom), articulatory encoding electrodes contributed the most to decoding performance. For text-decoding and speech-synthesis the precentral gyrus contributed slightly more across all percentiles.

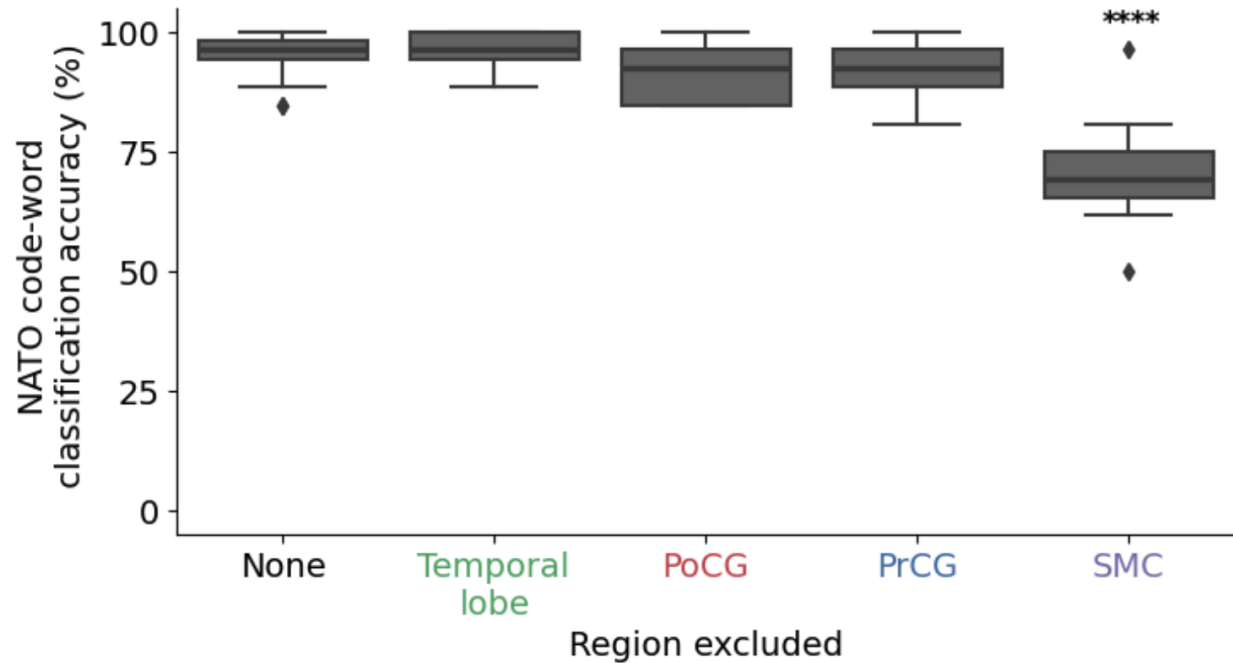


Figure S14. Region-exclusion analysis for NATO code words. Effect of excluding anatomical regions (PoCG: postcentral gyrus, PrCG: precentral gyrus, SMC: sensorimotor cortex) on NATO code-word classification accuracies. Significance markers indicate comparisons against the full-model condition (None). (**** $P < 0.0001$, two-sided Wilcoxon signed-rank test with 10-way Bonferroni correction, full comparisons are given in Table S9). Distributions are over 19 blocks after the NATO code-word classifier was frozen (see Fig. 2h)

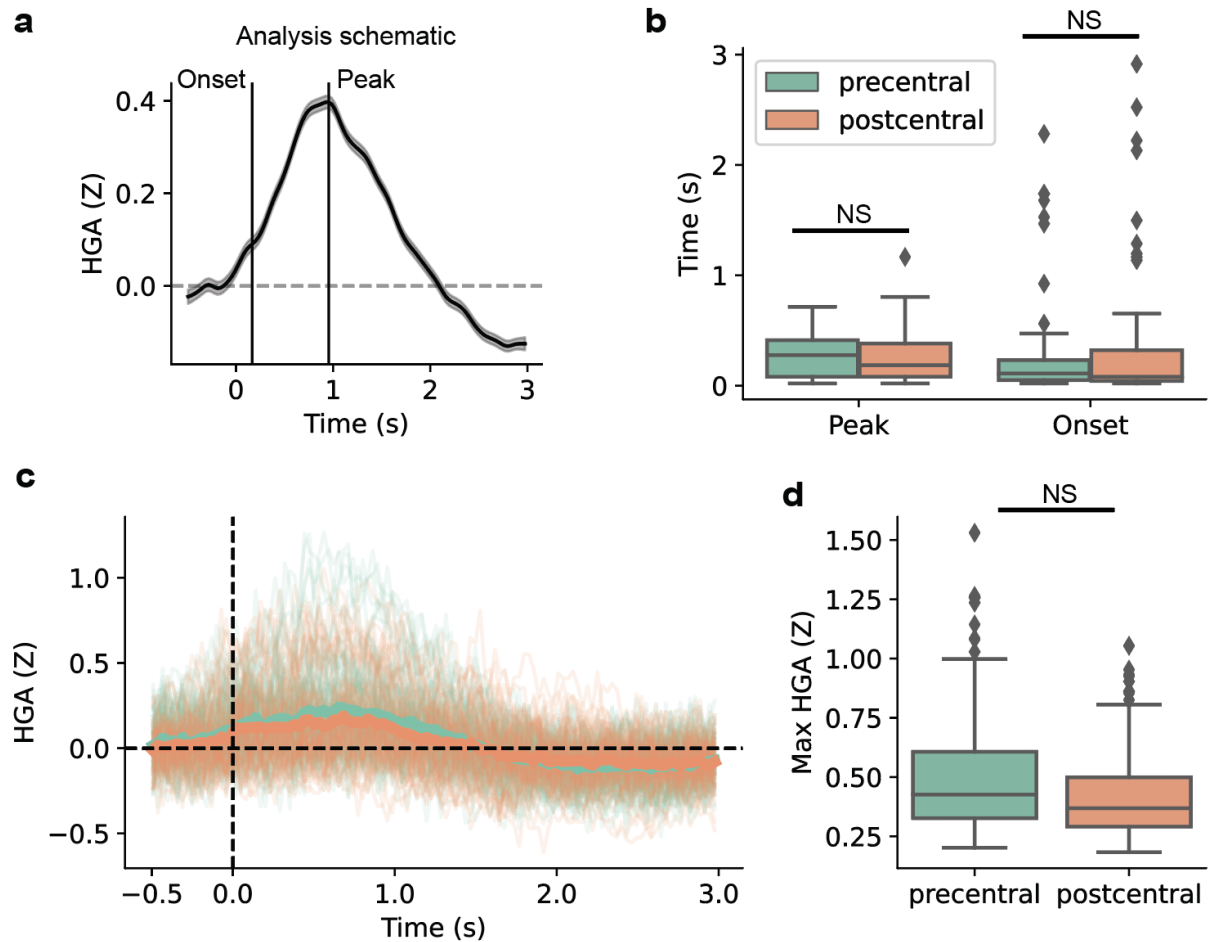


Figure S15. Timing comparison between precentral and postcentral gyri. (a) Schematic of the timing comparison analysis. For each speech-responsive electrode, we computed the trial averaged high-gamma amplitude (HGA ERP). The onset time was defined as the first timepoint at which the HGA ERP was statistically different than zero. The peak time was defined as the time at which the HGA ERP reached its peak. See methods for more detail on ERP computation for each electrode. (b) Peak and onset times for electrodes in the precentral and postcentral gyri (NS: $P > 0.01$, Two sided Mann-Whitney U-tests). (c) Visualization of trial-averaged HGA for precentral and postcentral electrodes. Each line indicates a single electrode, and bolded lines indicate region averages. (d) The peak HGA of ERPs for electrodes in the precentral and postcentral gyri (NS: $P > 0.01$, Two sided Mann-Whitney U-test).

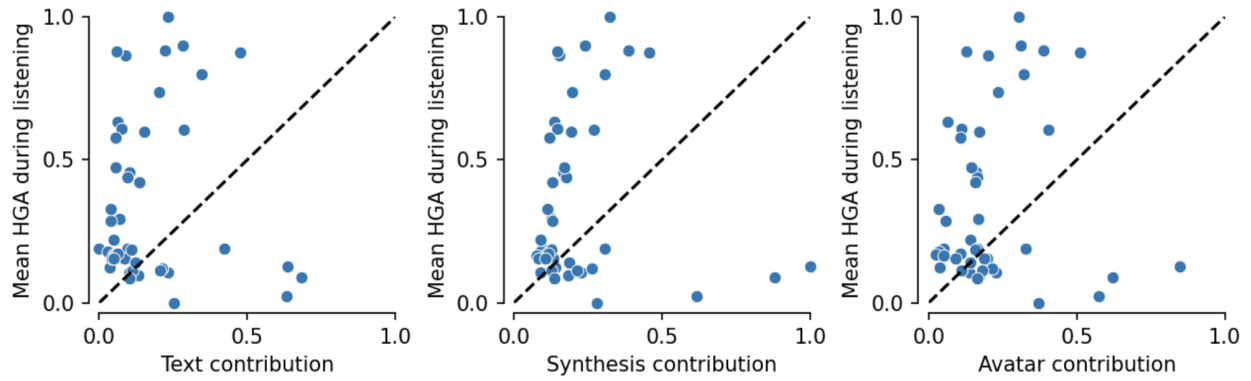


Figure S16. Relationship between temporal lobe decoding contributions and auditory responses. Each point is a temporal-lobe electrode. The electrode contribution, computed the same as in Fig. 6, is plotted against the median temporal-lobe high-gamma amplitude (HGA) in the 0-2 s window aligned to onset of auditory presentation of sentences (normalized between 0-1). Black dotted lines indicate unity ($y=x$). There is no significant correlation between HGA during listening and electrode contribution to text-decoding (left; $r = 0.017$, $P = 0.91$), speech-synthesis (middle; $r = -0.0052$, $P = 0.99$), and avatar direct-decoding (right; $r = 0.089$, $P = 0.51$).

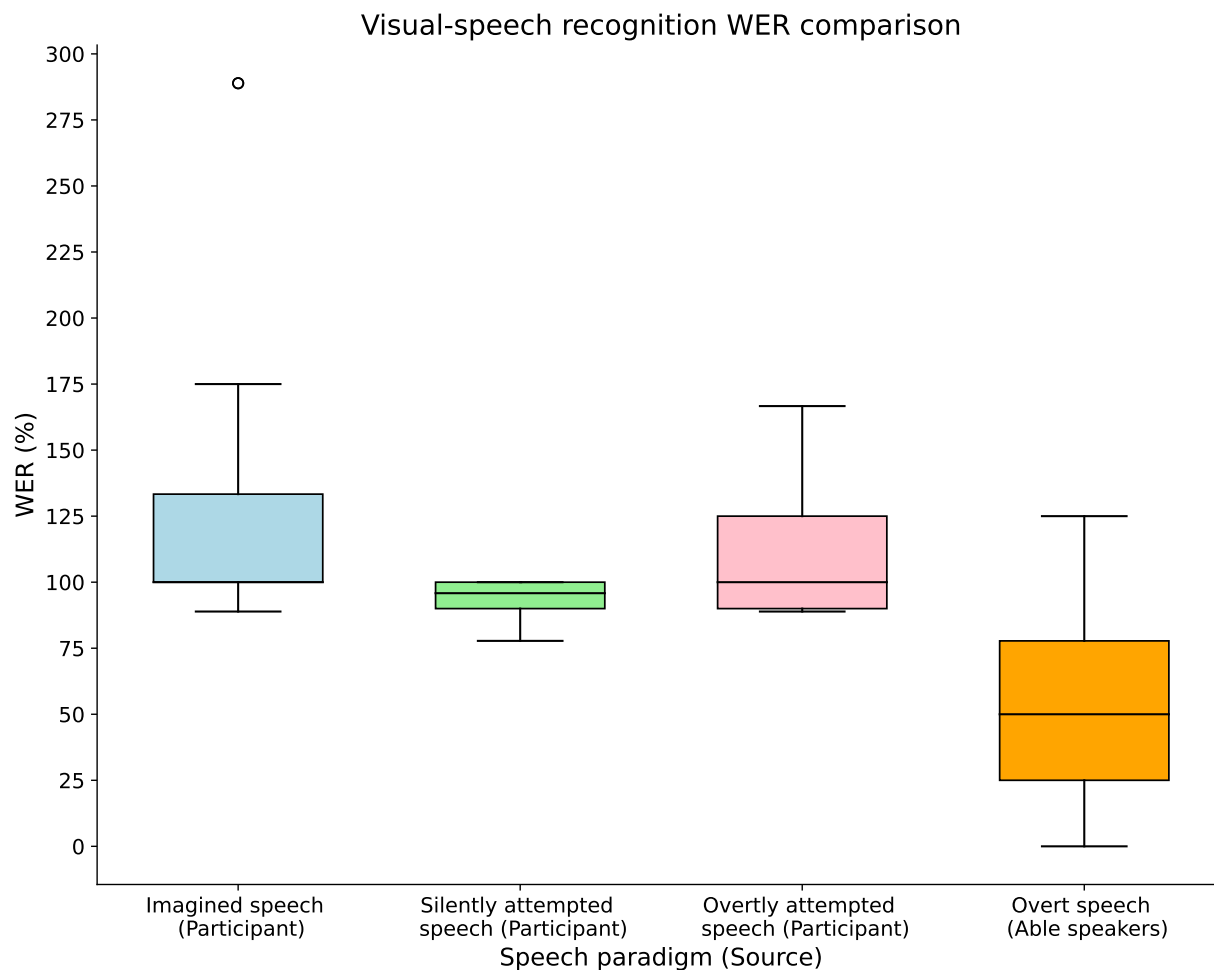


Figure S17. Visual-speech recognition for participant vs. able speakers. Visual-speech recognition results using AV-HuBERT to recognize speech from the participant as well as 8 neurotypical speakers. Imagined, silently attempted, and overtly attempted speech all had higher WERs than able speakers, with the best participant model having a median WER of 95.8% (99% CI [90.0, 125.0]) compared to 50% (99% CI [37.5, 62.5]) for the able speakers.

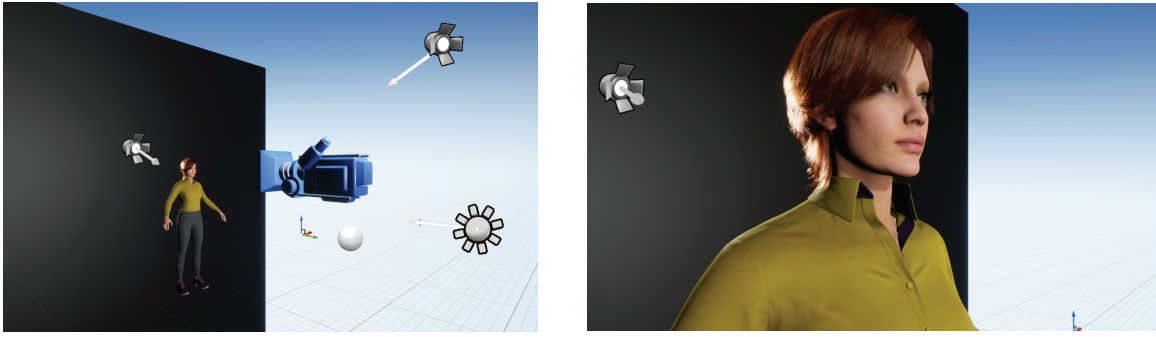


Figure S18. Virtual environment for avatar decoding. Virtual environment (designed in Unreal Engine 4.26) containing the camera and setup (left) for the "Vivian" MetaHuman's character (right).

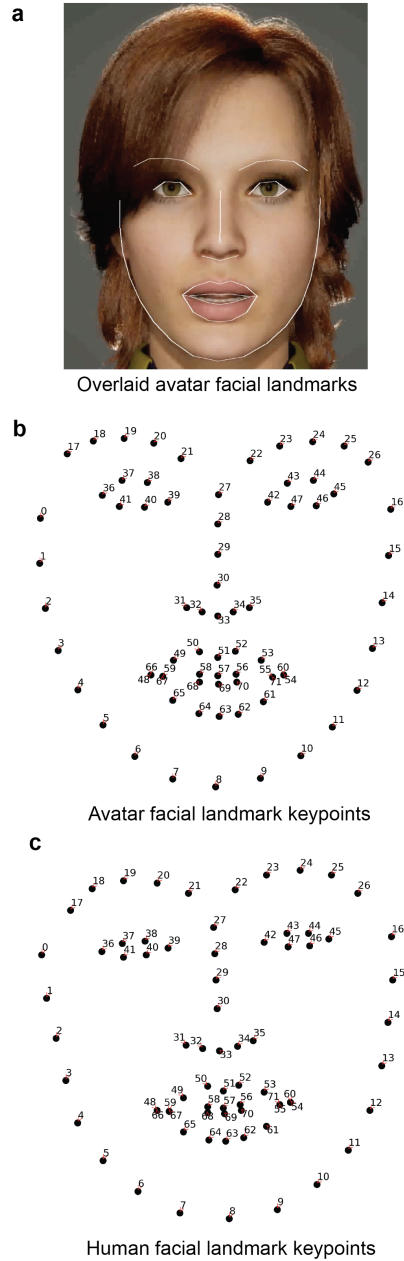


Figure S19. Example of dlib facial-landmark detection. **a** An example of detected facial landmarks overlaid on a frame selected from a video rendering of an avatar during a single trial and using the direct approach to avatar decoding, **b** An example set of plotted detected facial landmark key points from a video rendering of an avatar during a single trial and using the direct approach to avatar decoding, **c** An example set of plotted facial landmark key points that shows exemplar facial landmark detection of a human face. The original video frame was selected from one of our 8 volunteer speakers speaking a phrase from the 1024-word-**General** sentence set. The avatar and human key points are coherently and robustly tracked. All landmarks were tracked and detected using [16]. In **b** and **c**, the small red arrow points to the precise xy coordinate of the landmark tracked by each labeled keypoint. Note some landmarks are overlapping (e.g. keypoints 48 and 66).

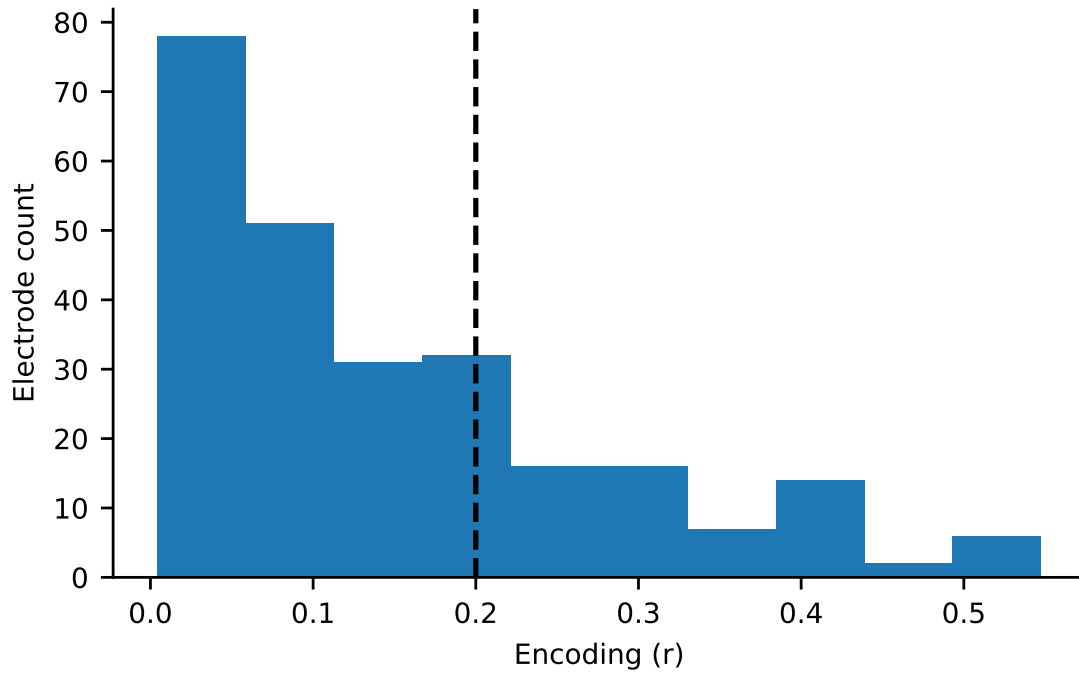


Figure S20. Distribution of phone-encoding r-values across electrodes. Shown are encoding r-values across electrodes from the linear encoding model trained to predict each electrode’s high-gamma activity from phoneme emission probabilities. The dashed black line indicates the cut-off for inclusion in subsequent clustering analysis (Fig. 5). 27.7% of electrodes met a threshold of $r > 0.2$ for inclusion [18].

Supplementary Table S1. Participant’s personalized voice MCD comparisons.

Dataset 1	Dataset 2	Statistic	Corrected P-value
1024-word-General B3 MCD	50-phrase-AAC chance MCD	2.07e+03	1.62e-42
1024-word-General B3 MCD	1024-word-General chance MCD	1.88e+02	1.42e-32
50-phrase-AAC B3 MCD	1024-word-General B3 MCD	4.98e+03	5.37e-26
50-phrase-AAC B3 MCD	50-phrase-AAC chance MCD	1.00e+00	9.39e-26
529-phrase-AAC B3 MCD	529-phrase-AAC chance MCD	7.80e+01	3.28e-25
50-phrase-AAC B3 MCD	529-phrase-AAC B3 MCD	6.04e+03	8.00e-12
529-phrase-AAC B3 MCD	1024-word-General B3 MCD	1.16e+04	2.34e-04

¹ Across dataset comparisons are two-sided Mann-Whitney U-tests whereas within-dataset comparisons are two-sided Wilcoxon signed-rank paired tests; all with 7-way Holm-Bonferonni correction for multiple comparisons. Comparisons use n=20 pseudo-blocks for the 1024-word-General sentence set, and n=15 pseudo-blocks for the AAC sentence sets.

Supplementary Table S2. Illustrative speech-synthesis examples.

Sentence set	Target sentence	Transcribed sentence	WER (%)	Percentile (%)	MCD (dB)
50-phrase-AAC	Will you do me a favor	Will you do me a favor	0	39	1.9
	What do you think about that	What do you think about that	0	39	2.53
	Wait for the rest of them	Wait for the rest of them	0	39	2.73
	Great to see you again	Great to see you again	0	39	2.84
	Wait for the rest of them	Wait for the rest of them	0	39	2.93
	Tell me about yourself	Tell me about yourself	0	39	3.02
	I think you are wonderful	I think you are wonderful	0	39	3.22
	Let me tell you what i did	Let me tell you what i did	0	39	3.34
	What have you been doing	What have you been doing	0	39	3.44
	Thanks a lot it really helps	Thanks a lot it really helps	0	39	3.57
	I thought it would be good for me	I thought it would be good for me	0	39	3.76
	Do you really think so	Do you really think so	0	39	4.3
	I thought it would be good for me	I saw it would be good for me	12	81	3.95
	Believe me it is better	Believe me it is bad	20	89	2.95
	Give me a few minutes	Can he meet for a few minutes	80	96	4.16
529-phrase-AAC	All the time	All the time	0	26	2.16
	It is the truth	It is the truth	0	26	2.66
	Will you be here	Will you be here	0	26	2.89
	I will still need it	I will still need it	0	26	3.02
	I do not have much choice	I do not have much choice	0	26	3.18
	Forget about it	Forget about it	0	26	3.43
	As soon as possible	As soon as possible	0	26	3.63
	I am doing well	I am doing well	0	26	4.13
	When will i see you next	When will i see you	17	55	2.78
	How would you feel	How how would you feel	25	61	4.04
	There is more over there	There is near nor there	40	68	4.17
	No longer	To no longer	50	73	5.67
	It feels good	It feel hurt	67	81	4.58
	I need help now	I still have time	75	86	7.66
	Well it sure looks like it	What else is important	100	93	5.03
1024-word-General	Did you like it	Did you like it	0	7	2.39
	This is not right	This is not right	0	7	2.55
	I want to see him	I want to see him	0	7	3.14
	What does she want	What does she want	0	7	3.28
	Let me think about it	Let me think about it	0	7	3.64
	I have to leave now	I have to leave now	0	7	3.74
	Why would you do that	Why will you do that	20	17	2.59
	Where do we go now	But here we go now	40	30	4.54
	Where does he work	Where does it walk	50	37	4.24
	No one else heard it	No one will skip	60	47	3.87
	Have you found a place to stay	So found a play for today	71	56	4.86
	That must be him	Now make me him	75	64	5.81
	Maybe you should be	But you seeing me	88	85	5.89
	Should i say it	Too hard to get	100	94	5.47

Supplementary Table S3. Comparisons for dlib traces with the direct approach.

Articulator	Dataset 1	Dataset 2	Statistic ¹	Corrected P-value ²
Jaw	Avatar-Person	Person-Person	2.49e+04	1.00e-12
Jaw	Avatar-Person	Chance, Avatar-Person	2.20e+04	1.20e-41
Jaw	Person-Person	Chance, Person-Person	2.56e+05	2.58e-114
Lip aperture	Avatar-Person	Person-Person	2.23e+04	1.11e-16
Lip aperture	Avatar-Person	Chance, Avatar-Person	2.19e+04	3.37e-41
Lip aperture	Person-Person	Chance, Person-Person	2.57e+05	9.39e-117
Mouth width	Avatar-Person	Person-Person	3.32e+04	7.36e-04
Mouth width	Avatar-Person	Chance, Avatar-Person	2.18e+04	2.74e-40
Mouth width	Person-Person	Chance, Person-Person	2.57e+05	8.35e-117

¹ Each comparison is a two-sided Mann-Whitney U-test between dlib facial-landmark feature correlations for the avatar (decoded using the direct approach) and healthy-speaker videos, with n=19 pseudo-blocks for each of the 8 speakers (yielding 152 data points for avatar-person comparisons) and n=19 pseudo-blocks for each of the 28 combinations of pairs of speakers (yielding 532 data points for person-person comparisons).

² 9-way Holm-Bonferroni correction for multiple comparisons.

Supplementary Table S4. Comparisons for articulatory gesture decoding using the direct-decoding approach.

Articulator	Dataset 1	Dataset 2	Statistic ¹	Corrected P-value ²
Upper lip pull	1024-word-General	1024-word-General Chance	4.00e+00	8.01e-05
Upper lip pull	50-phrase-AAC	50-phrase-AAC Chance	0.00e+00	9.77e-04
Upper lip pull	529-phrase-AAC	529-phrase-AAC Chance	0.00e+00	9.77e-04
Lower lip pull	1024-word-General	1024-word-General Chance	0.00e+00	3.05e-05
Lower lip pull	50-phrase-AAC	50-phrase-AAC Chance	0.00e+00	9.77e-04
Lower lip pull	529-phrase-AAC	529-phrase-AAC Chance	0.00e+00	9.77e-04
Nostril flare	1024-word-General	1024-word-General Chance	7.80e+01	3.30e-01
Nostril flare	50-phrase-AAC	50-phrase-AAC Chance	1.80e+01	1.51e-02
Nostril flare	529-phrase-AAC	529-phrase-AAC Chance	2.60e+01	5.54e-02
Lower lip tuck	1024-word-General	1024-word-General Chance	2.10e+01	3.40e-03
Lower lip tuck	50-phrase-AAC	50-phrase-AAC Chance	0.00e+00	9.77e-04
Lower lip tuck	529-phrase-AAC	529-phrase-AAC Chance	2.00e+00	9.77e-04
Jaw opening	1024-word-General	1024-word-General Chance	0.00e+00	3.05e-05
Jaw opening	50-phrase-AAC	50-phrase-AAC Chance	0.00e+00	9.77e-04
Jaw opening	529-phrase-AAC	529-phrase-AAC Chance	0.00e+00	9.77e-04
Compression	1024-word-General	1024-word-General Chance	3.00e+00	7.63e-05
Compression	50-phrase-AAC	50-phrase-AAC Chance	0.00e+00	9.77e-04
Compression	529-phrase-AAC	529-phrase-AAC Chance	0.00e+00	9.77e-04
Adduction	1024-word-General	1024-word-General Chance	9.00e+00	3.15e-04
Adduction	50-phrase-AAC	50-phrase-AAC Chance	0.00e+00	9.77e-04
Adduction	529-phrase-AAC	529-phrase-AAC Chance	0.00e+00	9.77e-04
Lip flare	1024-word-General	1024-word-General Chance	2.20e+01	3.40e-03
Lip flare	50-phrase-AAC	50-phrase-AAC Chance	0.00e+00	9.77e-04
Lip flare	529-phrase-AAC	529-phrase-AAC Chance	4.00e+00	9.77e-04
Tongue tip raise	1024-word-General	1024-word-General Chance	0.00e+00	3.05e-05
Tongue tip raise	50-phrase-AAC	50-phrase-AAC Chance	0.00e+00	9.77e-04
Tongue tip raise	529-phrase-AAC	529-phrase-AAC Chance	0.00e+00	9.77e-04
Tongue body raise	1024-word-General	1024-word-General Chance	3.00e+00	7.63e-05
Tongue body raise	50-phrase-AAC	50-phrase-AAC Chance	0.00e+00	9.77e-04
Tongue body raise	529-phrase-AAC	529-phrase-AAC Chance	0.00e+00	9.77e-04
Rounding	1024-word-General	1024-word-General Chance	0.00e+00	3.05e-05
Rounding	50-phrase-AAC	50-phrase-AAC Chance	0.00e+00	9.77e-04
Rounding	529-phrase-AAC	529-phrase-AAC Chance	0.00e+00	9.77e-04
Lower lip push	1024-word-General	1024-word-General Chance	0.00e+00	3.05e-05
Lower lip push	50-phrase-AAC	50-phrase-AAC Chance	0.00e+00	9.77e-04
Lower lip push	529-phrase-AAC	529-phrase-AAC Chance	0.00e+00	9.77e-04
Retraction	1024-word-General	1024-word-General Chance	0.00e+00	3.05e-05
Retraction	50-phrase-AAC	50-phrase-AAC Chance	0.00e+00	9.77e-04
Retraction	529-phrase-AAC	529-phrase-AAC Chance	0.00e+00	9.77e-04
Tongue retraction	1024-word-General	1024-word-General Chance	1.00e+00	3.43e-05
Tongue retraction	50-phrase-AAC	50-phrase-AAC Chance	0.00e+00	9.77e-04
Tongue retraction	529-phrase-AAC	529-phrase-AAC Chance	0.00e+00	9.77e-04
Pinching	1024-word-General	1024-word-General Chance	5.10e+01	8.81e-02
Pinching	50-phrase-AAC	50-phrase-AAC Chance	0.00e+00	9.77e-04
Pinching	529-phrase-AAC	529-phrase-AAC Chance	1.00e+00	9.77e-04
Tongue advance	1024-word-General	1024-word-General Chance	0.00e+00	3.05e-05
Tongue advance	50-phrase-AAC	50-phrase-AAC Chance	0.00e+00	9.77e-04
Tongue advance	529-phrase-AAC	529-phrase-AAC Chance	0.00e+00	9.77e-04

¹ Each comparison is a two-sided Wilcoxon signed-rank test between correlations from real-time decoded articulatory gestures (generated using the direct approach) and reference gestures across n=20 pseudo-blocks for the 1024-word-General sentence set and n=15 pseudo-blocks for the 50-phrase-AAC and 529-phrase-AAC sentence sets.

² 16-way Holm-Bonferroni correction for multiple comparisons (corresponding to the 16 gesture categories).

Supplementary Table S5. Comparisons for acoustic approach to avatar animation.

Articulator	Dataset 1	Dataset 2	Statistic ¹	Corrected P-value ²
Lower lip push	1024-word-General	1024-word-General Chance	0.00e+00	3.05e-05
Lower lip push	50-phrase-AAC	50-phrase-AAC Chance	0.00e+00	9.77e-04
Lower lip push	529-phrase-AAC	529-phrase-AAC Chance	0.00e+00	9.77e-04
Pinching	1024-word-General	1024-word-General Chance	6.00e+00	3.05e-05
Pinching	50-phrase-AAC	50-phrase-AAC Chance	0.00e+00	9.77e-04
Pinching	529-phrase-AAC	529-phrase-AAC Chance	0.00e+00	9.77e-04
Upper lip pull	1024-word-General	1024-word-General Chance	0.00e+00	3.05e-05
Upper lip pull	50-phrase-AAC	50-phrase-AAC Chance	0.00e+00	9.77e-04
Upper lip pull	529-phrase-AAC	529-phrase-AAC Chance	0.00e+00	9.77e-04
Lip flare	1024-word-General	1024-word-General Chance	0.00e+00	3.05e-05
Lip flare	50-phrase-AAC	50-phrase-AAC Chance	0.00e+00	9.77e-04
Lip flare	529-phrase-AAC	529-phrase-AAC Chance	0.00e+00	9.77e-04
Lower lip pull	1024-word-General	1024-word-General Chance	0.00e+00	3.05e-05
Lower lip pull	50-phrase-AAC	50-phrase-AAC Chance	0.00e+00	9.77e-04
Lower lip pull	529-phrase-AAC	529-phrase-AAC Chance	0.00e+00	9.77e-04
Jaw opening	1024-word-General	1024-word-General Chance	0.00e+00	3.05e-05
Jaw opening	50-phrase-AAC	50-phrase-AAC Chance	0.00e+00	9.77e-04
Jaw opening	529-phrase-AAC	529-phrase-AAC Chance	0.00e+00	9.77e-04
Tongue body raise	1024-word-General	1024-word-General Chance	0.00e+00	3.05e-05
Tongue body raise	50-phrase-AAC	50-phrase-AAC Chance	0.00e+00	9.77e-04
Tongue body raise	529-phrase-AAC	529-phrase-AAC Chance	0.00e+00	9.77e-04
Retraction	1024-word-General	1024-word-General Chance	0.00e+00	3.05e-05
Retraction	50-phrase-AAC	50-phrase-AAC Chance	0.00e+00	9.77e-04
Retraction	529-phrase-AAC	529-phrase-AAC Chance	0.00e+00	9.77e-04
Nostril flare	1024-word-General	1024-word-General Chance	0.00e+00	3.05e-05
Nostril flare	50-phrase-AAC	50-phrase-AAC Chance	0.00e+00	9.77e-04
Nostril flare	529-phrase-AAC	529-phrase-AAC Chance	0.00e+00	9.77e-04
Tongue tip raise	1024-word-General	1024-word-General Chance	0.00e+00	3.05e-05
Tongue tip raise	50-phrase-AAC	50-phrase-AAC Chance	0.00e+00	9.77e-04
Tongue tip raise	529-phrase-AAC	529-phrase-AAC Chance	0.00e+00	9.77e-04
Compression	1024-word-General	1024-word-General Chance	0.00e+00	3.05e-05
Compression	50-phrase-AAC	50-phrase-AAC Chance	0.00e+00	9.77e-04
Compression	529-phrase-AAC	529-phrase-AAC Chance	0.00e+00	9.77e-04
Tongue advance	1024-word-General	1024-word-General Chance	0.00e+00	3.05e-05
Tongue advance	50-phrase-AAC	50-phrase-AAC Chance	0.00e+00	9.77e-04
Tongue advance	529-phrase-AAC	529-phrase-AAC Chance	0.00e+00	9.77e-04
Tongue retraction	1024-word-General	1024-word-General Chance	1.00e+00	3.05e-05
Tongue retraction	50-phrase-AAC	50-phrase-AAC Chance	0.00e+00	9.77e-04
Tongue retraction	529-phrase-AAC	529-phrase-AAC Chance	0.00e+00	9.77e-04
Adduction	1024-word-General	1024-word-General Chance	0.00e+00	3.05e-05
Adduction	50-phrase-AAC	50-phrase-AAC Chance	0.00e+00	9.77e-04
Adduction	529-phrase-AAC	529-phrase-AAC Chance	0.00e+00	9.77e-04
Lower lip tuck	1024-word-General	1024-word-General Chance	0.00e+00	3.05e-05
Lower lip tuck	50-phrase-AAC	50-phrase-AAC Chance	0.00e+00	9.77e-04
Lower lip tuck	529-phrase-AAC	529-phrase-AAC Chance	0.00e+00	9.77e-04
Rounding	1024-word-General	1024-word-General Chance	0.00e+00	3.05e-05
Rounding	50-phrase-AAC	50-phrase-AAC Chance	0.00e+00	9.77e-04
Rounding	529-phrase-AAC	529-phrase-AAC Chance	0.00e+00	9.77e-04

¹ Each comparison is a two-sided Wilcoxon signed-rank test between correlations from real-time decoded articulatory gestures (generated using the acoustic approach) and reference gestures across n=20 pseudo-blocks for the 1024-word-General sentence set and n=15 pseudo-blocks for the 50-phrase-AAC and 529-phrase-AAC sentence sets.

² 16-way Holm-Bonferroni correction for multiple comparisons (corresponding to the 16 gesture categories).

Supplementary Table S6. Comparisons for dlib traces with the acoustic approach.

Articulator	Dataset 1	Dataset 2	Statistic ¹	Corrected P-value ²
Jaw	Avatar-Person	Person-Person	4.09e+04	8.36e-01
Jaw	Avatar-Person	Chance, Avatar-Person	2.30e+04	2.00e-49
Jaw	Person-Person	Chance, Person-Person	2.56e+05	1.62e-114
Lip aperture	Avatar-Person	Person-Person	4.23e+04	7.88e-01
Lip aperture	Avatar-Person	Chance, Avatar-Person	2.30e+04	2.36e-49
Lip aperture	Person-Person	Chance, Person-Person	2.58e+05	3.95e-119
Mouth width	Avatar-Person	Person-Person	3.64e+04	1.89e-01
Mouth width	Avatar-Person	Chance, Avatar-Person	2.22e+04	1.67e-43
Mouth width	Person-Person	Chance, Person-Person	2.58e+05	2.40e-118

¹ Each comparison is a two-sided Mann-Whitney U-test between dlib facial-landmark feature correlations for the avatar (decoded using the acoustic approach) and healthy-speaker videos, with n=19 pseudo-blocks for each of the 8 speakers (yielding 152 data points for avatar-person comparisons) and n=19 pseudo-blocks for each of the 28 combinations of pairs of speakers (yielding 532 data points for person-person comparisons).

² 9-way Holm-Bonferroni correction for multiple comparisons.

Supplementary Table S7. Exclusion comparisons between anatomical regions.

Task ¹	Region excluded 1	Region excluded 2	Statistic ²	Corrected P-value ³
Text WER	SMC	temporal lobe	0.00e+00	8.94e-07
Text WER	SMC	chance	8.00e+00	1.04e-05
Text WER	SMC	none	0.00e+00	8.94e-07
Text WER	SMC	postcentral	0.00e+00	8.94e-07
Text WER	SMC	precentral	0.00e+00	8.94e-07
Text WER	temporal lobe	chance	0.00e+00	8.94e-07
Text WER	temporal lobe	none	8.90e+01	1.65e-01
Text WER	temporal lobe	postcentral	9.10e+01	1.65e-01
Text WER	temporal lobe	precentral	7.30e+01	5.89e-02
Text WER	chance	none	0.00e+00	8.94e-07
Text WER	chance	postcentral	0.00e+00	8.94e-07
Text WER	chance	precentral	0.00e+00	8.94e-07
Text WER	none	postcentral	2.40e+01	2.63e-03
Text WER	none	precentral	1.10e+01	4.29e-04
Text WER	postcentral	precentral	9.50e+01	3.06e-01
Synthesis MCD	SMC	temporal lobe	0.00e+00	2.86e-05
Synthesis MCD	SMC	chance	0.00e+00	2.86e-05
Synthesis MCD	SMC	none	0.00e+00	2.86e-05
Synthesis MCD	SMC	postcentral	1.00e+00	2.86e-05
Synthesis MCD	SMC	precentral	6.00e+00	1.07e-04
Synthesis MCD	temporal lobe	chance	0.00e+00	2.86e-05
Synthesis MCD	temporal lobe	none	1.00e+00	2.86e-05
Synthesis MCD	temporal lobe	postcentral	9.40e+01	7.01e-01
Synthesis MCD	temporal lobe	precentral	4.80e+01	6.55e-02
Synthesis MCD	chance	none	0.00e+00	2.86e-05
Synthesis MCD	chance	postcentral	0.00e+00	2.86e-05
Synthesis MCD	chance	precentral	0.00e+00	2.86e-05
Synthesis MCD	none	postcentral	0.00e+00	2.86e-05
Synthesis MCD	none	precentral	0.00e+00	2.86e-05
Synthesis MCD	postcentral	precentral	3.20e+01	1.46e-02
NATO code-word accuracy	SMC	temporal lobe	0.00e+00	3.81e-05
NATO code-word accuracy	SMC	none	0.00e+00	3.81e-05
NATO code-word accuracy	SMC	postcentral	0.00e+00	3.81e-05
NATO code-word accuracy	SMC	precentral	0.00e+00	3.81e-05
NATO code-word accuracy	temporal lobe	none	1.50e+01	7.15e-01
NATO code-word accuracy	temporal lobe	postcentral	8.00e+00	1.35e-02
NATO code-word accuracy	temporal lobe	precentral	8.50e+00	2.01e-02
NATO code-word accuracy	none	postcentral	7.00e+00	3.21e-02
NATO code-word accuracy	none	precentral	5.00e+00	1.25e-02
NATO code-word accuracy	postcentral	precentral	5.40e+01	7.28e-01
Avatar DTW mean correlation	SMC	temporal lobe	5.09e+03	7.37e-01
Avatar DTW mean correlation	SMC	chance	3.14e+02	5.11e-23
Avatar DTW mean correlation	SMC	none	1.54e+03	3.96e-14
Avatar DTW mean correlation	SMC	postcentral	4.82e+03	4.07e-01
Avatar DTW mean correlation	SMC	precentral	4.82e+03	4.07e-01
Avatar DTW mean correlation	temporal lobe	chance	0.00e+00	1.62e-25
Avatar DTW mean correlation	temporal lobe	none	4.07e+03	9.30e-03
Avatar DTW mean correlation	temporal lobe	postcentral	5.36e+03	1.00e+00
Avatar DTW mean correlation	temporal lobe	precentral	5.76e+03	1.00e+00
Avatar DTW mean correlation	chance	none	4.80e+01	3.90e-25
Avatar DTW mean correlation	chance	postcentral	1.81e+02	4.45e-24
Avatar DTW mean correlation	chance	precentral	5.10e+01	3.90e-25
Avatar DTW mean correlation	none	postcentral	2.30e+03	8.65e-10
Avatar DTW mean correlation	none	precentral	3.39e+03	6.48e-05
Avatar DTW mean correlation	postcentral	precentral	5.75e+03	1.00e+00

¹ Abbreviations: Word error rate (WER); Sensorimotor cortex (SMC); Mel-cepstral distortion (MCD); Mean DTW correlation between facial landmarks from video of avatar and healthy speakers (r) (Avatar DTW mean correlation)

² Each comparison is a two-sided Wilcoxon signed-rank test between n=25 text WER pseudoblocks, n=20 synthesis pseudoblocks, n=152 avatar comparisons (19 pseudo-blocks for 8 healthy speakers), or n=19 NATO blocks

³ 15-way Holm-Bonferroni correction for multiple comparisons. 10-way Holm-Bonferroni for NATO code-word accuracy

Supplementary Table S8. Exclusion comparisons between electrode densities.

Task ¹	Density 1	Density 2	Statistic ²	P-value ³
Text WER	chance	high density	0.00e+00	1.79e-07
Text WER	chance	low density	0.00e+00	1.79e-07
Text WER	high density	low density	2.40e+01	3.18e-04
Synthesis MCD	chance	high density	0.00e+00	5.72e-06
Synthesis MCD	chance	low density	0.00e+00	5.72e-06
Synthesis MCD	high density	low density	9.00e+00	6.29e-05
Avatar DTW mean correlation	chance	high density	4.80e+01	5.57e-26
Avatar DTW mean correlation	chance	low density	1.90e+01	4.72e-26
Avatar DTW mean correlation	high density	low density	4.34e+03	6.59e-03

¹ Abbreviations: Word error rate (WER); Mel-cepstral distortion (MCD); Mean DTW correlation between facial landmarks from video of avatar and healthy speakers (r) (Avatar DTW mean correlation)

² Each comparison is a two-sided Wilcoxon signed-rank test between $n=25$ text pseudoblocks, $n=20$ synthesis pseudoblocks, or $n=152$ avatar comparisons (19 pseudo-blocks for 8 healthy speakers)

³ 3-way Holm-Bonferroni correction for multiple comparisons.

Supplementary Table S9. User experience survey.

Modality	Participant feedback ¹
Text decoding	<p>”Text decoding is the building blocks of the speech synthesis and the avatar, it may be less exciting but it is necessary. We experimented doing free-style and I can see it as helpful. I personally took online university courses and it would be very helpful when writing papers. I had a fifteen page paper once and the text decoder would have helped so much. The ideal scenario is for the connection to be cordless.”</p>
Speech synthesis	<p>”First, the simple fact of hearing a voice similar to your own is emotional. Being able to have the ability to speak aloud is very important. The first 7 years after my stroke, all I used was a letterboard. My husband was so sick of having to get up and translate the letterboard for me. We didn’t argue because he didn’t give me a chance to argue back. As you can imagine, this frustrated me greatly! When I had the ability to talk for myself was huge! Again, the ideal situation would be for it to be wireless. Being able to speak free-style would be ideal also.”</p>
Avatar control	<p>”Before the study started I was asked for my moonshot. My moonshot was to become a counselor and use the system to talk to my clients. I think the avatar would make them more at ease.”</p>

¹ The participant was asked for her general feedback for each modality. She used a Tobii Dynavox to compose written feedback.

Supplementary Table S10. Text RNN neural-decoding model hyperparameter values.

Sentence set	Hyperparameter description	Final Value
1024-word-General sentence set	Kernel size (and stride)	4
	Number of GRU layers	3
	Hidden units per GRU layer	500
	Dropout	0.4
	Jitter amount j	0.5
	Additive noise level σ_n	0.0027
	Scale min α_{min}	0.955
	Scale max α_{max}	1.07
	Max temporal mask length b	0.871
	Temporal mask probability p	0.0478
	Channel-wise noise σ_{ch}	0.0283
50-phrase-AAC and 529-phrase-AAC sentence sets	Kernel size (and stride)	2
	Number of GRU layers	3
	Hidden units per GRU layer	512
	Dropout	0.6

Supplementary Table S11. NATO code word and hand-motor movement decoder hyperparameters.

Hyperparameter description	Final Value
Kernel size (and stride)	4
Number of GRU layers	2
Hidden units per GRU layer	274
Dropout	0.545
Jitter amount j	.237
Additive noise level σ_n	0.0027
Scale min α_{min}	0.955
Scale max α_{max}	1.07
Max temporal mask length b	0.871
Temporal mask probability p	0.0478
Channel-wise noise σ_{ch}	0.0283

Supplementary Table S12. Speech synthesis RNN neural-decoding model hyperparameters.

Sentence set	Hyperparameter description	Final Value
1024-word-General	Kernel size (and stride)	6
	Number of GRU layers	3
	Hidden units per GRU layer	260
	Dropout	0.7
	Batch size	16
529-phrase-AAC and 50-phrase-AAC	Kernel size (and stride)	6
	Number of GRU layers	3
	Hidden units per GRU layer	260
	Dropout	0.7
	Batch size	64

Supplementary Table S13. Articulatory gesture descriptions.

Articulatory gesture	Description
Tongue tip raise	Raise the tip of the tongue
Tongue retraction	Retraction of the tongue
Tongue body raise	Raise the body portion of tongue
Tongue advance	Tongue extends out of the mouth
Rounding	Lips are puckered
Pinching	Mouth corners are pressed and pulled back
Nostril flare	Nostrils open (e.g during a breath)
Upper lip pull	Upper lip is pulled upward
Lower lip tuck	Lower lip is tucked over teeth, as in during an F
Lower lip push	Lower lip pushed upward by movement in chin
Lower lip pull	Lower lip pulled down and gums exposed
Lip flare	Lips move to make 'SH' sound
Jaw opening	Opening of the jaw
Compression	Lips pursed without protrusion
Adduction	Upper lips rolls down and in, as in during an 'M' sound

¹ Reference articulatory gestures sampled at 100 Hz and generate via Speech Graphics' SG Com acoustic-to-articulatory inversion model.

² The gestures are continuous-valued activations of muscle movements that correspond to the degree each gesture is activated.

Supplementary Table S14. Avatar CTC decoding hyperparameters.

Sentence set	Hyperparameter description	Final Value
1024-word-General	Kernel size (and stride)	2
	Number of GRU layers	3
	Hidden units per GRU layer	256
	Dropout	0.3
529-phrase-AAC	Kernel size (and stride)	2
	Number of GRU layers	3
	Hidden units per GRU layer	256
	Dropout	0.7
50-phrase-AAC	Kernel size (and stride)	2
	Number of GRU layers	3
	Hidden units per GRU layer	256
	Dropout	0.7
All sets	Additive noise level σ_n	0.0027
	Scale min α_{min}	0.955
	Scale max α_{max}	1.07
	Max temporal mask length b	0.871
	Temporal mask probability p	0.0478
	Channel-wise noise σ_{ch}	0.0283
	Weight decay	1e-5

Supplementary references

1. Metzger, S. L. et al. Generalizable spelling using a speech neuroprosthesis in an individual with severe limb and vocal paralysis. *Nature Communications* **13**, 1–15 (2022).
2. Moses, D. A. et al. Neuroprosthesis for decoding speech in a paralyzed person with anarthria. *New England Journal of Medicine* **385**, 217–227 (2021).
3. Park, K. & Kim, J. g2pE <https://github.com/Kyubyong/g2p>. 2019.
4. Graves, A., Fernández, S., Gomez, F. & Schmidhuber, J. Connectionist temporal classification: labelling unsegmented sequence data with recurrent neural networks in *Proceedings of the 23rd international conference on Machine learning* (2006), 369–376.
5. Chung, J., Gulcehre, C., Cho, K. & Bengio, Y. Empirical evaluation of gated recurrent neural networks on sequence modeling. *arXiv preprint arXiv:1412.3555* (2014).
6. Loshchilov, I. & Hutter, F. Fixing Weight Decay Regularization in Adam. *CoRR abs/1711.05101*. [arXiv: 1711.05101](http://arxiv.org/abs/1711.05101). <http://arxiv.org/abs/1711.05101> (2017).
7. Yang, Y.-Y. et al. Torchaudio: Building blocks for audio and speech processing in *ICASSP 2022-2022 IEEE International Conference on Acoustics, Speech and Signal Processing (ICASSP)* (2022), 6982–6986.
8. Ney, H., Essen, U. & Kneser, R. On structuring probabilistic dependences in stochastic language modelling. *Computer Speech & Language* **8**, 1–38 (1994).
9. Kingma, D. P. & Ba, J. Adam: A method for stochastic optimization. *arXiv preprint arXiv:1412.6980* (2014).
10. Srivastava, N., Hinton, G., Krizhevsky, A., Sutskever, I. & Salakhutdinov, R. Dropout: a simple way to prevent neural networks from overfitting. *The journal of machine learning research* **15**, 1929–1958 (2014).
11. Hsu, W.-N. et al. Hubert: Self-supervised speech representation learning by masked prediction of hidden units. *IEEE/ACM Transactions on Audio, Speech, and Language Processing* **29**, 3451–3460 (2021).
12. Lakhotia, K. et al. On generative spoken language modeling from raw audio. *Transactions of the Association for Computational Linguistics* **9**, 1336–1354 (2021).
13. Ott, M. et al. fairseq: A Fast, Extensible Toolkit for Sequence Modeling in *Proceedings of NAACL-HLT 2019: Demonstrations* (2019).
14. Berger, M. A., Hofer, G. & Shimodaira, H. Carnival—combining speech technology and computer animation. *IEEE computer graphics and applications* **31**, 80–89 (2011).
15. Van den Oord, A., Vinyals, O. & Kavukcuoglu, K. Neural Discrete Representation Learning. *CoRR abs/1711.00937*. [arXiv: 1711.00937](http://arxiv.org/abs/1711.00937). <http://arxiv.org/abs/1711.00937> (2017).
16. King, D. E. Dlib-ml: A Machine Learning Toolkit. *Journal of Machine Learning Research* **10**, 1755–1758 (2009).
17. Salvador, S. & Chan, P. Toward accurate dynamic time warping in linear time and space. *Intelligent Data Analysis* **11**, 561–580 (2007).

- 821 18. Hullett, P. W., Hamilton, L. S., Mesgarani, N., Schreiner, C. E. & Chang, E. F. Human
822 superior temporal gyrus organization of spectrotemporal modulation tuning derived
823 from speech stimuli. *The Journal of Neuroscience* **36**, 2014–2026 (2016).

A high-performance neuroprosthesis for speech decoding and avatar control

This supplemental file contains the following items relating to the clinical-trial protocol registered on ClinicalTrials.gov (with ID NCT03698149), which the present work was performed under:

1. Original protocol (registered on October 4, 2018)
2. Final protocol (updated on August 23, 2022)
3. Summary of changes between the final and original protocols
4. Note about the exploratory nature of the clinical trial

CLINICAL PROTOCOL (original)

Title: A High-Performance ECoG-based Neural Interface for Communication and Neuroprosthetic Control

Study Sponsors/Investigators:

Redacted

Protocol Synopsis

Title	A High-Performance ECoG-based Neural Interface for Communication and Neuroprosthetic Control
Study Phase	Phase I
Device(s)	<p>Device Information: Devices to be used in this study are grouped below according to FDA approval.</p> <p>Cleared for temporary (<30 days) recording and monitoring of brain electrical activity under 510k:</p> <ul style="list-style-type: none"> • NeuroPort Array, PN 6248 (K070272, K110010) • NeuroPort System, PN 5416 (K060523, K090957) <p>Cleared for temporary (<30 day) use with recording, monitoring, and stimulation equipment for the recording, monitoring and stimulation of electrical signals on the surface of the brain under 510k:</p> <ul style="list-style-type: none"> • PMT Subdural Cortical Electrodes, Model #2110TX-128-005 (K082474) <p>The Blackrock Microsystems Neuroport Array connector pedestal, a subcomponent of the Blackrock Microsystems NeuroPort Array, will be laser bonded to the PMT Subdural Cortical Electrode by Blackrock Microsystems. As documented below, this specific approach has already been tested in non-human primates (over at least an 18-month period, see below regarding published report).</p> <p>Request for off-label use of the combined investigational device for 1 year, for the equivalent indication of recording and monitoring of brain electrical activity.</p>
Indication	Adults with neurological disorders (e.g. amyotrophic lateral sclerosis/ALS, spinal cord injury, multiple sclerosis, stroke) often develop disorders of movement and communication. We aim to determine the feasibility of ECoG based brain computer interface control of complex neuroprosthetic devices.
Sponsor Contacts	*Redacted*
Data Safety Monitor Board (DSMB)	*Redacted*

<p>Treatment</p>	<p>The Blackrock Microsystems NeuroPort Array connector pedestal, NeuroPort System, and PMT Subdural Cortical Electrodes are currently cleared for monitoring of patients for up to 30 days. Here we to aim to use these systems combined for at least a 1-year period in subjects with neurological illness and disorders of communication to test feasibility for both neuroprosthetic control and for decoding speech from neural activity.</p>
<p>Study Sites</p>	<ul style="list-style-type: none"> • *Redacted*
<p>Study Design</p>	<p>This is a single-center early feasibility study of the use of an ECoG-based neural interface for testing the feasibility of using ECoG signals to control complex devices for motor and speech control in adults affected by neurological disorders of movement.</p> <p>A PMT Subdural Cortical Electrode array, bonded to the Blackrock Microsystems NeuroPort Array pedestal, will be surgically placed directly on the brain surface over the motor and language cortices of subjects with disorders of motor control. After implantation of the electrode and pedestal, the Neuroport Biopotential Processing System will be connected to the Neuroport Array pedestal to monitor and record neural signals. With this ECoG-based neural interface, study patients will undergo training and assessment of their ability to control a wearable hand robotic exoskeleton and to determine if ECoG brain signals can be decoded for language communication. This will be performed in two phases.</p> <p><u>Phase 1: Optimize BCI system</u></p> <p>In Phase 1, we will optimize the entire system to reliably detect neural activity to ensure that the recorded signals are stable and free of artifacts. Moreover, we will ensure that the neural signals are converted in real-time into cursor movements. During this phase, we will primarily examine cursor based control, decoding of parameters and ‘disembodied’ control (i.e. the subjects’ arm will not interact with the mechanical system). This phase will be conducted in the outpatient office setting and/or the patient’s home environment, based on patient preference and needs. We anticipate that this phase will take approximately 1 month; however, this may be longer or shorter for each subject depending on the level of control achieved.</p> <p><u>Phase 2: Testing of BCI Control</u></p> <p>In Phase 2, we will test feasibility for both neuroprosthetic control and for decoding speech from neural activity. We will begin to perform experimental testing with the system for control of a custom wearable hand exoskeleton robot that</p>

	<p>meets criteria for a non-significant risk device. As outlined in the sections below, we have multiple safety features to ensure that there is minimal risk for injury during the embodiment phase (i.e. the subjects arm is interacting with the exoskeleton). Throughout this period, neural signals will be recorded and analyzed, and tasks will be performed toward the development, assessment, and improvement of the neural interface system. We will assess quality of performance using kinematic parameters while performing required tasks. We will analyze stability of neural recordings and performance. To measure stability of the neural representation we will analyze the neural correlates of imagined movements. We will also assess changes in spatial correlation scales and other redundancy measures during learning and stable performance. We anticipate that testing will be conducted in the outpatient office or home setting based on the patient's preference and needs.</p> <p>In this phase, we will also continue to perform experimental testing with the system for control of a virtual communicating interface. Throughout this period, neural signals will be recorded and analyzed, and tasks will be performed toward the development, assessment, and improvement of the communication interface.</p>
<p>Objectives</p>	<p>In eight patients with severe disorders of movement control, we will surgically implant PMT Subdural Cortical Electrodes on the brain surface over the motor and language cortices. The electrode will be bonded to a Blackrock Neuroport Array pedestal, which can be connected to the NeuroPort System in order to process and record neural activity in real time. Using this neural interface, we will condition the patient to be able to control a wearable hand robotic exoskeleton, communicate with a computer system for typing and perform speech output tasks. We will utilize optimal neural plasticity mechanisms, a novel decoder framework, and advanced language modeling during BCI conditioning.</p> <p>Hypothesis: The underlying hypothesis is that ECoG recordings will allow severely paralyzed individuals to skillfully control complex neuroprosthetic devices for movement and communication. A closely related hypothesis is that the well-known stability of ECoG signals will allow us to maximally engage neural mechanism of plasticity and thereby optimize long-term skilled acquisition.</p>
<p>Patient Population</p>	<p>Study subjects will be adults with severe motor impairment secondary to a neurological disorder.</p>

Inclusion Criteria

- Age > 21
- Limited ability to use upper limbs, based on neurological examination, due to stroke, amyotrophic lateral sclerosis (ALS), multiple sclerosis, cervical spinal cord injury, brainstem stroke, muscular dystrophy, myopathy or severe neuropathy
- Disability, defined by a 4 or greater score on the Modified Rankin Scale, must be severe enough to cause loss of independence and inability to perform activities of daily living.
- If stroke or spinal cord injury, at least 1 year has passed since onset of symptoms
- Must live within a two-hour drive of UCSF

Exclusion Criteria

- Pregnancy or breastfeeding
- Inability to understand and/or read English
- Inability to give consent
- Dementia, based on history, physical exam, and MMSE
- Active depression (BDI > 20) or other psychiatric illness (active general anxiety disorder, schizophrenia, bipolar disorder, obsessive-compulsive disorder (OCD), or personality disorders (e.g. multiple personality disorder, borderline personality disorder, etc.)
- History of suicide attempt or suicidal ideation
- History of substance abuse
- Co-morbidities including ongoing anticoagulation, uncontrolled hypertension, cancer, or major organ system failure
- Inability to comply with study follow-up visits
- Any prior intracranial surgery
- History of seizures
- Immunocompromised
- Has an active infection
- Has a CSF drainage system or an active CSF leak
- Requires diathermy, electroconvulsive therapy (ECT), or transcranial magnetic stimulation (TMS) to treat a chronic condition
- Has an implanted electronic device such as a neurostimulator, cardiac pacemaker/defibrillator or medication pump
- Allergies or known hypersensitivity to materials in the Blackrock NeuroPort Array pedestal (i.e. silicone, titanium) or the PMT Subdural Cortical Electrode (silicone, platinum iridium, nichrome)

Sample Size	8 patients
Efficacy Assessments	<u>Primary Endpoints:</u> Feasibility of control of a wearable exoskeleton device and a communication interface.
Safety Assessments	<ul style="list-style-type: none"> • Physical examination at all study visits • Perform functional test of the PMT/Blackrock combined neural interface system prior to implantation • Surgical/ or nonsurgical protocol-defined adverse events recorded on adverse events case report forms and use of protocol-defined procedures for adverse event management • Assessment of suicidality using Columbia Suicide Severity Rating Scale, and assessment of changes using the Beck Depression and Anxiety Inventories, <u>at monthly intervals.</u>

1.0 Patient Eligibility

Study subjects will be adults with severe motor impairment secondary to a neurological disorder.

Inclusion Criteria

- Age > 21
- Limited ability to use upper limbs, based on neurological examination, due to stroke, amyotrophic lateral sclerosis (ALS), multiple sclerosis, cervical spinal cord injury, brainstem stroke, muscular dystrophy, myopathy or severe neuropathy
- Disability, defined by a 4 or greater score on the Modified Rankin Scale, must be severe enough to cause loss of independence and inability to perform activities of daily living.
- If stroke or spinal cord injury, at least 1 year has passed since onset of symptoms
- Must live within a two-hour drive of UCSF

Exclusion Criteria

- Pregnancy or breastfeeding
- Inability to understand and/or read English
- Inability to give consent
- Dementia, based on history, physical exam, and MMSE
- Active depression (BDI > 20) or other psychiatric illness (active general anxiety disorder, schizophrenia, bipolar disorder, obsessive-compulsive disorder (OCD), or personality disorders (e.g. multiple personality disorder, borderline personality disorder, etc.)
- History of suicide attempt or suicidal ideation
- History of substance abuse
- Co-morbidities including ongoing anticoagulation, uncontrolled hypertension, cancer, or major organ system failure
- Inability to comply with study follow-up visits
- Any prior intracranial surgery
- History of seizures
- Immunocompromised
- Has an active infection
- Has a CSF drainage system or an active CSF leak
- Requires diathermy, electroconvulsive therapy (ECT), or transcranial magnetic stimulation (TMS) to treat a chronic condition
- Has an implanted electronic device such as a neurostimulator, cardiac pacemaker/defibrillator or medication pump
- Allergies or known hypersensitivity to materials in the Blackrock NeuroPort Array pedestal (i.e. silicone, titanium) or the PMT Subdural Cortical Electrode (silicone, platinum iridium, nichrome)

2.0 Study Device(s)

Cleared for same indication with off-label use of device for at least 1 year:

- Blackrock NeuroPort Array, PN 6248
- Blackrock NeuroPort System, PN 5416
- PMT Subdural Cortical Electrodes, Model #2110TX-128-005

3.0 Study Procedure

Study Duration: The duration of this pilot study will be 6 years. We expect that all 8 patients will be recruited in the first 4-5 years, and data collection, device development and analysis will be completed in 6 years.

Patient recruitment and clinical characterization: Patients with motor impairments secondary to neurological disorders will be recruited from clinics specializing in the treatment of stroke, ALS, and general neurological disorders, at UCSF and the San Francisco VA Medical Center.

Enrollment procedures: Prior to enrollment into the study, an informal phone interview to schedule an office-based evaluation will take place, followed by three outpatient screening visits. During the first outpatient visit we will describe the trial in detail and answer all questions. Should the participant choose to continue, we will schedule another visit to conduct a physical exam and to perform screening labs to determine eligibility. During this visit we will screen for eligibility by 1) acquiring patient demographics, 2) reviewing medical history and measuring vital signs, 3) ensuring patients are not currently pregnant or plan to become pregnant, 4) obtaining a list of current medications being taken, 5) ensuring MMSE scores are within a reasonable range (≥ 18 , also accounting for motor difficulties with taking the test), 6) obtain baseline patient-rated and investigator rated clinical global impression scales, 7) assess baseline health status with SF-36 Health Survey, 8) assess current depression and anxiety states with Beck Depression and Anxiety inventories (BDI and BAI, respectively), 9) determine suicidal ideation risk is minimal with Columbia Suicide Severity Rating Scale (C-SSRS) 10) perform a baseline neurological physical exam and 11) determine the disability rating using the modified Rankin Scale. An MRI and CT of the brain will also be obtained for future surgical planning and to further determine eligibility. Moreover, a ECG and chest x-ray will also be obtained. We will then schedule a third follow-up visit to review this data and to answer remaining questions.

Pre-operative care: Subjects will be administered Kefzol 2g IV within 60 minutes prior to surgical incision, and continued for 24 hours post-operatively. In case of allergy to Kefzol, Vancomycin 1gm IV will be used.

Surgery: After obtaining informed consent, subjects will undergo brief general anesthesia (typically ~ 3-4 hours) for the surgical procedure. This may be either IV or inhaled anesthetics. Patient will be given IV antibiotics prior to incision, and re-dosed if required. Induction and wake-up will take place in the operating room, and patients will be monitored in the post-anesthesia care unit (PACU) after surgery for 2-3 hours during the peri-operative period. Subject will then continue to recover on the surgical ward for 2 days.

Subjects will undergo surgical placement of an ECoG array over the nondominant (usually right-sided) sensorimotor and speech cortices. The basic operative procedure is similar to what is commonly performed for non-penetrating subdural grid placement in patients with intractable epilepsy, which is well tolerated and has few complications [35]. This surgery will be smaller in exposure given that coverage will be limited to the regions of interest, and

not broadly applied as used for epilepsy localization. Standard procedures for craniotomy at the surgical site will be followed. Briefly, a 5-6 cm curvilinear incision will be made over the anatomic hand representation of the cortex (i.e. "hand knob") which is located 3 cm lateral to the midline. Localization will be confirmed using intraoperative Brainlab stereotactic neuronavigation. A craniotomy will then be performed, exposing the dural surface. A wide slit in the dura will be opened.

After identifying the location for the electrode grid implant, the position for the pedestal connector is determined on the adjacent or contra-lateral skull surface and marked. A separate 2 cm scalp incision will be made for the pedestal connector. Holes will be drilled for connector placement and the connector will be secured to the skull with 8 small titanium screws. Once the connector is placed, the electrodes and wire bundle are gently manipulated to position the electrodes so that they are resting on the cortical surface over the area of interest. The nonpenetrating ECoG microarray will be sutured to the dura to secure its position. After successful placement of the electrode grid, the dura will be sutured closed in a watertight fashion and the bone flap will be replaced and secured in place with a standard titanium cranial fixation plates and screws.

The surgical site will be irrigated with antibiotic lactated ringers solution. The fascia and skin will be closed with absorbable sutures over the covered craniotomy with a slit accommodating the passage of the connector. The wound will be dressed with a sealed surgical bandage. The expected blood loss for this procedure is 50 cc. The expected operative time is 3-6 hours.

The ECoG electrode array is manufactured by PMT Corporation, and is already FDA-cleared for temporary (<30 days) clinical monitoring of neural signals (K082474). The PMT Subdural Cortical Electrodes are a chronically implantable array containing 128 electrodes, with an electrode spacing of 4 mm, capable of recording from areas of the central nervous system for extended periods of time. The electrode contacts are composed of medical grade platinum iridium, and embedded in a thin sheet of medical grade silastic. The model number 2110 indicates a platinum iridium wire and platinum iridium contacts. Platinum iridium is a mechanically robust alloy electrode material used in commercial DBS leads (Petrossians, Whalen and Weiland 2016). The electrodes' contacts are molded into a silicone rubber matrix in a fixed pattern. This identical electrode is used routinely at our institution and others for seizure localization. In the past ten years, we have not encountered any adverse inflammatory reactions or bleeding specific to the electrode arrays itself (over 100 cases). Insulated wires extend from each electrode through a flexible silicone tube to the connector on the pedestal.

Post-Operative Care: Subjects will be recovered in the intensive care unit and observed for 24 hours before transferring to the ward. A postoperative head CT will be obtained to evaluate for any hemorrhage and to confirm the position of the array. IV antibiotics (Kefzol will be used if there are no allergies) will be administered for 24 hours after surgery, followed by prophylactic antibiotics given up to suture removal plus 2 days. Patients will be switched to oral antibiotics as soon as possible. Subjects will undergo physical exam every day with monitoring of vital signs, neurological exam, and basic respiratory, cardiac, and gastrointestinal exams. In addition, the wound site will be inspected at all study visits.

Routine hygiene will consist of handwashing with soap/water and donning gloves using sterile technique when coming in contact with the percutaneous connector. The caregiver

and patient will be trained to clean the pedestal site according to specific instructions that will be given to them, to be performed at least once every seven days or as required.

An infection control protocol will be strictly followed. At early signs of infection or irritation the patient/caregiver should contact the study physician immediately. The surgical site will need to be cleaned twice or more during the day, while using extra meticulous hand hygiene. If skin erythema, edema, pain and/or warmth are present, the available drainage will be cultured and oral antibiotics will be started. Plain radiographs of the involved area, ESR, CRP, WBC, and blood cultures will be obtained. If there is no improvement within 72 hours, rapid progression of erythema, symptoms worsen, or if there are signs of systemic toxicity, parenteral antibiotics is warranted. If high fever or severe pain is present, nuchal rigidity, or progressive deterioration in level of consciousness, the participant should go to the hospital emergency room. All implanted hardware will be surgically removed if there is evidence of hardware infection.

Pain related to small craniotomies is usually self-limited. Pain scale ratings will be assessed every 4 hours and routine postoperative pain management will be used. This includes the following medications as needed: acetaminophen and/or Percocet (acetaminophen/hydrocodone). IV pain meds (morphine sulfate or dilaudid) will also be administered if needed. In our experience, most patients do not require IV analgesics beyond the first operative day for smaller craniotomies.

Study visits: As outlined above, system testing will occur through two phases. In the first phase, we will simply optimize the system; in the second phase, we will commence testing of the motor and communication neural interface systems.

In **Phase 1**, the main goal is to ensure reliable neural signal monitoring and optimization of the real-time systems. Initial study visits will occur at defined time points, similar to those normally used in clinical care. For example, we anticipate a visit at post-op day (POD) 10 and 14. During this time, we will simply monitor the neural signals and briefly test the real-time communication with the computer interface. We anticipate additional visits 1-3x/week, based on the patient's availability and preference, to continue to monitor signal stability and check for wound healing. During this phase, we will also offer in home testing of the system to minimize the burden. While the equipment may be kept at the subject's home, testing will only occur when study personnel are present. The total time period of Phase 1 will be approximately 1 months, the exact time will be customized for each patient.

In **Phase 2**, we will test feasibility for both neuroprosthetic control and for decoding speech from neural activity. We will begin to perform experimental testing with the system for control of a custom wearable hand exoskeleton robot that can be classified as a non-significant risk device. As shown in panel A, the exoskeleton system consists of a table top frame that allows x,y,z movement of the arm/hand (i.e. supported by a brace attached to the platform mount). Movements are limited to the natural workspace of each subject. The hand exoskeleton (panel B) will be mounted using a readily releasable magnetic mount. The hand system aims to allow control of the fingers and thumb using a motorized cable system attached to motors. This system will allow us to test restoration of reach to grasp functions in our subjects. As outlined in the Risk Analysis (Appendix D), we have multiple safety features to ensure that there is minimal risk for injury during the embodiment phase (i.e. the subjects interact with the exoskeleton).

Throughout this period, neural signals will be recorded and analyzed, and tasks will be performed toward the development, assessment, and improvement of the neural interface system. We will assess quality of performance using kinematic parameters while performing required tasks. We will analyze stability of neural recordings and performance. To measure stability of the neural representation we will analyze the neural correlates of imagined movements. We will also examine the stability of neural correlates on neuroprosthetic exoskeleton movements (e.g. spectral content, timing, spatial recruitment). We will assess changes in the spatial correlation scales and other redundancy measures during learning and stable performance. We anticipate that testing will be conducted in the outpatient office or home setting based on the patient's preference and needs.

In this phase, we will also continue to perform experimental testing with the system for control of a virtual communicating interface. Throughout this period, neural signals will be recorded and analyzed, and tasks will be performed toward the development, assessment, and improvement of the neural interface system. We will assess the ability to control a computer communication interface. To measure stability of the neural representation we will analyze the neural correlates of imagined speech. We will also examine the stability of neural correlates on a neuroprosthetic communication device (e.g. spectral content, timing, spatial recruitment).

Neural activity monitoring: Continuous neural signal data will be acquired from the 128-channel implanted PMT Subdural Cortical Electrodes and processed with the NeuroPort System hardware by Blackrock Microsystems. Broadly, the neural data will consist of ECoG neural activity from neurons in the vicinity of each recording electrode. The neural data will be actively monitored and recorded via the graphical user interface associated with the NeuroPort hardware commercially available via Blackrock. Data read and download are non-invasive and will be performed with the patient comfortably rested.

The NeuroPort System has been successfully deployed in monitoring neural activity in patients with motor control disorders (e.g. (Hochberg et al. 2012a, Pandarinath et al. 2015)). Blackrock Microsystems provides commercial software that allows real-time filtering, recording, and visualization of acquired neural data and also allows interfacing with other programming languages such as MATLAB (Mathworks, MA). Together, this allows the ability to create custom software such as communication device based on neural spiking activity, detailed further in the following section. Overall, the mix of commercial and custom software will allow for real-time signal processing, synchronization and control of the peripheral communication device, with parallel data streams to store data for offline analyses.

Online BMI control of a Wearable Hand Robotic Exoskeleton Device:

ECoG signals will be filtered and processed in real-time using a customized portable multi-channel neurophysiology workstation NeuroPort Biopotential Signal Processing System. We will bandpass each channel into multiple bands. Past experiments, including our own, suggest that movement related information is encoded in these bands.

Initialization Phase. We will use an adaptive filter to create a 'decoder' that maps neural activity to movement of the wearable exoskeleton device. Recent experiments suggest that such a filter can rapidly allow control of neuroprosthetic devices. We will train the filter

using ‘imagined movements’. As paretic/paralyzed patients will not have access to normal overt movement related neural signals, we will use the neural basis of imagined movements for training. We anticipate that during the initial training phase, the filter will establish a set of weights between the object and neural signals. During this training phase, patients will observe a computer cursor on a screen. In order to compare visual versus visual + proprioceptive/tactile feedback signals during decoder conditioning, we will use the exoskeleton setup for decoder conditioning. The arm and hand will move in a stereotyped fashion while the subjects are instructed to ‘imagine’ actively tracking its path. Of note, we have experience with similar control of an exoskeleton system ((Ganguly et al. 2011, Ganguly et al. 2009)). As prior and as outlined below, the current system is developed by UC Berkeley. They have long-standing experience with kinematic monitoring, limb dynamics and exoskeleton development (Matthew et al. 2015, Matthew et al. 2016, Oskarsson et al. 2016).

Training Phase. Subjects will be allowed to practice tasks associated with arms/hand and object manipulation. The position of the exoskeleton end effector coordinates (x, y, z) will be under direct neural control. Preliminary experiments with an exoskeleton system showed that end effector control (position and orientation of the wrist) was more intuitive and efficient than position control of individual joints. For this initial phase, the motion will be restricted to a 2-dimensional plane for reaching and grasping objects. There are currently 9 tasks which involve interactions with both static and dynamic environments with various fixtures. We will first limit movements to a 2D environment. The additional degree of freedom involving grasp will be included based on proficiency. In addition, given that ‘motivation’ and reward are known to influence the overall learning process, a gamed-based training environment with specific goals and scoring systems were developed to engage the subject intellectually and to provide additional enrichment during the training phase.

Testing Phase. To assess robustness and stability of control over days we will assess performance characteristics in three tasks. A) Standard center-out task where subjects have to move to the center, engage a grasp, then move to a target and disengage the grasp to release of an object such as a ball. The workspace will be at 95% of the patient’s natural reach. Target size will be kept at 5 cm. B) Reaching from a randomized starting and end position in the workspace of Task A. C) Task B except with the need to plan around obstacles that are placed in the direct path.

Online BMI control: Also during phase 2, neural activity will be used to control a real-time communication device using state of the art closed-loop decoders based on rapid changes in neural activity (Shanechi, Orsborn and Carmena 2016). The main advantage of such a decoder lies in its enhanced ability in discriminating user intent and its speed of operating at every event. Such decoders operate at much higher speeds (typically at 200Hz) over previously developed decoders that rely on averaging neural activity (typically at 10Hz). In addition, we will compare this decoder to more standard decoders (e.g. the Weiner Filter, the LMS filter, the Kalman filter and variants). As documented below, the main outcome measure will be the rate of communication using these approaches.

A virtual communication effector will be presented on a computer screen, custom written in the MATLAB programming environment. The interface between MATLAB and the NeuroPort System will be via commercial software provided by Blackrock Microsystems. The novel decoder will map neural activity to the communication interface. A language processing engine will be concurrently running in the background to model and predict the words and sentences. The following metrics will be utilized to measure performance of the decoder and communication device: selections per minute, accuracy, correct characters per minute (Bacher et al. 2015b) and the bitrate, an information theoretic approach to relate accuracy, time of task completion and complexity (Nuyujukian et al. 2014b, Thompson et al. 2014a). The performance of the novel decoder based communication device will be compared to traditional state space filtering decoders such as the Kalman Filter that has been previously successfully deployed in similar BMI paradigms (Gilja et al. 2012, Bacher et al. 2015b).

Development life cycle of the BMI motor control and communication software:

a) *Scope:* The intended use of the decoder is to allow the patient to achieve control of external devices and thereby select characters and letters to form sentences, as well as control a wearable hand exoskeleton. As such the operation of the BCI is therefore dependent on the functionality of the software.

b) *Platform:* The software will be developed on MATLAB (The Mathworks, MA) and MATLAB supported C/C++ complied programs (MEX files) and will be running on the data acquisition PC that interfaces with the Blackrock NeuroPort Array pedestal connector. We will use the software libraries that are part of the Blackrock Neuroport system to stream neural data into MATLAB in real-time.

c) *Inputs and outputs:* The inputs to the software will be the neural signals from the PMT Subdural Cortical Electrodes grid and the output of the software will consist of user controlled (via the user's neural signals) effector position, selections of characters, letters and numbers for communication purposes, in addition to control of a movements of a wearable hand exoskeleton.

d) *Components:* There are four distinct aspects of the software, three that operate 'behind the scenes' and one that serves as a Graphical User Interface for display. First, is the decoder itself that translates neural signals into user intentions. Second, is another parallel decoder that serves to discriminate when the patient has made a particular selection (or e.g. grasping actions). Third, is the software engine, that keeps track of the current selections made and generates a list of probable options using a statistical model of movement direction and language (Nadkarni, Ohno-Machado and Chapman 2011b). The fourth and final aspect of the decoder is the Graphical User Interface (GUI) that displays and controls the real-time position of end effector.

e) *Safety:* The software provides only visual feedback to the user and does not directly interface with the neural signal data acquisition process. The software only serves to allow the use to control the communication interface and the exoskeleton position.

f) *Planning phase:* In the planning phase, we will identify off-the-shelf components (such as language processing engines) and will aim to further refine and customize it in-house concurrently with the decoders and GUI.

g) *Development phase:* In the development phase, all components will be developed in parallel as discrete subunits of the overall functional system. A code repository will be maintained to keep track of the life cycle versions and code will be commented wherever

appropriate. During the development phase, debugging will be performed at every iteration and documented. The documentation and code will be maintained on secure hard drives.

h) Testing phase: There are two aspects of this phase. One is the performance testing of each of the four individual components and the other is the testing of the entire software. In lieu of actual neural signals, simulated neural signals will be delivered as input, with a known mapping between the input and output state as the ground truth is known a priori. This will allow testing the performance of the decoders (accuracy in estimated positions). The testing of the GUI and the software engine will be performed independently of the decoders by manually controlling the position of the effector. The testing of the GUI and the software engine will be assessed by the stability and reliability in updating effector position and exoskeleton movements, in the turnaround time of displaying the list of predictive words and actions based on current selections. The overall system testing will employ a combination of simulated neural signals and manual position control to assess the ability of the software in allowing a user to communicate and control a hand neuroprosthetic.

i) Error handling: Code will be written to specifically monitor potential sources of errors in real-time decoding due to either noise in neural signals or decoder weight drift that would necessitate recalibration and resetting of the GUI and software engine.

j) Software validation: The validation and formal design review for the overall software will be performed by members of the PI's laboratory not involved with the development and testing of the software prior to software deployment.

k) Resolution and maintenance: Active documentation and daily logs will be noted to keep track of the performance of the software and address issues such as version control, robustness and immediate resolution of unforeseen errors in the software.

Progression of phases: We anticipate phase 1 will last approximately 1 month, but will vary based on each subject. Phase 2 will last at a minimum 10-11 months, a total amount of time of at least 1 year after PMT Subdural Cortical Electrodes implantation and neural interface monitoring and testing, a timeframe which has been performed or exceeded without adverse effects by previous studies using the PMT Subdural Cortical Electrodes and Blackrock Microsystems NeuroPort Array pedestal and NeuroPort System. In this study, recordings were made over 666 days in a non-human primate with no adverse events related to the implanted devices (Degenhart et al. 2016). The ECoG array is identical to that used for subdural grid placement in patients with intractable epilepsy, which is well tolerated and has few complications (Chang et al. 2010).

Activation of the brain recording function: All data collection in the study visits will be initiated by the study staff.

Conclusion of study: For each enrolled subject, if there have been no serious adverse events, we will present the option to continue with the study at the end of a 1-year period. If the subject chooses, we will continue with testing for another year. We will formally present this option every year for a period of 5 years. Notably, the subject will be reminded that he/she will have the option for surgical removal of the device at any point.

Removal of the ECoG grid and Connector pedestal: At the conclusion of the study, or earlier if medically indicated, the subdural cortical electrodes and connector pedestal will be

surgically removed. The skin incision and bone flap will be reopened and the electrode will be removed and discarded. The dura will be sutured tightly. The galea and scalp will be sutured closed. The expected blood loss is minimal (less than 10 cc), and the expected operative time is 30 minutes.

4.0 Clinical Measurements

Primary

This is a pilot study to test feasibility in eight subjects.

For BCI motor control, we will use outcome measures that are frequently used in preclinical studies of neuroprostheses (e.g. accuracy and reliability of cursor and limb control). As outlined below, the primary goal will be to gather statistics regarding the best achievable control using ECoG signals and state-of-the-art methods to allow motor neuroprosthetic control. For each of the parameters below we aim to describe the statistics as the mean and the variance (Bacher et al. 2015a, Nadkarni et al. 2011a, Nuyujukian et al. 2014a, Shanechi et al. 2016, Thompson et al. 2014b). Ultimately, we will compare these values to a wealth of published data regarding movements in able-bodied subjects, e.g.(Bacher et al. 2015a).

1. *Quality of performance* will be assessed using kinematic parameters while performing the required tasks. We will assess stability of the trajectories in the tasks. We will then assess ability for generalization from any region in the workspace to another random point. Position errors from the selected trajectory of the task as well as velocity and acceleration will be studied in both joint space and the end effector space.
2. *Recording and Performance Stability*. We will use previously established metrics to analyze stability of neural recordings (Shanechi et al. 2016, Thompson et al. 2014b) and performance. To measure stability of the neural representation we will analyze the neural correlates of daily imagined movements. We will also examine the stability of the neural correlates of neuroprosthetic movements (e.g. spectral content, timing, spatial recruitment).
3. *Spatial Scale*. An important question for ECoG recordings is the optimal spatial scale for the electrode grid. This has implications for maximizing the amount of information that can be obtained from the recording setup but also for defining the design specifications of implantable electronics (e.g. power requirements could vary greatly depending on the spatial and temporal resolution of the neural data required). We will look at changes in the spatial correlation scales and other redundancy measures during learning and stable performance.

The following metrics will further be utilized to measure performance of the decoder and communication device: selections per minute, accuracy, correct characters per minute (Bacher et al. 2015b) and the bitrate, an information theoretic approach to relate accuracy, time of task completion and complexity (Nuyujukian et al. 2014b, Thompson et al. 2014a). Physiological measurements related to neural activity will include statistical assessments of z-scored activity from single electrodes as well as population dynamics. Physiological measurements related to oscillatory activity will include: wide spectrum power-spectral

analysis as well as using specific frequency domain for mean log power (i.e. in the delta, theta, alpha, beta, gamma bands), coupling between the phase of low frequency rhythms and broadband gamma amplitude (phase-amplitude coupling, abbreviated PAC) (Canolty et al. 2006, Miller et al. 2010, Tort et al.).

Clinical measures and physiological measurements will be collected and recorded by members of the research and clinical team.

5.0 Data Management

All clinical and physiological data will be stored in encrypted and password-protected computers in the PI's laboratory that is always locked. If the Neuroport System is stored in the participant's residence, all research data will be maintained in accordance with UCSF standard encryption policy. In publications or presentations of the data, data will be grouped by case number in chronological order with no name identification. All patients will be asked to sign a separate consent for audio-video recording. When presenting videotape data at scientific conferences, we will utilize only videos from patients who have consented to have their videos shown. De-identified electrophysiological data may be shared with other researchers at other institutions.

6.0 Statistical Methods and Data Analysis

To assess the performance of the decoder, analyses will be performed on the kinematics associated with control, such as time to reach a target, trajectory curvature etc., in conjunction with measures associated with the communication device such as the bit rate, accuracy, characters per minute. The statistical reliability of the decoder will be assessed by non-parametric data permutation wherein the learned mapping between neural activity and the effector position will be artificially broken down and shuffled. Field potential data will be analyzed using wide spectrum power-spectral analysis as well as using specific frequency domain for mean log power (i.e. in the delta, theta, alpha, beta, gamma bands). We will also examine coherence and cross-frequency coupling between the channels (Canolty et al. 2006, Miller et al. 2010, Tort et al.). Using a repeated measures ANOVA statistical analysis, summary statistics for power in relevant frequency bands, control related power changes, and indices of phase-amplitude coupling will be compared at different time-points of control. Additionally, bootstrap statistical tests and general linear mixed models can be utilized to investigate potential statistical effects, given the small sample size. Mean, median, variance and median absolute deviation describing the statistics of each of the measured outcome (such as accuracy, effector position control) will be recorded for each subject.

Sample size calculation: This is a pilot study to assess the feasibility of an ECoG based implantable BCI device in patients with motor control disorders using intracranial recordings, a communication interface and a wearable hand exoskeleton. The collected pilot data will aid in determining the feasibility, reliability and future directions of the brain machine interface for communication and motor control. In addition, the pilot data will be used to formulate more detailed hypothesis on neural plasticity and BMI control in humans. As such, there is no formal sample size requirement for this pilot study.

Criteria for study success that would justify a larger subsequent trial:

- 1) Ability to use ECoG-based neural activity to control a neuroprosthetic device and communication interface.
- 2) No permanent serious adverse events occur (such as trauma with long-term motor deficit).
- 3) Benefits to the patient in regaining a sense of control over the ability to exert motor control and communicate in an efficient manner.

7.0 Regulatory Requirements

Prior to the start of the study, the following documents will be collected and filed:

- Signed protocol signature page
- Curriculum vitae of the PIs and Sub-investigators, updated within 2 years
- Current medical licenses for the PIs and all Sub-investigators
- Financial disclosure form signed by the PIs and all Sub-investigators
- Copy of the IRB approval letter for the study and the IRB Membership List
- Investigator Agreement

Investigator Obligations

Redacted will be responsible for ensuring that all study site personnel, adhere to all FDA regulations and guidelines regarding clinical trials, including guidelines for GCP (including the archiving of essential documents), both during and after study completion. Additionally, they are responsible for the subject's compliance to the study protocol.

All information obtained during the conduct of the study with respect to the patients' state of health will be regarded as confidential. This is detailed in the written information provided to the patient. An agreement for disclosure of any such information will be obtained in writing and will be signed by the patient.

Informed Consent

The investigators will obtain and document informed consent for each patient screened for this study. All patients will be informed in writing of the nature of the protocol and investigational therapy, its possible hazards, and their right to withdraw at any time, and will sign a form indicating their consent to participate prior to the initiation of study procedures.

Institutional Review Board

This protocol and relevant supporting data are to be submitted to the appropriate IRB for review and approval before the study can be initiated (UCSF, Human Research Protection Program, 3333 California Street, Suite 315, San Francisco, CA, 94118, FWA#00000068; IRB Registration 00000229, Lisa Denney, HRRP Director). Amendments to the protocol will also be submitted to the IRB prior to implementation of the change. The PIs are responsible for informing the IRB of the progress of the study and for obtaining annual IRB renewal. The IRB must be informed at the time of completion of the study and should be provided with a summary of the results of the study by the PIs. The PIs must notify the IRB in writing of any SAE or any unexpected AE according to ICH guidelines.

Data safety monitoring board (DSMB) and safety monitoring plan

Treatment emergent adverse events that are assessed by the principal investigators as possibly, probably, or definitely related to surgical implantation or chronic cortical recording AND are unexpected or meet seriousness criteria (death, immediately life threatening, hospitalization >24 hours, persistent or significant disability, or significant

intervention required to prevent one of the previously-stated outcomes) will be recorded and reported to the IRB, device manufacturer and the FDA via the MedWatch online voluntary reporting form within 10 working days of the study team's knowledge of the event.

All such events will also be reported to the data safety monitor board (DSMB), led by a neurosurgeon at our home institution, who does not have direct involvement in this study but who has expertise in implantable devices, pain management and neurosurgery. The DSMB will meet regularly to review data related to the clinical trial, provide guidance and feedback, and review any adverse event reports. Treatment-related adverse events assessed as definitely, probably, or possibly related to study procedures and either serious or unexpected, noted by any study personnel will be reported within 10 working days of their knowledge of the event to the DSMB. The DSMB will then advise the PI on potential changes in procedures to improve safety. The safety endpoint will consist of all adverse events.

Throughout the clinical trial, should a serious adverse event occur that is assessed to be surgery related or not, or related to the presence of the electrode system, such as infection, the device will be removed and the study halted for the patient. Removal will be accomplished by re-opening the original incisions, temporary removal of the bone, and removal of the PMT Subdural Cortical Electrodes from the brain and NeuroPort Array pedestal from the skull. The dura will be re-sewn together and the bone fixed again with titanium screws

Furthermore, if there is a serious surgical or non-surgical adverse event, or with the onset of suicidality, the study will be halted for the patient.

If two patients meet one or more of these criteria (i. serious surgical or nonsurgery-related adverse event, or ii. onset of suicidality), the study will be halted until information is reviewed by the DSMB and FDA.

8.0 References

- Ajiboye, A. B., J. D. Simeral, J. P. Donoghue, L. R. Hochberg & R. F. Kirsch (2012) Prediction of imagined single-joint movements in a person with high-level tetraplegia. *IEEE Trans Biomed Eng*, 59, 2755-65.
- Anderson, K. D. (2004) Targeting recovery: priorities of the spinal cord-injured population. *J Neurotrauma*, 21, 1371-83.
- Bacher, D., B. Jarosiewicz, N. Y. Masse, S. D. Stavisky, J. D. Simeral, K. Newell, E. M. Oakley, S. S. Cash, G. Friehs & L. R. Hochberg (2015a) Neural Point-and-Click Communication by a Person With Incomplete Locked-In Syndrome. *Neurorehabil Neural Repair*, 29, 462-71.
- Bacher, D., B. Jarosiewicz, N. Y. Masse, S. D. Stavisky, J. D. Simeral, K. Newell, E. M. Oakley, S. S. Cash, G. Friehs & L. R. Hochberg (2015b) Neural point-and-click communication by a person with incomplete locked-in syndrome. *Neurorehabilitation and neural repair*, 29, 462-471.
- Bensmaia, S. J. & L. E. Miller (2014) Restoring sensorimotor function through intracortical interfaces: progress and looming challenges. *Nat Rev Neurosci*, 15, 313-25.
- Birbaumer, N., N. Ghanayim, T. Hinterberger, I. Iversen, B. Kotchoubey, A. Kubler, J. Perelmouter, E. Taub & H. Flor (1999) A spelling device for the paralysed. *Nature*, 398, 297-8.
- Bouchard, K. E., N. Mesgarani, K. Johnson & E. F. Chang (2013) Functional organization of human sensorimotor cortex for speech articulation. *Nature*, 495, 327-32.
- Bouton, C. E., A. Shaikhouni, N. V. Annetta, M. A. Bockbrader, D. A. Friedenberg, D. M. Nielson, G. Sharma, P. B. Sederberg, B. C. Glenn, W. J. Mysiw, A. G. Morgan, M. Deogaonkar & A. R. Rezai (2016) Restoring cortical control of functional movement in a human with quadriplegia. *Nature*, 533, 247-50.
- Canolty, R. T., E. Edwards, S. S. Dalal, M. Soltani, S. S. Nagarajan, H. E. Kirsch, M. S. Berger, N. M. Barbaro & R. T. Knight (2006) High gamma power is phase-locked to theta oscillations in human neocortex. *Science*, 313, 1626-8.
- Carmena, J. M., M. A. Lebedev, R. E. Crist, J. E. O'Doherty, D. M. Santucci, D. F. Dimitrov, P. G. Patil, C. S. Henriquez & M. A. Nicolelis (2003) Learning to control a brain-machine interface for reaching and grasping by primates. *PLoS Biol*, 1, E42.
- Chang, E. F., J. W. Rieger, K. Johnson, M. S. Berger, N. M. Barbaro & R. T. Knight (2010) Categorical speech representation in human superior temporal gyrus. *Nat Neurosci*, 13, 1428-32.
- Chao, Z. C., Y. Nagasaka & N. Fujii (2010) Long-term asynchronous decoding of arm motion using electrocorticographic signals in monkeys. *Front Neuroengineering*, 3, 3.
- Chestek, C. A., V. Gilja, P. Nuyujukian, R. J. Kier, F. Solzbacher, S. I. Ryu, R. R. Harrison & K. V. Shenoy (2009) HermesC: Low-Power Wireless Neural Recording System for Freely Moving Primates. *Ieee Transactions on Neural Systems and Rehabilitation Engineering*, 17, 330-338.
- Churchland, M. M., J. P. Cunningham, M. T. Kaufman, J. D. Foster, P. Nuyujukian, S. I. Ryu & K. V. Shenoy (2012) Neural population dynamics during reaching. *Nature*, 487, 51-6.
- Collinger, J. L., S. Foldes, T. M. Bruns, B. Wodlinger, R. Gaunt & D. J. Weber (2013) Neuroprosthetic technology for individuals with spinal cord injury. *J Spinal Cord Med*, 36, 258-72.

- Degenhart, A. D., J. Eles, R. Dum, J. L. Mischel, I. Smalianchuk, B. Endler, R. C. Ashmore, E. C. Tyler-Kabara, N. G. Hatsopoulos, W. Wang, A. P. Batista & X. T. Cui (2016) Histological evaluation of a chronically-implanted electrocorticographic electrode grid in a non-human primate. *J Neural Eng*, 13, 046019.
- Ganguly, K. & J. M. Carmena (2009) Emergence of a stable cortical map for neuroprosthetic control. *PLoS Biol*, 7, e1000153.
- Ganguly, K., D. F. Dimitrov, J. D. Wallis & J. M. Carmena (2011) Reversible large-scale modification of cortical networks during neuroprosthetic control. *Nat Neurosci*, 14, 662-7.
- Ganguly, K., L. Secundo, G. Ranade, A. Orsborn, E. F. Chang, D. F. Dimitrov, J. D. Wallis, N. M. Barbaro, R. T. Knight & J. M. Carmena (2009) Cortical representation of ipsilateral arm movements in monkey and man. *J Neurosci*, 29, 12948-56.
- Gilja, V., C. A. Chestek, I. Diester, J. M. Henderson, K. Deisseroth & K. V. Shenoy (2011) Challenges and opportunities for next-generation intracortically based neural prostheses. *IEEE Trans Biomed Eng*, 58, 1891-9.
- Gilja, V., P. Nuyujukian, C. A. Chestek, J. P. Cunningham, M. Y. Byron, J. M. Fan, M. M. Churchland, M. T. Kaufman, J. C. Kao & S. I. Ryu (2012) A high-performance neural prosthesis enabled by control algorithm design. *Nature neuroscience*, 15, 1752-1757.
- Hochberg, L. R., D. Bacher, B. Jarosiewicz, N. Y. Masse, J. D. Simeral, J. Vogel, S. Haddadin, J. Liu, S. S. Cash & P. van der Smagt (2012a) Reach and grasp by people with tetraplegia using a neurally controlled robotic arm. *Nature*, 485, 372-375.
- Hochberg, L. R., D. Bacher, B. Jarosiewicz, N. Y. Masse, J. D. Simeral, J. Vogel, S. Haddadin, J. Liu, S. S. Cash, P. van der Smagt & J. P. Donoghue (2012b) Reach and grasp by people with tetraplegia using a neurally controlled robotic arm. *Nature*, 485, 372-5.
- Hochberg, L. R., M. D. Serruya, G. M. Friehs, J. A. Mukand, M. Saleh, A. H. Caplan, A. Branner, D. Chen, R. D. Penn & J. P. Donoghue (2006) Neuronal ensemble control of prosthetic devices by a human with tetraplegia. *Nature*, 442, 164-71.
- Homer, M. L., A. V. Nurmikko, J. P. Donoghue & L. R. Hochberg (2013) Sensors and decoding for intracortical brain computer interfaces. *Annu Rev Biomed Eng*, 15, 383-405.
- Huggins, J. E., P. A. Wren & K. L. Gruis (2011) What would brain-computer interface users want? Opinions and priorities of potential users with amyotrophic lateral sclerosis. *Amyotroph Lateral Scler*, 12, 318-24.
- Kennedy, P. R. (1994) 'Locked-in' patients. *Neurology*, 44, 366-7.
- Kennedy, P. R. & R. A. Bakay (1998) Restoration of neural output from a paralyzed patient by a direct brain connection. *Neuroreport*, 9, 1707-11.
- Kim, S. P., J. D. Simeral, L. R. Hochberg, J. P. Donoghue & M. J. Black (2008a) Neural control of computer cursor velocity by decoding motor cortical spiking activity in humans with tetraplegia. *Journal of Neural Engineering*, 5, 455-76.
- (2008b) Neural control of computer cursor velocity by decoding motor cortical spiking activity in humans with tetraplegia. *J Neural Eng*, 5, 455-76.
- Kubler, A., B. Kotchoubey, J. Kaiser, J. R. Wolpaw & N. Birbaumer (2001) Brain-computer communication: unlocking the locked in. *Psychol Bull*, 127, 358-75.
- Leuthardt, E. C., K. J. Miller, G. Schalk, R. P. Rao & J. G. Ojemann (2006) Electrocorticography-based brain computer interface--the Seattle experience. *IEEE Trans Neural Syst Rehabil Eng*, 14, 194-8.

- Leuthardt, E. C., G. Schalk, J. Roland, A. Rouse & D. W. Moran (2009) Evolution of brain-computer interfaces: going beyond classic motor physiology. *Neurosurg Focus*, 27, E4.
- Leuthardt, E. C., G. Schalk, J. R. Wolpaw, J. G. Ojemann & D. W. Moran (2004) A brain-computer interface using electrocorticographic signals in humans. *J Neural Eng*, 1, 63-71.
- Matthew, R. P., E. J. Mica, W. Meinhold, J. A. Loeza, M. Tomizuka & R. Bajcsy (2015) Initial investigation into the effect of an Active/Passive exoskeleton on hammer curl performance in healthy subjects. *Conf Proc IEEE Eng Med Biol Soc*, 2015, 3607-10.
- Matthew, R. P., V. Shia, G. Venture & R. Bajcsy (2016) Generating physically realistic kinematic and dynamic models from small data sets: An application for sit-to-stand actions. *Conf Proc IEEE Eng Med Biol Soc*, 2016, 2173-2178.
- Miller, K. J., D. Hermes, C. J. Honey, M. Sharma, R. P. Rao, M. den Nijs, E. E. Fetz, T. J. Sejnowski, A. O. Hebb, J. G. Ojemann, S. Makeig & E. C. Leuthardt (2010) Dynamic modulation of local population activity by rhythm phase in human occipital cortex during a visual search task. *Front Hum Neurosci*, 4, 197.
- Monti, M. M., A. Vanhauzenhuyse, M. R. Coleman, M. Boly, J. D. Pickard, L. Tshibanda, A. M. Owen & S. Laureys (2010) Willful modulation of brain activity in disorders of consciousness. *N Engl J Med*, 362, 579-89.
- Morrell, M. J. & R. N. S. S. i. E. S. Group (2011) Responsive cortical stimulation for the treatment of medically intractable partial epilepsy. *Neurology*, 77, 1295-304.
- Nadkarni, P. M., L. Ohno-Machado & W. W. Chapman (2011a) Natural language processing: an introduction. *J Am Med Inform Assoc*, 18, 544-51.
- Nadkarni, P. M., L. Ohno-Machado & W. W. Chapman (2011b) Natural language processing: an introduction. *Journal of the American Medical Informatics Association*, 18, 544-551.
- Nicolelis, M. A. & M. A. Lebedev (2009) Principles of neural ensemble physiology underlying the operation of brain-machine interfaces. *Nat Rev Neurosci*, 10, 530-40.
- Nuyujukian, D. S., J. Voutsinas, L. Bernstein & S. S. Wang (2014a) Medication use and multiple myeloma risk in Los Angeles County. *Cancer Causes Control*, 25, 1233-7.
- Nuyujukian, P., J. C. Kao, J. M. Fan, S. D. Stavisky, S. I. Ryu & K. V. Shenoy (2014b) Performance sustaining intracortical neural prostheses. *Journal of neural engineering*, 11, 066003.
- Oskarsson, B., N. C. Joyce, E. De Bie, A. Nicorici, R. Bajcsy, G. Kurillo & J. J. Han (2016) Upper extremity 3-dimensional reachable workspace assessment in amyotrophic lateral sclerosis by Kinect sensor. *Muscle Nerve*, 53, 234-41.
- Pandarinath, C., V. Gilja, C. H. Blabe, P. Nuyujukian, A. A. Sarma, B. L. Sorice, E. N. Eskandar, L. R. Hochberg, J. M. Henderson & K. V. Shenoy (2015) Neural population dynamics in human motor cortex during movements in people with ALS. *Elife*, 4, e07436.
- Pasley, B. N., S. V. David, N. Mesgarani, A. Flinker, S. A. Shamma, N. E. Crone, R. T. Knight & E. F. Chang (2012) Reconstructing speech from human auditory cortex. *Plos Biology*, 10, e1001251.
- Schalk, G., K. J. Miller, N. R. Anderson, J. A. Wilson, M. D. Smyth, J. G. Ojemann, D. W. Moran, J. R. Wolpaw & E. C. Leuthardt (2008) Two-dimensional movement control using electrocorticographic signals in humans. *J Neural Eng*, 5, 75-84.
- Schwartz, A. B. (2004) Cortical neural prosthetics. *Annu Rev Neurosci*, 27, 487-507.

- Schwartz, A. B., X. T. Cui, D. J. Weber & D. W. Moran (2006) Brain-controlled interfaces: movement restoration with neural prosthetics. *Neuron*, 52, 205-20.
- Selzer, M. E., S. Clarke, L. G. Cohen, G. Kwakkel & R. H. Miller. 2014. *Textbook of neural repair and rehabilitation*. Cambridge: Cambridge University Press.
- Shanechi, M. M., A. L. Orsborn & J. M. Carmena (2016) Robust Brain-Machine Interface Design Using Optimal Feedback Control Modeling and Adaptive Point Process Filtering. *PLoS Comput Biol*, 12, e1004730.
- Shenoy, K. V. & J. M. Carmena (2014) Combining decoder design and neural adaptation in brain-machine interfaces. *Neuron*, 84, 665-80.
- Simeral, J. D., S. P. Kim, M. J. Black, J. P. Donoghue & L. R. Hochberg (2011) Neural control of cursor trajectory and click by a human with tetraplegia 1000 days after implant of an intracortical microelectrode array. *J Neural Eng*, 8, 025027.
- Slutzky, M. W., L. R. Jordan, E. W. Lindberg, K. E. Lindsay & L. E. Miller (2011) Decoding the rat forelimb movement direction from epidural and intracortical field potentials. *J Neural Eng*, 8, 036013.
- Spataro, R., M. Ciriaco, C. Manno & V. La Bella (2014) The eye-tracking computer device for communication in amyotrophic lateral sclerosis. *Acta Neurol Scand*, 130, 40-5.
- Taylor, D. M., S. I. Tillery & A. B. Schwartz (2002) Direct cortical control of 3D neuroprosthetic devices. *Science*, 296, 1829-32.
- Thompson, D. E., L. R. Quitadamo, L. Mainardi, S. Gao, P.-J. Kindermans, J. D. Simeral, R. Fazel-Rezai, M. Matteucci, T. H. Falk & L. Bianchi (2014a) Performance measurement for brain-computer or brain-machine interfaces: a tutorial. *Journal of neural engineering*, 11, 035001.
- Thompson, D. E., L. R. Quitadamo, L. Mainardi, K. U. Laghari, S. Gao, P. J. Kindermans, J. D. Simeral, R. Fazel-Rezai, M. Matteucci, T. H. Falk, L. Bianchi, C. A. Chestek & J. E. Huggins (2014b) Performance measurement for brain-computer or brain-machine interfaces: a tutorial. *J Neural Eng*, 11, 035001.
- Tort, A. B., R. Komorowski, H. Eichenbaum & N. Kopell (2010) Measuring phase-amplitude coupling between neuronal oscillations of different frequencies. *J Neurophysiol*, 104, 1195-210.
- Wolpaw, J. R., N. Birbaumer, D. J. McFarland, G. Pfurtscheller & T. M. Vaughan (2002) Brain-computer interfaces for communication and control. *Clin Neurophysiol*, 113, 767-91.

CLINICAL PROTOCOL

(updated 8/23/2022)

Title:

A High-Performance ECoG-based Neural Interface for Communication and Neuroprosthetic Control

Protocol:

FDA reference number: G170242

UCSF-BMI-ECoG-2022-06

Study Sponsors/Investigators:

Redacted

Protocol Synopsis

<p>Title</p>	<p>A High-Performance ECoG-based Neural Interface for Communication and Neuroprosthetic Control</p>
<p>Study Phase</p>	<p>Phase I</p>
<p>Device(s)</p>	<p>Device Information: Devices to be used in this study are grouped below according to FDA approval.</p> <p>Cleared for temporary (<30 days) recording and monitoring of brain electrical activity under 510k:</p> <ul style="list-style-type: none"> • NeuroPort Array, PN 6248 (K070272, K110010) <p>Seeking Special 510(k) (not yet submitted to FDA):</p> <ul style="list-style-type: none"> • Digital NeuroPort System (Modification to existing NeuroPort System - K042626) <p>Cleared for temporary (<30 day) use with recording, monitoring, and stimulation equipment for the recording, monitoring and stimulation of electrical signals on the surface of the brain under 510k:</p> <ul style="list-style-type: none"> • PMT Subdural Cortical Electrodes, Model #2110TX-253-001 (K082474) • PMT Subdural Cortical Electrodes, Model #2110TX-128-005 (K082474) <p>Not cleared:</p> <ul style="list-style-type: none"> • Blackrock Microsystems 256-channel pedestal connector (see Appendix E for justification of use) • Blackrock Microsystems CerePlex E256 digital head stage <p>The Blackrock Microsystems NeuroPort Array connector pedestal, a subcomponent of the Blackrock Microsystems NeuroPort Array, or the 256-channel Blackrock Microsystems connector pedestal will be laser bonded to the PMT Subdural Cortical Electrode by Blackrock Microsystems. As documented below, the combination device including the Blackrock Microsystems NeuroPort Array connector pedestal laser bonded to the PMT Subdural Cortical Electrode has already been tested in non-human primates (over at least an 18-month period, see below regarding published report).</p> <p>Request for off-label use of the combined investigational device for 1 year, for the equivalent indication of recording and monitoring of brain electrical activity.</p>

Indication	Adults with neurological disorders (e.g. amyotrophic lateral sclerosis/ALS, spinal cord injury, multiple sclerosis, stroke) often develop disorders of movement and communication. We aim to determine the feasibility of ECoG based brain computer interface control of complex neuroprosthetic devices.
Sponsor Contacts	*Redacted*
Data Safety Monitor Board (DSMB)	*Redacted*
Treatment	The Blackrock Microsystems NeuroPort Array connector pedestal, NeuroPort system, and PMT Subdural Cortical Electrodes are currently cleared for monitoring of patients for up to 30 days. The Blackrock Microsystems 256-channel NeuroPort connector pedestal and CerePlex E256 digital head stage are not cleared by the FDA. Blackrock has modifications to the NeuroPort system for which they are seeking special 510(k) clearance. Here we to aim to use these systems combined for at least a 1-year period in subjects with neurological illness and disorders of communication to test feasibility for both neuroprosthetic control and for decoding speech from neural activity.
Study Sites	*Redacted*

<p>Study Design</p>	<p>This is a single-center early feasibility study of the use of an ECoG-based neural interface for testing the feasibility of using ECoG signals to control complex devices for motor and speech control in adults affected by neurological disorders of movement.</p> <p>A PMT Subdural Cortical Electrode array, bonded to the Blackrock Microsystems NeuroPort Array pedestal or to the 256-channel NeuroPort pedestal, will be surgically placed directly on the brain surface over the motor and language cortices of subjects with disorders of motor control. After implantation of the electrode and pedestal, the NeuroPort Biopotential Processing System will be connected to the NeuroPort Array pedestal, or to the 256-channel NeuroPort pedestal, to monitor and record neural signals. With this ECoG-based neural interface, study patients will undergo training and assessment of their ability to control assistive robotic arms and to determine if ECoG brain signals can be decoded for language communication. This will be performed in two phases.</p> <p><u>Phase 1: Optimize BCI system</u></p> <p>In Phase 1, we will optimize the entire system to reliably detect neural activity to ensure that the recorded signals are stable and free of artifacts. Moreover, we will ensure that the neural signals are converted in real-time into cursor movements. During this phase, we will primarily examine cursor based control, decoding of parameters and ‘disembodied’ control (i.e. the subjects’ arm will not interact with the mechanical system). This phase will be conducted in the outpatient office setting and/or the patient’s home environment, based on patient preference and needs. We anticipate that this phase will take approximately 1 month; however, this may be longer or shorter for each subject depending on the level of control achieved.</p> <p><u>Phase 2: Testing of BCI Control</u></p> <p>In Phase 2, we will test feasibility for both neuroprosthetic control and for decoding speech from neural activity. We will begin to perform experimental testing with the system for control of an assistive robotic arms that meets criteria for a non-significant risk device. As outlined in the sections below, we have multiple safety features to ensure that there is minimal risk for injury during use of the robotic arms, including subject contact during object interaction and the embodiment phase (i.e. the subjects arm is interacting with the exoskeleton). Throughout this period, neural signals will be recorded and analyzed, and tasks will be performed toward the development, assessment, and improvement of the neural interface system. We will assess quality of performance using kinematic parameters while performing required tasks. We will analyze stability of neural recordings and performance. To measure stability of the neural representation we will analyze the neural correlates of imagined movements. We will also assess changes in spatial correlation scales and other redundancy measures during learning and stable performance. We anticipate that testing will be conducted in the outpatient office or home setting based on the patient’s preference and needs.</p>
----------------------------	--

	<p>In this phase, we will also continue to perform experimental testing with the system for control of a virtual communicating interface. Throughout this period, neural signals will be recorded and analyzed, and tasks will be performed toward the development, assessment, and improvement of the communication interface.</p>
--	---

<p>Objectives</p>	<p>In eight patients with severe disorders of movement control, we will surgically implant PMT Subdural Cortical Electrodes on the brain surface over the motor and language cortices. The electrode will be bonded to a Blackrock NeuroPort Array pedestal or the Blackrock 256-channel NeuroPort pedestal, which can be connected to the Digital NeuroPort system in order to process and record neural activity in real time. Using this neural interface, we will condition the patient to be able to control assistive robotic arms, communicate with a computer system for typing and perform speech output tasks. We will utilize optimal neural plasticity mechanisms, a novel decoder framework, and advanced language modeling during BCI conditioning.</p> <p>Hypothesis: The underlying hypothesis is that ECoG recordings will allow severely paralyzed individuals to skillfully control complex neuroprosthetic devices for movement and communication. A closely related hypothesis is that the well-known stability of ECoG signals will allow us to maximally engage neural mechanism of plasticity and thereby optimize long-term skilled acquisition.</p>
--------------------------	---

<p>Patient Population</p>	<p>Study subjects will be adults with severe motor impairment secondary to a neurological disorder.</p> <p><u>Inclusion Criteria</u></p> <ul style="list-style-type: none"> ● Age 21-75 years old ● Limited ability to use upper limbs and limited ability to use speech, based on neurological examination by a board-certified neurological specialist, due to stroke, spastic quadriplegic cerebral palsy (with no significant cognitive deficits based on formal neuropsychological testing), amyotrophic lateral sclerosis (ALS), multiple sclerosis, cervical spinal cord injury, brainstem stroke, muscular dystrophy, myopathy or severe neuropathy ● Disability, defined by a 4 or greater score on the Modified Rankin Scale, must be severe enough to cause loss of independence and inability to perform activities of daily living. ● If stroke or spinal cord injury, at least 1 year has passed since onset of symptoms ● Must live within a two-hour drive of UCSF <p><u>Exclusion Criteria</u></p> <ul style="list-style-type: none"> ● Pregnancy or breastfeeding ● Inability to understand and/or read English ● Inability to give consent ● Dementia, based on history, physical exam, and MMSE ● Active depression (BDI > 20) or other psychiatric illness (active general anxiety disorder, schizophrenia, bipolar disorder, obsessive-compulsive disorder (OCD), or personality disorders (e.g. multiple personality disorder, borderline personality disorder, etc.) ● History of suicide attempt or suicidal ideation within one's lifetime prior to enrollment, confirmed by a baseline negative Columbia Suicide Severity Rating Scale (C-SSRS) ● Comorbidities including uncontrolled hypertension, cancer, or major organ system failure. ● History of intracranial surgery ● History of substance abuse within the last year ● Ongoing anticoagulation which cannot be stopped in the peri-procedural period. ● Inability to comply with study follow-up visits ● Immunocompromised ● Has an active infection ● Has a CSF drainage system or an active CSF leak ● Requires diathermy, electroconvulsive therapy (ECT), or transcranial magnetic stimulation (TMS) to treat a chronic condition ● Has an implanted electronic device such as a neurostimulator, cardiac pacemaker/defibrillator or medication pump
----------------------------------	---

	<ul style="list-style-type: none">• Allergies or known hypersensitivity to materials in the Blackrock NeuroPort Array pedestal or Blackrock 256-channel pedestal (i.e. silicone, titanium) or the PMT Subdural Cortical Electrode (silicone, platinum iridium, nichrome)
--	--

Sample Size	8 patients
Efficacy Assessments	<u>Primary Endpoints:</u> Feasibility of control of assistive robotic arms and a communication interface.
Safety Assessments	<ul style="list-style-type: none"> ● Physical examination at all study visits ● Perform functional test of the PMT/Blackrock combined neural interface system prior to implantation ● Surgical/ or nonsurgical protocol-defined adverse events recorded on adverse events case report forms and use of protocol-defined procedures for adverse event management ● Assessment of suicidality using Columbia Suicide Severity Rating Scale, and assessment of changes using the Beck Depression and Anxiety Inventories, <u>at monthly intervals.</u>

Table of Contents

Title Page

i. Protocol Synopsis

ii. Table of Contents

iii. Investigator Agreement / Protocol Signature Page

1. Introduction

2. Clinical Study Outline & Study Objectives

3. Investigational Plan

4. Patient Eligibility

5. Study Device

6. Study Procedure

7. Clinical Measurements and Procedures

8. Data Management

9. Statistical Methods and Data Analysis

10. Regulatory Requirements

11. References

12. Appendices

Investigator Agreement / Protocol Signature Page

Redacted

1.0

Introduction

Restoration of function with assistive robotic arms and a communication interface are important goals of BCIs. Multiple neurological disorders can result in severe bilateral upper limb weakness or paralysis. Surveys of patients with quadriplegia provide important guidance about specific rehabilitation needs and preferences as well as targets for intervention. A survey of patients with tetraplegia resulting from SCI found that restoration of arm and hand function was of highest priority (Anderson 2004). Similarly, patients with ALS reported that direct neural control of a robotic arm would be of great importance (Huggins, Wren and Gruis 2011). While there has been extensive research into each disease process, little has been proven to be clinically effective for the rehabilitation of this chronic disability (Wolpaw et al. 2002).

In patients with conditions such as high cervical SCI, basilar strokes or advanced ALS, the effects can be particularly devastating as tetraplegia may be accompanied by paralysis of oral structures, leading to the loss of voluntary vocal function. Individuals with severe traumatic brain injury or high cervical injuries who require mechanical ventilation may also have limited capacity to communicate (Kennedy 1994, Kubler et al. 2001, Monti et al. 2010). Standard augmentative and alternative communication (AAC) devices are widely available but may not be suitable for individuals with severe or complete paralysis of the voluntary motor system (Selzer et al. 2014). For example, the most commonly used devices are gaze trackers that allow computer cursor control through eye movements (Spataro et al. 2014). However, eye tracking may have a limited role in advanced cases of ALS and after brainstem strokes, where eye movements are frequently affected (Birbaumer et al. 1999, Kennedy and Bakay 1998). They also require sustained visual attention and may create a high cognitive burden. Thus, it remains critical to develop novel technologies to help restore communication as well as upper limb function.

Brain-Computer Interfaces (BCIs) are a very promising method to significantly improve quality of life by restoring upper extremity function and communication ability in patients with motor and speech disabilities. Over the past decade, the rate and sophistication of research involving invasive BCIs have rapidly increased. BMIs have the potential to seamlessly integrate the computational power of artificial electronic systems with that of the nervous system. Multiple neural signals can be used in a BCI, including non-invasive EEG signals and other neural signals such as spikes and electrocorticography (ECoG) that require invasive placement of electrodes. Non-invasive BCIs have been studied for at least two decades. Known limitations of surface EEG recordings are a low 'signal-to-noise' and contamination by muscle activity (Wolpaw et al. 2002). Recent studies suggest that BMIs using invasive recording of neural signals (spikes or ECoG) can allow more rapid intuitive control over complex devices (Carmena et al. 2003, Leuthardt et al. 2009, Leuthardt et al. 2004, Schwartz et al. 2006, Taylor, Tillery and Schwartz 2002). A large basic science and clinical effort is currently devoted to BMIs based on invasive recordings of action potentials. However, it is increasingly clear that there are significant limits on possible translation of spikes

based recordings. It does not readily permit reliable long-term recordings (Chestek et al. 2009, Ganguly and Carmena 2009, Gilja et al. 2011, Hochberg et al. 2006).

Electrocorticography (ECoG) offers a promising alternative for BMIs (Pasley et al. 2012, Bouchard et al. 2013, Slutzky et al. 2011, Leuthardt et al. 2006, Ganguly et al. 2009). ECoG has the potential to serve as a robust source of neural signals that can be integrated into a clinically viable device. Specifically, it can be: (1) stably recorded over long-periods of time, (2) possesses sufficient ‘signal-to-noise’ and (3) is known to be rich in information about neural processes, (4) can allow long-term rapid control of multiple degrees of freedom (DOF). Because ECoG arrays lie on the brain surface, they can be stably monitored for very long periods of time (Nadkarni, Ohno-Machado and Chapman 2011a, Thompson et al. 2014b). This approach has been demonstrated clinically in tens of thousands of patients that have had arrays or stimulating electrodes made of the same materials implanted for years (for indications such as pain, movement disorders, or newer closed loop devices for epilepsy) (Nadkarni et al. 2011a).

A significant limitation of current ECoG studies and models is the use of able-bodied subjects in whom motor and sensory pathways are intact. The overwhelming majority of BMI experiments do not monitor physical movements or EMG signals during online BMI control. In addition, intact sensory feedback would likely facilitate learning BMI control. Disabled patients may not have access to such training signals (Bensmaia and Miller 2014). Moreover, it is well known that there is a major reorganization of sensorimotor areas following injury (e.g. after spinal cord injury) (Canolty et al. 2006, Churchland et al. 2012, Miller et al. 2010, Tort et al. 2010). Thus, it remains quite difficult to predict generalization of ECoG-based neuroprosthetic control to disabled patients. It remains unclear if ECoG based control of complex devices can be achieved in paralyzed patients.

Thus, this proposal aims to test feasibility of controlling assistive robotic arms and a communication interface using invasive electrocorticography (ECoG) in subjects with extensive motor disabilities. There have been two main approaches to BCI control, i.e. control of a motor prosthetic (mBCI) or a communication interface (cBCI) (Bensmaia and Miller 2014, Homer et al. 2013, Nicolelis and Lebedev 2009, Schwartz 2004, Shenoy and Carmena 2014). In general, the broader framework for communication is similar to motor control. In a motor BCI, a participant’s intention to move is translated into commands for device control. The components of a motor BMI are (1) recordings of neural activity (2) algorithms to transform the neural activity into control signals, (3) an external device driven by these control signals and (4) feedback regarding the current state. Initial studies in able-bodied non-human primates as well as human subjects (e.g. undergoing epilepsy surgical monitoring) have demonstrated the general feasibility of neuroprosthetic control using ECoG based recordings (Leuthardt et al. 2006, Chao, Nagasaka and Fujii 2010, Schalk et al. 2008).

We propose to conduct an early feasibility (i.e. pilot clinical) trial of ECoG-based BMIs in subjects with motor disability. Preclinical studies have suggested that ECoG based recordings provide a viable alternative for clinical translation of BMI technology; however, it remains unclear if complex control can be achieved in patients with neurological disorders. This study will utilize devices cleared by the FDA for the same indication of recording and monitoring of brain electrical activity, but with off label use of the device for at least 1 year to meet the objectives outlined above. Specifically, we will use the Blackrock NeuroPort Array pedestal, or the Blackrock 256-channel

pedestal (not currently cleared by FDA), laser-bonded to PMT Subdural Cortical Electrodes, and connected to the NeuroPort Biopotential Signal Processing System, to acquire neural data. The digitized data will then be transmitted to a personal computer and decoded to direct motion of assistive robotic arms and a communication interface. This will allow individuals to use ECoG neural activity to control complex neuroprosthetic devices. **Demonstration of reliable prosthetic control using ECoG signals in disabled subjects would represent a major milestone. It would strongly motivate the development of implantable wireless ECoG recording systems that can be integrated with assistive robotic devices.**

The Blackrock Microsystems NeuroPort system and the NeuroPort Array have been successfully used in humans with neurological disorders. Several human studies have demonstrated successful long-term implantation of neuroprosthetic control using the Blackrock Microsystem NeuroPort microelectrode array with the NeuroPort system (Hochberg et al. 2012b, Hochberg et al. 2006, Kim et al. 2008a, Ajiboye et al. 2012, Simeral et al. 2011, Bouton et al. 2016). Thus far, at least six patients with tetraplegia have been implanted and monitored with the Blackrock NeuroPort Array and NeuroPort system from published reports. This human data supports chronic implantation of the devices in human patient populations by showing: 1) Chronic stable recordings from the cortex using the NeuroPort Signal Processing system connected to the Blackrock NeuroPort Array may be maintained for at least 5 years. 2) Extensive experience with the decoding of the neural data in humans using these devices 3) Proof of concept that individuals with tetraplegia resulting from neurological injuries could readily use motor cortex neural signals to control a computer cursor after an injury
3) Lack of significant adverse events associated with the devices observed over years after implantation

In this study, the PMT Subdural Cortical Electrodes will replace the Blackrock Microsystems NeuroPort Array microelectrode array for monitoring recordable electrical brain activity. The NeuroPort Array pedestal, or the Blackrock Microsystems 256-channel pedestal, will be bonded to the PMT Subdural Cortical Electrodes (in place of the Blackrock Microsystems NeuroPort Array electrode) in a custom-ordered device collaboratively built by the Blackrock Microsystems and PMT Corporation and sterilized by PMT Corporation. The feasibility of this approach has been demonstrated **in a non-human primate study (i.e. the PMT ECoG grid was connected to a Blackrock Microsystems pedestal connector to monitor neural signals for ~ 18 months)** (Degenhart et al. 2016). After implantation, the study explored the host-tissue response to the subdural ECoG grid implanted for 666 d, focusing on both cortical tissue health and fibrosis at the implant site, while also validating device performance by examining neural responses to overt reaching movements. They found that cortical thickness and neuronal density were both unaffected by the ECoG array implantation. As expected, the grid itself was found to be encapsulated in a fibrous envelope upon explantation. Despite this encapsulation, robust modulation of ECoG signals in recordings conducted 18 months after implantation were observed.

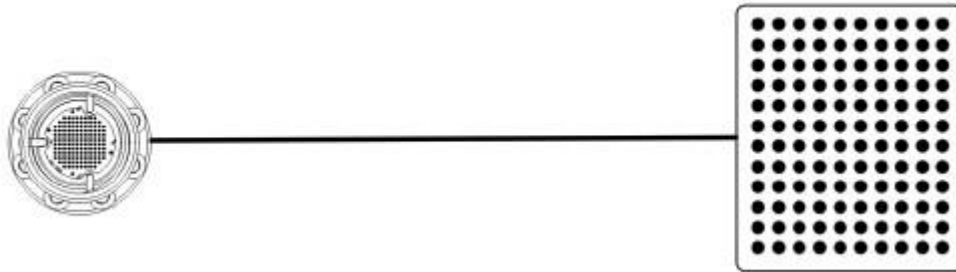


Figure 1: Diagram of pedestal connected to a 128-channel ECoG array

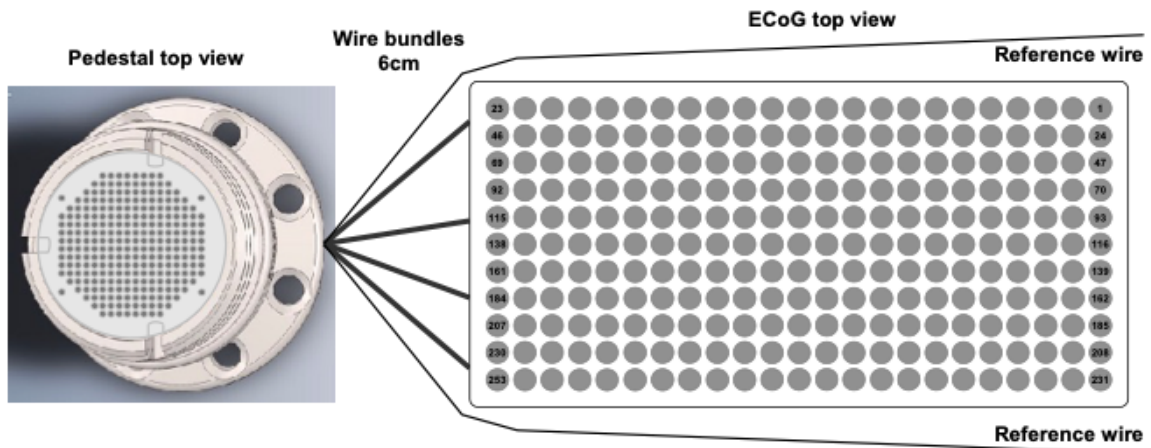


Figure 2: Diagram of pedestal connected to a 253-channel ECoG array

The current literature indicates that ECoG may provide a means by which stable chronic cortical recordings can be obtained with little neural tissue damage, and with a safety level comparable to chronic intracranial device implantations for the treatment of PD. For example, in human subjects, subdural ECoG arrays have been implanted in patients with epilepsy for over 1 year with corroborating evidence of viable long-term neural recordings (Morrell and Group 2011). The primary safety endpoint was achieved whereby the SAE rate for the ECoG system over the first 28 days (device related and not device related) was not worse than the prespecified literature-derived comparator for implantation of intracranial electrodes for seizure localization and epilepsy surgery. Moreover, the SAE rate for the ECoG system during the implant and first 84 days was not worse than the prespecified literature-derived comparator with DBS for PD (Morrell and Group 2011).

2.0 Clinical Study Outline

This study will use the Blackrock Microsystems NeuroPort Biopotential Signal Processing system to record data from the Blackrock Microsystems NeuroPort Array pedestal, or the 256-channel Blackrock Microsystems pedestal, bonded to PMT Subdural Cortical electrodes implanted over cortical areas over a period of at least 1 year. The processed neural signals received by the system will allow us to test the feasibility of training patients to use their neural activity to control assistive robotic arms and a communication interface.

2.1 Study Objectives

This study will allow us to test the feasibility of conditioning individuals with impaired motor ability to be able to control assistive robotic arms and a communication device using ECoG signals.

3.0 Investigational Plan

We aim to conduct a small pilot study to assess the feasibility of translating an ECoG-based interface to control complex neuroprosthetic devices in a severely disabled patient population. **Our underlying hypothesis is that ECoG recordings will allow disabled individuals to skillfully exert motor control of assistive robotic arms and generate verbal output using a computer communication interface.**

In a cohort of 8 subjects, we propose to record and monitor neural signals using subdural electrodes and a mounting and processing system which are already FDA cleared for the general indications of recording and monitoring of brain electrical activity. Specifically, the 510(k) documentation for the Blackrock NeuroPort system and NeuroPort Array states that it "is for temporary (< 30 days) recording and monitoring of brain electrical activity" (K060523 and K090957). The 510K documentation for the PMT Subdural Cortical Electrodes states that it is "cleared for temporary (<30 day) use with recording, monitoring, and stimulation equipment for the recording, monitoring and stimulation of electrical signals on the surface of the brain" (K082474). The Blackrock Microsystems 256-channel pedestal and 256-channel Blackrock Microsystems CereplexE256 digital headstage will also be used in this study (Appendix E). The Blackrock NeuroPort Biopotential Signal Processing System and NeuroPort Electrode Array have been used in human translational clinical studies to record neural activity over a number of months and years and enabled tetraplegic patients to volitionally control computer cursor position and an anthropomorphic prosthetic limb with 7 degrees-of-freedom (Ajiboye et al. 2012, Bouton et al. 2016, Collinger et al. 2013, Hochberg et al. 2012b, Hochberg et al. 2006, Kim et al. 2008b, Simeral et al. 2011). The PMT Subdural Cortical Electrodes have been used extensively in patients for epilepsy monitoring. The combination device of Blackrock Microsystems NeuroPort system, NeuroPort Array pedestal, and PMT Subdural Cortical Electrodes has been implanted in a nonhuman primate to successfully monitor overt reaching movements for 666 days without signal degradation or without significant damage to the brain cortex. We propose to perform long-term

monitoring and testing with the Blackrock/PMT combined system over similar time scales as the aforementioned studies, with the aim of motor and communication control.

We further propose that our investigational device will bear the statement, “CAUTION – Investigational device. Limited by United States law to investigational use.”; all devices that will be used in this study will be labeled for investigational use and all labels and labeling will contain the investigational device statement .

Upon UCSF Institutional Review Board (IRB) approval of our investigational plan and protocol, we propose to conduct testing in two phases for each subject. We anticipate that study visits will be conducted in the outpatient office and/or home setting based on participant preference and other practicalities.

This is a single-center study of the use of a ECoG-based neural interface for testing the feasibility of using ECoG signals to control complex devices for motor and speech control in adults affected by neurological disorders with severely impaired motor and communication.

PMT Subdural Cortical Electrodes will be surgically placed directly on the brain surface over the motor and language cortices of subjects with severe disorders of motor control and communication. After implantation of the electrode, study patients will undergo training and assessment of their ability to control assistive robotic arms and determine if ECoG brain signals can be decoded for language communication. This will be performed in two phases.

Phase 1: Optimize BCI system

In Phase 1, we will optimize the entire system to reliably detect neural activity to ensure that the recorded signals are stable and free of artifacts. Moreover, we will ensure that the neural signals can be converted in real-time into cursor or external object movements. This phase will be conducted in the outpatient office setting and/or the patient’s home environment, based on patient preference and needs. We anticipate that this phase will take ~1 month; we will, however, specifically tailor the period for each subject.

Phase 2: Testing of BCI Control

In Phase 2, we will test feasibility for both neuroprosthetic control and for decoding speech from neural activity. We will begin experimental testing with the system for control of assistive robotic arms that is classified as a non-significant risk device. As outlined in the sections below, we have multiple safety features to ensure that there is minimal risk for injury during use of the robotic arms, including subject contact during object interaction and the embodiment phase (i.e. the subject's arm is interacting with the exoskeleton).

Throughout this period, neural signals will be recorded and analyzed, and tasks will be performed toward the development, assessment, and improvement of the neural interface system. We anticipate that testing will be conducted in the outpatient office or home setting based on the patient’s preference and needs. In this phase, we will also continue to perform experimental testing with the communication interface; we will assess the ability to control a communication interface. We anticipate that this phase will take a minimum of 10-11 months.

4.0 Patient Eligibility

Study subjects will be adults with severe motor impairment secondary to a neurological disorder.

Inclusion Criteria

- Age 21-75 years old
- Limited ability to use upper limbs and limited ability to use speech, based on neurological examination by a board-certified neurological specialist, due to stroke, spastic quadriplegic cerebral palsy (with no significant cognitive deficits based on formal neuropsychological testing), amyotrophic lateral sclerosis (ALS), multiple sclerosis, cervical spinal cord injury, brainstem stroke, muscular dystrophy, myopathy or severe neuropathy
- Disability, defined by a 4 or greater score on the Modified Rankin Scale, must be severe enough to cause loss of independence and inability to perform activities of daily living.
- If stroke or spinal cord injury, at least 1 year has passed since onset of symptoms
- Must live within a two-hour drive of UCSF

Exclusion Criteria

- Pregnancy or breastfeeding
- Inability to understand and/or read English
- Inability to give consent
- Dementia, based on history, physical exam, and MMSE
- Active depression (BDI > 20) or other psychiatric illness (active general anxiety disorder, schizophrenia, bipolar disorder, obsessive-compulsive disorder (OCD), or personality disorders (e.g. multiple personality disorder, borderline personality disorder, etc.)
- History of suicide attempt or suicidal ideation within one's lifetime prior to enrollment, confirmed by a baseline negative Columbia Suicide Severity Rating Scale (C-SSRS)
- Comorbidities including uncontrolled hypertension, cancer, or major organ system failure.
- History of intracranial surgery
- History of substance abuse within the last year
- Ongoing anticoagulation which cannot be stopped in the peri-procedural period.
- Inability to comply with study follow-up visits
- Immunocompromised
- Has an active infection
- Has a CSF drainage system or an active CSF leak
- Requires diathermy, electroconvulsive therapy (ECT), or transcranial magnetic stimulation (TMS) to treat a chronic condition
- Has an implanted electronic device such as a neurostimulator, cardiac pacemaker/defibrillator or medication pump
- Allergies or known hypersensitivity to materials in the Blackrock NeuroPort Array pedestal or the Blackrock 256-channel pedestal (i.e. silicone, titanium) or the PMT Subdural Cortical Electrode (silicone, platinum iridium, nichrome)

5.0

Study Device(s)

Cleared for same indication with off-label use of device for at least 1 year:

- Blackrock NeuroPort Array, PN 6248
- Blackrock NeuroPort system, PN 5416
- PMT Subdural Cortical Electrodes, Model #2110TX-128-005, Model #2110TX-253-001

Modifications to Blackrock NeuroPort System with same indication with off-label use of device for at least 1 year:

- Digital Hub, 10480
- NeuroPlex E, 10908

Not cleared:

- Blackrock Microsystems 256-channel pedestal connector (see Appendix E for justification of use)
- Blackrock Microsystems 256-channel CereplexE256 digital headstage (see Appendix E for justification of use)

6.0 Study Procedure

Study Duration: The duration of this pilot study will be 6 years. We expect that all 8 patients will be recruited in the first 4-5 years, and data collection, device development and analysis will be completed in 6 years.

Patient recruitment and clinical characterization: Patients with motor impairments secondary to neurological disorders will be recruited from clinics specializing in the treatment of stroke, ALS, and general neurological disorders, at UCSF.

Enrollment procedures: Prior to enrollment into the study, an informal phone interview to schedule an office-based evaluation will take place, followed by three outpatient screening visits. During the first outpatient visit we will describe the trial in detail and answer all questions. Should the participant choose to continue, we will schedule another visit to conduct a physical exam and to perform screening labs to determine eligibility. During this visit we will screen for eligibility by 1) acquiring patient demographics, 2) reviewing medical history and measuring vital signs, 3) ensuring patients are not currently pregnant or plan to become pregnant, 4) obtaining a list of current medications being taken, 5) ensuring MMSE scores are within a reasonable range (≥ 18 , also accounting for motor difficulties with taking the test), 6) obtain baseline patient-rated and investigator rated clinical global impression scales, 7) assess baseline health status with SF-36 Health Survey, 8) assess current depression and anxiety states with Beck Depression and Anxiety inventories (BDI and BAI, respectively), 9) determine suicidal ideation risk is minimal with Columbia Suicide Severity Rating Scale (C-SSRS) 10) perform a baseline neurological physical exam and 11) determine the disability rating using the modified Rankin Scale. An MRI and CT of the brain will also be obtained for future surgical planning and to further determine eligibility. Moreover, a ECG and chest x-ray will also be obtained. We will then schedule a third follow-up visit to review this data and to answer remaining questions.

Pre-operative care: Subjects will be administered Kefzol 2g IV within 60 minutes prior to surgical incision, and continued for 24 hours post-operatively. In case of allergy to Kefzol, Vancomycin 1gm IV will be used.

Surgery: After obtaining informed consent, subjects will undergo brief general anesthesia (typically ~ 3-4 hours) for the surgical procedure. This may be either IV or inhaled anesthetics. Patient will be given IV antibiotics prior to incision, and re-dosed if required. Induction and wake up will take place in the operating room, and patients will be monitored in the post-anesthesia care unit (PACU) after surgery for 2-3 hours during the peri-operative period. Subject will then continue to recover on the surgical ward for 2 days.

Subjects will undergo surgical placement of an ECoG array over the dominant (usually left-sided) sensorimotor and speech cortices. The basic operative procedure is similar to what is commonly performed for non-penetrating subdural grid placement in patients with intractable epilepsy, which is well tolerated and has few complications [35]. This surgery will be smaller in exposure given that coverage will be limited to the regions of interest, and not broadly applied as used for epilepsy localization. For placement of the 253-channel electrocorticography array, the craniotomy will be the same size as for the 128-channel array. The craniotomy will also be smaller in exposure compared with the broader exposure for epilepsy localization, which usually includes placement of two 128-channel electrocorticography arrays. Standard procedures for craniotomy at the surgical site will be followed. Briefly, a 5-6 cm curvilinear incision will be made over the anatomic hand representation of the cortex (i.e. “hand knob”) which is located 3 cm lateral to the midline. Localization will be confirmed using intraoperative BrainLab stereotactic neuronavigation. A craniotomy will then be performed, exposing the dural surface. A wide slit in the dura will be opened.

After identifying the location for the electrode grid implant, the position for the pedestal connector is determined on the adjacent or contra-lateral skull surface and marked. A separate 2 cm scalp incision will be made for the pedestal connector. Holes will be drilled for connector placement and the connector will be secured to the skull with 8 small titanium screws. Once the connector is placed, the electrodes and wire bundle are gently manipulated to position the electrodes so that they are resting on the cortical surface over the area of interest. The nonpenetrating ECoG microarray will be sutured to the dura to secure its position. After successful placement of the electrode grid, the dura will be sutured closed in a watertight fashion and the bone flap will be replaced and secured in place with standard titanium cranial fixation plates and screws.

The surgical site will be irrigated with antibiotic lactated ringers solution. The fascia and skin will be closed with absorbable sutures over the covered craniotomy with a slit accommodating the passage of the connector. The wound will be dressed with a sealed surgical bandage. The expected blood loss for this procedure is 50 cc. The expected operative time is 3-6 hours.

The ECoG electrode array is manufactured by PMT Corporation, and is already FDA-cleared for temporary (<30 days) clinical monitoring of neural signals (K082474). The PMT Subdural Cortical Electrodes are a chronically implantable array containing 128 or 253 electrodes, with an electrode spacing of 4 mm or 3mm, capable of recording from areas of the central nervous system for extended periods of time. The electrode contacts are composed of medical grade platinum iridium, and embedded in a thin sheet of medical grade silastic. The model number 2110 indicates a platinum iridium wire and platinum iridium contacts. Platinum iridium is a mechanically robust alloy electrode material used in commercial DBS leads (Petrossians, Whalen and Weiland 2016).

The electrodes’ contacts are molded into a silicone rubber matrix in a fixed pattern. PMT Corporation electrodes are used routinely at our institution and others for seizure localization. In the past ten years, we have not encountered any adverse inflammatory reactions or bleeding specific to the electrode arrays itself (over 100 cases). Insulated wires extend from each electrode through a flexible silicone tube to the connector on the pedestal.

Post-Operative Care: Subjects will be recovered in the intensive care unit and observed for 24 hours before transferring to the ward. A postoperative head CT will be obtained to evaluate for any hemorrhage and to confirm the position of the array. IV antibiotics (Kefzol will used if there are no allergies) will be administered for 24 hours after surgery, followed by prophylactic antibiotics given up to suture removal plus 2 days. Patients will be switched to oral antibiotics as soon as possible. Subjects will undergo physical exam every day with monitoring of vital signs, neurological exam, and basic respiratory, cardiac, and gastrointestinal exams. In addition, the wound site will be inspected at all study visits.

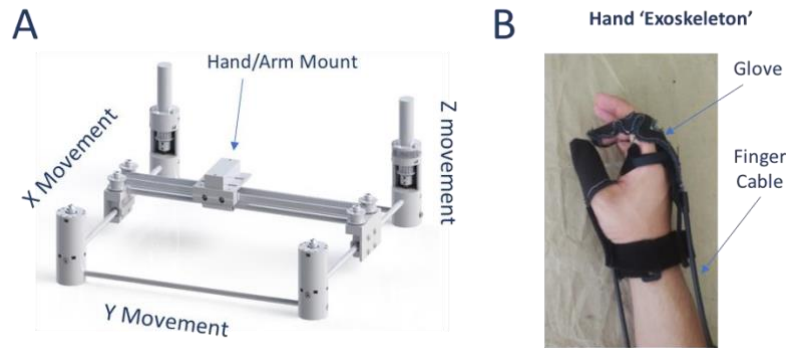
Routine hygiene will consist of handwashing with soap/water and donning gloves using sterile technique when coming in contact with the percutaneous connector. The caregiver and patient will be trained to clean the pedestal site according to specific instructions that will be given to them, to be performed at least once every seven days or as required.

An infection control protocol will be strictly followed. At early signs of infection or irritation the patient/caregiver should contact the study physician immediately. The surgical site will need to be cleaned twice or more during the day, while using extra meticulous hand hygiene. If skin erythema, edema, pain and/or warmth are present, the available drainage will be cultured and oral antibiotics will be started. Plain radiographs of the involved area, ESR, CRP, WBC, and blood cultures will be obtained. If there is no improvement within 72 hours, rapid progression of erythema, symptoms worsen, or if there are signs of systemic toxicity, parenteral antibiotics is warranted. If high fever or severe pain is present, nuchal rigidity, or progressive deterioration in level of consciousness, the participant should go to the hospital emergency room. All implanted hardware will be surgically removed if there is evidence of hardware infection.

Pain related to small craniotomies is usually self-limited. Pain scale ratings will be assessed every 4 hours and routine postoperative pain management will be used. This includes the following medications as needed: acetaminophen and/or Percocet (acetaminophen/hydrocodone). IV pain meds (morphine sulfate or dilaudid) will also be administered if needed. In our experience, most patients do not require IV analgesics beyond the first operative day for smaller craniotomies.

Study visits: As outlined above, system testing will occur through two phases. In the first phase, we will simply optimize the system; in the second phase, we will commence testing of the motor and communication neural interface systems.

In **Phase 1**, the main goal is to ensure reliable neural signal monitoring and optimization of the real-time systems. Initial study visits will occur at defined time points, similar to those normally used in clinical care. For example, we anticipate a visit at post-op day (POD) 10 and 14. During this time, we will simply monitor the neural signals and briefly test the real-time communication with the computer interface. We anticipate additional visits 1-3x/week, based on the patient's availability and preference, to continue to monitor signal stability and check for wound healing. During this phase, we will also offer in home testing of the system to minimize the burden. While the equipment may be kept at the subject's home, testing will only occur when study personnel are present. The total time period of Phase 1 will be approximately 1 months, the exact time will be customized for each patient.



In **Phase 2**, we will test feasibility for both neuroprosthetic control and for decoding speech from neural activity. We will begin to perform experimental testing with the system for control of assistive robotic arms including a custom wearable hand exoskeleton robot and a surface mounted robotic arm which can be classified as non-significant risk devices. As shown in panel A, the exoskeleton system consists of a table top frame that allows x,y,z movement of the arm/hand (i.e. supported by a brace attached to the platform mount). Movements are limited to the natural workspace of each subject. The hand exoskeleton (panel B) will be mounted using a readily releasable magnetic mount. The hand system aims to allow control of the fingers and thumb using a motorized cable system attached to motors. This system will allow us to test restoration of reach to grasp functions in our subjects. The surface mounted robotic arm is a commercially available investigational device for installation on wheelchairs of users with functional limitations or upper body disabilities. It is designed to support active tasks such as eating, drinking, and personal hygiene. There are three options available for control of the robotic arm, including joystick control, a graphical user interface, and an option offering developers to customize control of the robotic arm through a software interface. This system will allow us to test control of a surface mounted robotic assistive arm. However, for the purposes of this study, we will not mount the robotic arm on a wheelchair, but rather to a tabletop. There will be no direct physical contact between the Kinova robot arm and gripper and the participant. In addition, the participant is positioned greater than 48 inches away from the base of the robotic arm, rendering it physically impossible for the robot to contact the participant. As outlined in the Risk Analysis (Appendix B), we have multiple safety features to ensure that there is minimal risk for injury during the embodiment and use phase (i.e. the subjects interact with the exoskeleton and surface mounted robotic arm).

Throughout this period, neural signals will be recorded and analyzed, and tasks will be performed toward the development, assessment, and improvement of the neural interface system. We will assess quality of performance using kinematic parameters while performing required tasks. We will analyze stability of neural recordings and performance. To measure stability of the neural representation we will analyze the neural correlates of imagined movements. We will also examine the stability of neural correlates on neuroprosthetic control (e.g. spectral content, timing, spatial recruitment). We will assess changes in the spatial correlation scales and other redundancy measures during learning and stable performance. We anticipate that testing will be conducted in the outpatient office or home setting based on the patient's preference and needs.

In this phase, we will also continue to perform experimental testing with the system for control of a virtual communicating interface. Throughout this period, neural signals will be recorded and analyzed, and tasks will be performed toward the development, assessment, and improvement of the neural interface system. We will assess the ability to control a computer communication interface. To measure stability of the neural representation we will analyze the neural correlates of imagined speech. We will also examine the stability of neural correlates on a neuroprosthetic communication device (e.g. spectral content, timing, spatial recruitment).

Neural activity monitoring: Continuous neural signal data will be acquired from the 253 or 128channel implanted PMT Subdural Cortical Electrodes and processed with the Digital NeuroPort system hardware by Blackrock Microsystems. Broadly, the neural data will consist of ECoG neural activity from neurons in the vicinity of each recording electrode. The neural data will be actively monitored and recorded via the graphical user interface associated with the NeuroPort hardware commercially available via Blackrock. Data read and download are non-invasive and will be performed with the patient comfortably rested. For both the 128 and 253-channel system, the patient will have one or two high-definition multimedia interface (HDMI) connections from the digital headstage to the digital hub for data acquisition. To mitigate the risk of any pulling, snagging, or tension to this connection, we will position our patients such that there is no activity between the digital headstage and the digital hub. Additionally, to further mitigate any risk of head movement which could lead to pulling, we will offer our patients neck support during each session.

The NeuroPort system has been successfully deployed in monitoring neural activity in patients with motor control disorders (e.g. (Hochberg et al. 2012a, Pandarinath et al. 2015)). Blackrock Microsystems provides commercial software that allows real-time filtering, recording, and visualization of acquired neural data and also allows interfacing with other programming languages such as MATLAB (Mathworks, MA) or Python (Python Software Foundation, VA). Together, this allows the ability to create custom software such as communication device based on neural spiking activity, detailed further in the following section. Overall, the mix of commercial and custom software will allow for real-time signal processing, synchronization, and control of the peripheral communication device, with parallel data streams to store data for offline analyses.

Online BMI control of Assistive Robotic Arm Devices:

ECoG signals will be filtered and processed in real-time using a customized portable multi-channel neurophysiology workstation NeuroPort Biopotential Signal Processing System. We will bandpass each channel into multiple bands. Past experiments, including our own, suggest that movement related information is encoded in these bands.

Initialization Phase.

We will train a ‘decoder’ that maps neural activity to the movement of an assistive robotic arm device. Recent experiments suggest that such methods can rapidly allow control of neuroprosthetic devices. We will train the neural decoder using ‘imagined movements’. As paretic/paralyzed patients will not have access to normal overt movement related neural signals, we will use the neural basis of imagined movements for training. During the training phase, patients will observe a

computer screen with either a cursor or a simulated robotic arm. Initial online decoder performance can be assessed in this virtual environment. We will then aim to transition to physical control of the assistive robotic arm devices (with all the safety constraints outlined in this submission).

In order to compare visual versus visual + proprioceptive/tactile feedback signals during decoder conditioning, we will use the exoskeleton setup for decoder conditioning. The arm and hand will move in a stereotyped fashion while the subjects are instructed to ‘imagine’ actively tracking its path. Of note, we have experience with similar control of an exoskeleton system (Ganguly et al. 2011, Ganguly et al. 2009). As prior and as outlined below, the current system is developed by the Robert Matthews, PhD and Ruzena Bajcsy, PhD (UC Berkeley). They have long-standing experience with kinematic monitoring, limb dynamics and exoskeleton development (Matthew et al. 2015, Matthew et al. 2016, Oskarsson et al. 2016).

The training of the Kinova robot arm will occur with the arm mounted on a table in front of him. The participant will be positioned greater than 48 inches from the robot to be outside the physical reach of the robotic arm and to account for any error. In this case, the subject will be able to control the endpoint of the Kinova robot along with orientation of its gripper and the grasper. Participants will practice object interactions such as picking up a ball and moving it to a second location. Testing of the robotic arm will only be performed with research study personnel present. Participants and caregivers will not use the robotic arm outside of testing with study personnel. In addition, the Kinova robotic arm will only be powered by a wall electrical outlet, and not by battery power.

While testing is conducted with the table mounted robotic arm, experimenters will visualize all channels of data in real-time and monitor for large variations in the recorded neural signals to detect the presence of noise or artifacts that may suggest electromagnetic interference. Additionally, we have implemented detections to determine if the recorded signals significantly differ from historical values or the baseline values recorded at the start of the session. If significant variations are detected, we will power off the robotic arm to determine if it is the source of the noise.

Training Phase. Subjects will be allowed to practice tasks associated with arms/hand and object manipulation. The position of the robotic arm end effector coordinates (x, y, z) will be under direct neural control. Preliminary experiments with an exoskeleton system showed that end effector control (position and orientation of the wrist) was more intuitive and efficient than position control of individual joints. For this initial phase, the motion will be restricted to a 2-dimensional plane for reaching and grasping objects. There are currently 9 tasks which involve interactions with both static and dynamic environments with various fixtures. We will first limit movements to a 2D environment. The additional degree of freedom involving grasp will be included based on proficiency. In addition, given that ‘motivation’ and reward are known to influence the overall learning process, a gamed-based training environment with specific goals and scoring systems were developed to engage the subject intellectually and to provide additional enrichment during the training phase.

Testing Phase. To assess robustness and stability of control over days we will assess performance characteristics in three tasks. A) Standard center-out task where subjects have to move to the center, engage a grasp, then move to a target and disengage the grasp to release an object such as a ball.

The workspace will be at 95% of the patient's natural reach. Target size will be kept at 5 cm. B) Reaching from a randomized starting and end position in the workspace of Task A. C) Task B except with the need to plan around obstacles that are placed in the direct path.

Online BMI control: Also during phase 2, neural activity will be used to control a real-time communication device using state of the art closed-loop decoders based on rapid changes in neural activity (Shanechi, Orsborn and Carmena 2016). The main advantage of such a decoder lies in its enhanced ability in discriminating user intent and its speed of operating at every event. Such decoders operate at much higher speeds (typically at 200Hz) over previously developed decoders that rely on averaging neural activity (typically at 10Hz). In addition, we will compare this decoder to more standard decoders (e.g. the Weiner Filter, the LMS filter, the Kalman filter and variants). As documented below, the main outcome measure will be the rate of communication using these approaches.

A virtual communication effector will be presented on a computer screen, custom written in the MATLAB or Python programming environment. The interface between MATLAB or Python and the Digital NeuroPort system will be via custom software or commercial software provided by Blackrock Microsystems. The novel decoder will map neural activity to the communication interface. A language processing engine will be concurrently running in the background to model and predict the words and sentences. The following metrics will be utilized to measure performance of the decoder and communication device: selections per minute, accuracy, correct characters per minute (Bacher et al. 2015b) and the bitrate, an information theoretic approach to relate accuracy, time of task completion and complexity (Nuyujukian et al. 2014b, Thompson et al. 2014a). The performance of the novel decoder based communication device will be compared to traditional state space filtering decoders such as the Kalman Filter that has been previously successfully deployed in similar BMI paradigms (Gilja et al. 2012, Bacher et al. 2015b).

Development life cycle of the BMI motor control and communication software:

a) *Scope:* The intended use of the decoder is to allow the patient to achieve control of external devices and thereby select characters and letters to form sentences, as well as control assistive robotic arm devices. As such the operation of the BCI is therefore dependent on the functionality of the software.

b) *Platform:* The software will be developed on MATLAB (The Mathworks, MA) and MATLAB supported C/C++ compiled programs (MEX files) or (Python Software Foundation, VA) and will be running on the data acquisition PC that interfaces with the Blackrock NeuroPort Array pedestal connector or on a separate real-time processing machine (as in [Moses*, Metzger*, Liu* et al., 2021]). We will use the software libraries that are part of the Blackrock Digital NeuroPort system, potentially in coordination with custom software, to stream neural data into MATLAB or Python in real-time. All neural data will be streamed through the Blackrock Microsystems Neural Signal Processor before streamed by HDMI cord to MATLAB or Python in real-time.

c) *Inputs and outputs:* The inputs to the software will be the neural signals from the PMT Subdural Cortical Electrodes grid and the output of the software will consist of user controlled (via

the user's neural signals) effector position, selections of characters, letters and numbers for communication purposes, in addition to control of a movements of assistive robotic arms.

d) Components: There are four distinct aspects of the software, three that operate 'behind the scenes' and one that serves as a Graphical User Interface for display. First, is the decoder itself that translates neural signals into user intentions. Second, is another parallel decoder that serves to discriminate when the patient has made a particular selection (or e.g. grasping actions). Third, is the software engine that keeps track of the current selections made and generates a list of probable options using a statistical model of movement direction and language (Nadkarni, Ohno-Machado and Chapman 2011b). The fourth and final aspect of the decoder is the Graphical User Interface (GUI) that displays and controls the real-time position of the end effector.

e) Safety: The software provides only visual feedback to the user and does not directly interface with the neural signal data acquisition process. The software only serves to allow the use to control the communication interface and the robotic arm position.

f) Planning phase: In the planning phase, we will identify off-the-shelf components (such as language processing engines) and will aim to further refine and customize it in-house concurrently with the decoders and GUI.

g) Development phase: In the development phase, all components will be developed in parallel as discrete subunits of the overall functional system. A code repository will be maintained to keep track of the life cycle versions and code will be commented wherever appropriate. During the development phase, debugging will be performed at every iteration and documented. The documentation and code will be maintained on secure hard drives.

h) Testing phase: There are two aspects of this phase. One is the performance testing of each of the four individual components and the other is the testing of the entire software. In lieu of actual neural signals, simulated neural signals will be delivered as input, with a known mapping between the input and output state as the ground truth is known a priori. This will allow testing the performance of the decoders (accuracy in estimated positions). The testing of the GUI and the software engine will be performed independently of the decoders by manually controlling the position of the effector. The testing of the GUI and the software engine will be assessed by the stability and reliability in updating effector position and robotic arm movements, in the turnaround time of displaying the list of predictive words and actions based on current selections. The overall system testing will employ a combination of simulated neural signals and manual position control to assess the ability of the software in allowing a user to communicate and control a hand neuroprosthetic. *i) Error handling:* Code will be written to specifically monitor potential sources of errors in realtime decoding due to either noise in neural signals or decoder weight drift that would necessitate recalibration and resetting of the GUI and software engine.

j) Software validation: The validation and formal design review for the overall software will be performed by members of the PI's laboratory not involved with the development and testing of the software prior to software deployment.

k) Resolution and maintenance: Active documentation and daily logs will be noted to keep track of the performance of the software and address issues such as version control, robustness and immediate resolution of unforeseen errors in the software.

Progression of phases: We anticipate phase 1 will last approximately 1 month but will vary based on each subject. Phase 2 will last at a minimum 10-11 months, a total amount of time of at least 1 year after PMT Subdural Cortical Electrodes implantation and neural interface monitoring and testing, a timeframe which has been performed or exceeded without adverse effects by previous

studies using the PMT Subdural Cortical Electrodes and Blackrock Microsystems NeuroPort Array pedestal, and NeuroPort system. In this study, recordings were made over 666 days in a non-human primate with no adverse events related to the implanted devices (Degenhart et al. 2016). The ECoG array is identical in manufacture and material to that used for subdural grid placement in patients with intractable epilepsy, which is well tolerated and has few complications (Chang et al. 2010).

Activation of the brain recording function: All data collection in the study visits will be initiated by the study staff.

Conclusion of study: For each enrolled subject, if there have been no serious adverse events, we will present the option to continue with the study at the end of a 1-year period. If the subject chooses, we will continue with testing for another year. We will formally present this option every year for a period of 5 years. Notably, the subject will be reminded that he/she will have the option for surgical removal of the device at any point.

Removal of the ECoG grid and Connector pedestal: At the conclusion of the study, or earlier if medically indicated, the subdural cortical electrodes and connector pedestal will be surgically removed. The skin incision and bone flap will be reopened and the electrode will be removed and discarded. The dura will be sutured tightly. The galea and scalp will be sutured closed. The expected blood loss is minimal (less than 10 cc), and the expected operative time is 30 minutes.

7.0

Clinical Measurements

Primary

This is a pilot study to test feasibility in eight subjects.

For BCI motor control, we will use outcome measures that are frequently used in preclinical studies of neuroprostheses (e.g. accuracy and reliability of cursor and limb control). As outlined below, the primary goal will be to gather statistics regarding the best achievable control using ECoG signals and state-of-the-art methods to allow motor neuroprosthetic control. For each of the parameters below we aim to describe the statistics as the mean and the variance (Bacher et al. 2015a, Nadkarni et al. 2011a, Nuyujukian et al. 2014a, Shanechi et al. 2016, Thompson et al. 2014b). Ultimately, we will compare these values to a wealth of published data regarding movements in able-bodied subjects, e.g.(Bacher et al. 2015a).

1. *Quality of performance* will be assessed using kinematic parameters while performing the required tasks. We will assess stability of the trajectories in the tasks. We will then assess the ability for generalization from any region in the workspace to another random point. Position errors from the selected trajectory of the task as well as velocity and acceleration will be studied in both joint space and the end effector space.
2. *Recording and Performance Stability.* We will use previously established metrics to analyze stability of neural recordings (Shanechi et al. 2016, Thompson et al. 2014b) and performance. To measure stability of the neural representation we will analyze the neural correlates of daily imagined movements. We will also examine the stability of the neural correlates of neuroprosthetic movements (e.g. spectral content, timing, spatial recruitment).
3. *Spatial Scale.* An important question for ECoG recordings is the optimal spatial scale for the electrode grid. This has implications for maximizing the amount of information that can be obtained from the recording setup but also for defining the design specifications of implantable electronics (e.g. power requirements could vary greatly depending on the spatial and temporal resolution of the neural data required). We will look at changes in the spatial correlation scales and other redundancy measures during learning and stable performance.

The following metrics will further be utilized to measure performance of the decoder and communication device: selections per minute, accuracy, correct characters per minute (Bacher et al. 2015b) and the bitrate, an information theoretic approach to relate accuracy, time of task completion and complexity (Nuyujukian et al. 2014b, Thompson et al. 2014a). Physiological measurements related to neural activity will include statistical assessments of z-scored activity from single electrodes as well as population dynamics. Physiological measurements related to oscillatory activity will include: wide spectrum power-spectral analysis as well as using specific frequency

domain for mean log power (i.e. in the delta, theta, alpha, beta, gamma bands), coupling between the phase of low frequency rhythms and broadband gamma amplitude (phase-amplitude coupling, abbreviated PAC) (Canolty et al. 2006, Miller et al. 2010, Tort et al.).

Clinical measures and physiological measurements will be collected and recorded by members of the research and clinical team.

8.0

Data Management

All clinical and physiological data will be stored in encrypted and password-protected computers in the PI's laboratory that is always locked. If the Digital NeuroPort system is stored in the participant's residence, all research data will be maintained in accordance with UCSF standard encryption policy. In publications or presentations of the data, data will be grouped by case number in chronological order with no name identification. All patients will be asked to sign a separate consent for audio-video recording. When presenting videotape data at scientific conferences, we will utilize only videos from patients who have consented to have their videos shown. De-identified electrophysiological data may be shared with other researchers at other institutions.

9.0 Statistical Methods and Data Analysis

To assess the performance of the decoder, analyses will be performed on the kinematics associated with control, such as time to reach a target, trajectory curvature etc., in conjunction with measures associated with the communication device such as the bit rate, accuracy, characters per minute. The statistical reliability of the decoder will be assessed by non-parametric data permutation wherein the learned mapping between neural activity and the effector position will be artificially broken down and shuffled. Field potential data will be analyzed using wide spectrum power-spectral analysis as well as using specific frequency domain for mean log power (i.e. in the delta, theta, alpha, beta, gamma bands). We will also examine coherence and cross-frequency coupling between the channels (Canolty et al. 2006, Miller et al. 2010, Tort et al.). Using a repeated measures ANOVA statistical analysis, summary statistics for power in relevant frequency bands, control related power changes, and indices of phase-amplitude coupling will be compared at different timepoints of control. Additionally, bootstrap statistical tests and general linear mixed models can be utilized to investigate potential statistical effects, given the small sample size. Mean, median, variance and median absolute deviation describing the statistics of each of the measured outcomes (such as accuracy, effector position control) will be recorded for each subject.

Sample size calculation: This is a pilot study to assess the feasibility of an ECoG based implantable BCI device in patients with motor control disorders using intracranial recordings, a communication interface and assistive robotic arms. The collected pilot data will aid in determining the feasibility, reliability and future directions of the brain machine interface for communication and motor control. In addition, the pilot data will be used to formulate more detailed hypothesis on neural plasticity and BMI control in humans. As such, there is no formal sample size requirement for this pilot study.

Criteria for study success that would justify a larger subsequent trial:

1. Ability to use ECoG-based neural activity to control a neuroprosthetic device and communication interface.
2. No permanent serious adverse events occur (such as trauma with long-term motor deficit).
3. Benefits to the patient in regaining a sense of control over the ability to exert motor control and communicate in an efficient manner.

10.0

Regulatory Requirements

Prior to the start of the study, the following documents will be collected and filed:

- Signed protocol signature page
- Curriculum vitae of the PIs and Sub-investigators, updated within 2 years
- Current medical licenses for the PIs and all Sub-investigators
- Financial disclosure form signed by the PIs and all Sub-investigators
- Copy of the IRB approval letter for the study and the IRB Membership List
- Investigator Agreement

Investigator Obligations

Redacted will be responsible for ensuring that all study site personnel adhere to all FDA regulations and guidelines regarding clinical trials, including guidelines for GCP (including the archiving of essential documents), both during and after study completion.

Additionally, they are responsible for the subject's compliance to the study protocol.

All information obtained during the conduct of the study with respect to the patients' state of health will be regarded as confidential. This is detailed in the written information provided to the patient. An agreement for disclosure of any such information will be obtained in writing and will be signed by the patient.

Informed Consent

The investigators will obtain and document informed consent for each patient screened for this study. All patients will be informed in writing of the nature of the protocol and investigational therapy, its possible hazards, and their right to withdraw at any time, and will sign a form indicating their consent to participate prior to the initiation of study procedures.

Institutional Review Board

This protocol and relevant supporting data are to be submitted to the appropriate IRB for review and approval before the study can be initiated (UCSF, Human Research Protection Program, 3333 California Street, Suite 315, San Francisco, CA, 94118, FWA#00000068; IRB Registration 00000229, Lisa Denney, HRRP Director). Amendments to the protocol will also be submitted to the IRB prior to implementation of the change. The PIs are responsible for informing the IRB of the progress of the study and for obtaining annual IRB renewal. The IRB must be informed at the time of completion of the study and should be provided with a summary of the results of the study by the PIs. The PIs must notify the IRB in writing of any SAE or any unexpected AE according to ICH guidelines.

Data safety monitoring board (DSMB) and safety monitoring plan

Treatment emergent adverse events that are assessed by the principal investigators as possibly, probably, or definitely related to surgical implantation or chronic cortical recording AND are unexpected or meet seriousness criteria (death, immediately life threatening, hospitalization >24 hours, persistent or significant disability, or significant intervention required to prevent one of the previously-stated outcomes) will be recorded and reported to the IRB, device manufacturer and the FDA via the MedWatch online voluntary reporting form within 10 working days of the study team's knowledge of the event.

All such events will also be reported to the data safety monitor board (DSMB), *Redacted*, who does not have direct involvement in this study but who has expertise in implantable devices, pain management and neurosurgery. The DSMB will meet regularly to review data related to the clinical trial, provide guidance and feedback, and review any adverse event reports. Treatment-related adverse events assessed as definitely, probably, or possibly related to study procedures and either serious or unexpected, noted by any study personnel will be reported within 10 working days of their knowledge of the event to the DSMB. The DSMB will then advise the PI on potential changes in procedures to improve safety. The safety endpoint will consist of all adverse events.

A Data and Safety Monitoring Board (DSMB), which includes an independent Medical Monitor and Neuroethics expert, will regularly assess reports of unanticipated study-related events. As a part of the DSMB, the independent medical monitor will receive mandatory adverse event reporting in the same timeframe as the DSMB. Apart from this, a report of accumulated adverse event data will be provided on a quarterly basis to the independent medical monitor for review.

Surgical and/or non-Surgical protocol defined adverse events will be recorded on adverse event case report forms. Any serious or unanticipated adverse events will be promptly reported to the DSMB, NIDCD, IRB and FDA in line with regulatory policies.

Throughout the clinical trial, should a serious adverse event occur that is assessed to be related to the presence or surgical implantation of the electrode system, such as infection, the device will be removed and the study halted for the patient. Removal will be accomplished by re-opening the original incisions, temporary removal of the bone, and removal of the PMT Subdural Cortical Electrodes from the brain and NeuroPort Array pedestal from the skull. The dura will be re-sewn together and the bone fixed again with titanium screws

Furthermore, if there is a serious surgical or non-surgical adverse event, or with the onset of suicidality, the study will be halted for the patient.

If two patients meet one or more of these criteria (i. serious surgical or nonsurgery-related adverse event, or ii. onset of suicidality), the study will be halted until information is reviewed by the DSMB and FDA.

References

- Ajiboye, A. B., J. D. Simeral, J. P. Donoghue, L. R. Hochberg & R. F. Kirsch (2012) Prediction of imagined single-joint movements in a person with high-level tetraplegia. *IEEE Trans Biomed Eng*, 59, 2755-65.
- Anderson, K. D. (2004) Targeting recovery: priorities of the spinal cord-injured population. *J Neurotrauma*, 21, 1371-83.
- Bacher, D., B. Jarosiewicz, N. Y. Masse, S. D. Stavisky, J. D. Simeral, K. Newell, E. M. Oakley, S. S. Cash, G. Friehs & L. R. Hochberg (2015a) Neural Point-and-Click Communication by a Person With Incomplete Locked-In Syndrome. *Neurorehabil Neural Repair*, 29, 46271.
- Bacher, D., B. Jarosiewicz, N. Y. Masse, S. D. Stavisky, J. D. Simeral, K. Newell, E. M. Oakley, S. S. Cash, G. Friehs & L. R. Hochberg (2015b) Neural point-and-click communication by a person with incomplete locked-in syndrome. *Neurorehabilitation and neural repair*, 29, 462-471.
- Bensmaia, S. J. & L. E. Miller (2014) Restoring sensorimotor function through intracortical interfaces: progress and looming challenges. *Nat Rev Neurosci*, 15, 313-25.
- Birbaumer, N., N. Ghanayim, T. Hinterberger, I. Iversen, B. Kotchoubey, A. Kubler, J. Perelmouter, E. Taub & H. Flor (1999) A spelling device for the paralysed. *Nature*, 398, 297-8.
- Bouchard, K. E., N. Mesgarani, K. Johnson & E. F. Chang (2013) Functional organization of human sensorimotor cortex for speech articulation. *Nature*, 495, 327-32.
- Bouton, C. E., A. Shaikhoui, N. V. Annetta, M. A. Bockbrader, D. A. Friedenberg, D. M. Nielson, G. Sharma, P. B. Sederberg, B. C. Glenn, W. J. Mysiw, A. G. Morgan, M. Deogaonkar & A. R. Rezai (2016) Restoring cortical control of functional movement in a human with quadriplegia. *Nature*, 533, 247-50.
- Canolty, R. T., E. Edwards, S. S. Dalal, M. Soltani, S. S. Nagarajan, H. E. Kirsch, M. S. Berger, N. M. Barbaro & R. T. Knight (2006) High gamma power is phase-locked to theta oscillations in human neocortex. *Science*, 313, 1626-8.
- Carmena, J. M., M. A. Lebedev, R. E. Crist, J. E. O'Doherty, D. M. Santucci, D. F. Dimitrov, P. G. Patil, C. S. Henriquez & M. A. Nicolelis (2003) Learning to control a brain-machine interface for reaching and grasping by primates. *PLoS Biol*, 1, E42.
- Chang, E. F., J. W. Rieger, K. Johnson, M. S. Berger, N. M. Barbaro & R. T. Knight (2010) Categorical speech representation in human superior temporal gyrus. *Nat Neurosci*, 13, 1428-32.
- Chao, Z. C., Y. Nagasaka & N. Fujii (2010) Long-term asynchronous decoding of arm motion using electrocorticographic signals in monkeys. *Front Neuroengineering*, 3, 3.
- Chestek, C. A., V. Gilja, P. Nuyujukian, R. J. Kier, F. Solzbacher, S. I. Ryu, R. R. Harrison & K. V. Shenoy (2009) HermesC: Low-Power Wireless Neural Recording System for Freely Moving Primates. *Ieee Transactions on Neural Systems and Rehabilitation Engineering*, 17, 330-338.
- Churchland, M. M., J. P. Cunningham, M. T. Kaufman, J. D. Foster, P. Nuyujukian, S. I. Ryu & K. V. Shenoy (2012) Neural population dynamics during reaching. *Nature*, 487, 51-6.
- Collinger, J. L., S. Foldes, T. M. Bruns, B. Wodlinger, R. Gaunt & D. J. Weber (2013) Neuroprosthetic technology for individuals with spinal cord injury. *J Spinal Cord Med*, 36, 258-72.

- Degenhart, A. D., J. Eles, R. Dum, J. L. Mischel, I. Smalianchuk, B. Endler, R. C. Ashmore, E. C. Tyler-Kabara, N. G. Hatsopoulos, W. Wang, A. P. Batista & X. T. Cui (2016) Histological evaluation of a chronically-implanted electrocorticographic electrode grid in a non-human primate. *J Neural Eng*, 13, 046019.
- Ganguly, K. & J. M. Carmena (2009) Emergence of a stable cortical map for neuroprosthetic control. *PLoS Biol*, 7, e1000153.
- Ganguly, K., D. F. Dimitrov, J. D. Wallis & J. M. Carmena (2011) Reversible large-scale modification of cortical networks during neuroprosthetic control. *Nat Neurosci*, 14, 662-7.
- Ganguly, K., L. Secundo, G. Ranade, A. Orsborn, E. F. Chang, D. F. Dimitrov, J. D. Wallis, N. M. Barbaro, R. T. Knight & J. M. Carmena (2009) Cortical representation of ipsilateral arm movements in monkey and man. *J Neurosci*, 29, 12948-56.
- Gilja, V., C. A. Chestek, I. Diester, J. M. Henderson, K. Deisseroth & K. V. Shenoy (2011) Challenges and opportunities for next-generation intracortically based neural prostheses. *IEEE Trans Biomed Eng*, 58, 1891-9.
- Gilja, V., P. Nuyujukian, C. A. Chestek, J. P. Cunningham, M. Y. Byron, J. M. Fan, M. M. Churchland, M. T. Kaufman, J. C. Kao & S. I. Ryu (2012) A high-performance neural prosthesis enabled by control algorithm design. *Nature neuroscience*, 15, 1752-1757.
- Hochberg, L. R., D. Bacher, B. Jarosiewicz, N. Y. Masse, J. D. Simeral, J. Vogel, S. Haddadin, J. Liu, S. S. Cash & P. van der Smagt (2012a) Reach and grasp by people with tetraplegia using a neurally controlled robotic arm. *Nature*, 485, 372-375.
- Hochberg, L. R., D. Bacher, B. Jarosiewicz, N. Y. Masse, J. D. Simeral, J. Vogel, S. Haddadin, J. Liu, S. S. Cash, P. van der Smagt & J. P. Donoghue (2012b) Reach and grasp by people with tetraplegia using a neurally controlled robotic arm. *Nature*, 485, 372-5.
- Hochberg, L. R., M. D. Serruya, G. M. Friehs, J. A. Mukand, M. Saleh, A. H. Caplan, A. Branner, D. Chen, R. D. Penn & J. P. Donoghue (2006) Neuronal ensemble control of prosthetic devices by a human with tetraplegia. *Nature*, 442, 164-71.
- Homer, M. L., A. V. Nurmikko, J. P. Donoghue & L. R. Hochberg (2013) Sensors and decoding for intracortical brain computer interfaces. *Annu Rev Biomed Eng*, 15, 383-405.
- Huggins, J. E., P. A. Wren & K. L. Gruis (2011) What would brain-computer interface users want? Opinions and priorities of potential users with amyotrophic lateral sclerosis. *Amyotroph Lateral Scler*, 12, 318-24.
- Kennedy, P. R. (1994) 'Locked-in' patients. *Neurology*, 44, 366-7.
- Kennedy, P. R. & R. A. Bakay (1998) Restoration of neural output from a paralyzed patient by a direct brain connection. *Neuroreport*, 9, 1707-11.
- Kim, S. P., J. D. Simeral, L. R. Hochberg, J. P. Donoghue & M. J. Black (2008a) Neural control of computer cursor velocity by decoding motor cortical spiking activity in humans with tetraplegia. *Journal of Neural Engineering*, 5, 455-76.
- (2008b) Neural control of computer cursor velocity by decoding motor cortical spiking activity in humans with tetraplegia. *J Neural Eng*, 5, 455-76.
- Kubler, A., B. Kotchoubey, J. Kaiser, J. R. Wolpaw & N. Birbaumer (2001) Brain-computer communication: unlocking the locked in. *Psychol Bull*, 127, 358-75.
- Leuthardt, E. C., K. J. Miller, G. Schalk, R. P. Rao & J. G. Ojemann (2006) Electrocorticography-based brain computer interface--the Seattle experience. *IEEE Trans Neural Syst Rehabil Eng*, 14, 194-8.

- Leuthardt, E. C., G. Schalk, J. Roland, A. Rouse & D. W. Moran (2009) Evolution of braincomputer interfaces: going beyond classic motor physiology. *Neurosurg Focus*, 27, E4.
- Leuthardt, E. C., G. Schalk, J. R. Wolpaw, J. G. Ojemann & D. W. Moran (2004) A braincomputer interface using electrocorticographic signals in humans. *J Neural Eng*, 1, 6371.
- Matthew, R. P., E. J. Mica, W. Meinhold, J. A. Loeza, M. Tomizuka & R. Bajcsy (2015) Initial investigation into the effect of an Active/Passive exoskeleton on hammer curl performance in healthy subjects. *Conf Proc IEEE Eng Med Biol Soc*, 2015, 3607-10.
- Matthew, R. P., V. Shia, G. Venture & R. Bajcsy (2016) Generating physically realistic kinematic and dynamic models from small data sets: An application for sit-to-stand actions. *Conf Proc IEEE Eng Med Biol Soc*, 2016, 2173-2178.
- Miller, K. J., D. Hermes, C. J. Honey, M. Sharma, R. P. Rao, M. den Nijs, E. E. Fetz, T. J. Sejnowski, A. O. Hebb, J. G. Ojemann, S. Makeig & E. C. Leuthardt (2010) Dynamic modulation of local population activity by rhythm phase in human occipital cortex during a visual search task. *Front Hum Neurosci*, 4, 197.
- Monti, M. M., A. Vanhauzenhuyse, M. R. Coleman, M. Boly, J. D. Pickard, L. Tshibanda, A. M. Owen & S. Laureys (2010) Willful modulation of brain activity in disorders of consciousness. *N Engl J Med*, 362, 579-89.
- Morrell, M. J. & R. N. S. S. i. E. S. Group (2011) Responsive cortical stimulation for the treatment of medically intractable partial epilepsy. *Neurology*, 77, 1295-304.
- Moses, D.A., Metzger, S.L., Liu, J.R., et al., (2021) Neuroprosthesis for Decoding Speech in a Paralyzed Person with Anarthria. *N Engl J Med*, 385, 217-227.
- Nadkarni, P. M., L. Ohno-Machado & W. W. Chapman (2011a) Natural language processing: an introduction. *J Am Med Inform Assoc*, 18, 544-51.
- Nadkarni, P. M., L. Ohno-Machado & W. W. Chapman (2011b) Natural language processing: an introduction. *Journal of the American Medical Informatics Association*, 18, 544-551.
- Nicolelis, M. A. & M. A. Lebedev (2009) Principles of neural ensemble physiology underlying the operation of brain-machine interfaces. *Nat Rev Neurosci*, 10, 530-40.
- Nuyujukian, D. S., J. Voutsinas, L. Bernstein & S. S. Wang (2014a) Medication use and multiple myeloma risk in Los Angeles County. *Cancer Causes Control*, 25, 1233-7.
- Nuyujukian, P., J. C. Kao, J. M. Fan, S. D. Stavisky, S. I. Ryu & K. V. Shenoy (2014b) Performance sustaining intracortical neural prostheses. *Journal of neural engineering*, 11, 066003.
- Oskarsson, B., N. C. Joyce, E. De Bie, A. Nicorici, R. Bajcsy, G. Kurillo & J. J. Han (2016) Upper extremity 3-dimensional reachable workspace assessment in amyotrophic lateral sclerosis by Kinect sensor. *Muscle Nerve*, 53, 234-41.
- Pandarinath, C., V. Gilja, C. H. Blabe, P. Nuyujukian, A. A. Sarma, B. L. Sorice, E. N. Eskandar, L. R. Hochberg, J. M. Henderson & K. V. Shenoy (2015) Neural population dynamics in human motor cortex during movements in people with ALS. *Elife*, 4, e07436.
- Pasley, B. N., S. V. David, N. Mesgarani, A. Flinker, S. A. Shamma, N. E. Crone, R. T. Knight & E. F. Chang (2012) Reconstructing speech from human auditory cortex. *Plos Biology*, 10, e1001251.
- Schalk, G., K. J. Miller, N. R. Anderson, J. A. Wilson, M. D. Smyth, J. G. Ojemann, D. W. Moran, J. R. Wolpaw & E. C. Leuthardt (2008) Two-dimensional movement control using electrocorticographic signals in humans. *J Neural Eng*, 5, 75-84.

- Schwartz, A. B. (2004) Cortical neural prosthetics. *Annu Rev Neurosci*, 27, 487-507.
- Schwartz, A. B., X. T. Cui, D. J. Weber & D. W. Moran (2006) Brain-controlled interfaces: movement restoration with neural prosthetics. *Neuron*, 52, 205-20.
- Selzer, M. E., S. Clarke, L. G. Cohen, G. Kwakkel & R. H. Miller. 2014. *Textbook of neural repair and rehabilitation*. Cambridge: Cambridge University Press.
- Shanechi, M. M., A. L. Orsborn & J. M. Carmena (2016) Robust Brain-Machine Interface Design Using Optimal Feedback Control Modeling and Adaptive Point Process Filtering. *PLoS Comput Biol*, 12, e1004730.
- Shenoy, K. V. & J. M. Carmena (2014) Combining decoder design and neural adaptation in brain-machine interfaces. *Neuron*, 84, 665-80.
- Simeral, J. D., S. P. Kim, M. J. Black, J. P. Donoghue & L. R. Hochberg (2011) Neural control of cursor trajectory and click by a human with tetraplegia 1000 days after implant of an intracortical microelectrode array. *J Neural Eng*, 8, 025027.
- Slutzky, M. W., L. R. Jordan, E. W. Lindberg, K. E. Lindsay & L. E. Miller (2011) Decoding the rat forelimb movement direction from epidural and intracortical field potentials. *J Neural Eng*, 8, 036013.
- Spataro, R., M. Ciriaco, C. Manno & V. La Bella (2014) The eye-tracking computer device for communication in amyotrophic lateral sclerosis. *Acta Neurol Scand*, 130, 40-5.
- Taylor, D. M., S. I. Tillery & A. B. Schwartz (2002) Direct cortical control of 3D neuroprosthetic devices. *Science*, 296, 1829-32.
- Thompson, D. E., L. R. Quitadamo, L. Mainardi, S. Gao, P.-J. Kindermans, J. D. Simeral, R. Fazel-Rezai, M. Matteucci, T. H. Falk & L. Bianchi (2014a) Performance measurement for brain-computer or brain-machine interfaces: a tutorial. *Journal of neural engineering*, 11, 035001.
- Thompson, D. E., L. R. Quitadamo, L. Mainardi, K. U. Laghari, S. Gao, P. J. Kindermans, J. D. Simeral, R. Fazel-Rezai, M. Matteucci, T. H. Falk, L. Bianchi, C. A. Chestek & J. E. Huggins (2014b) Performance measurement for brain-computer or brain-machine interfaces: a tutorial. *J Neural Eng*, 11, 035001.
- Tort, A. B., R. Komorowski, H. Eichenbaum & N. Kopell (2010) Measuring phase-amplitude coupling between neuronal oscillations of different frequencies. *J Neurophysiol*, 104, 1195-210.
- Wolpaw, J. R., N. Birbaumer, D. J. McFarland, G. Pfurtscheller & T. M. Vaughan (2002) Brain-computer interfaces for communication and control. *Clin Neurophysiol*, 113, 767-91.

Summary of Changes

1. Correction to our Clinical Protocol (page 30) wording to make it more precise and reflect the intended and appropriate device explanation criteria.

Before Correction:

“Throughout the clinical trial, should a serious adverse event occur that is assessed to be surgery related or not, or related to the presence of the electrode system, such as infection, the device will be removed and the study halted for the patient.”

After Correction:

“Throughout the clinical trial, should a serious adverse event occur that is assessed to be related to the presence or surgical implantation of the electrode system, such as infection, the device will be removed and the study halted for the patient.”

2. Change from the Blackrock Microsystems NeuroPort Biopotential Signal Processing system, otherwise known as the NeuroPort system (K060523, K090957), to utilize the newest versions of the Front End Amplifier and its power supply, and the Patient Cable, which are the Digital Hub 128, its power supply, and the NeuroPlex E, respectively.
3. Minor corrections to the wording of several exclusion criteria.

Before correction:

- Co-morbidities including ongoing anticoagulation, uncontrolled hypertension, cancer, or major organ system failure.
- History of substance abuse
- History of suicide attempt or suicidal ideation
- Allergies or known hypersensitivity to materials in the Blackrock NeuroPort Array pedestal (i.e. silicone, titanium) or the PMT Subdural Cortical Electrode (i.e. silicone, platinum iridium, nichrome)

After correction:

- Co-morbidities including uncontrolled hypertension, cancer, or major organ system failure.
 - Ongoing anticoagulation which cannot be stopped in the peri-procedural period.
 - History of substance abuse within the last year.
 - History of suicide attempt or suicidal ideation within one’s lifetime prior to enrollment, confirmed by a baseline negative Columbia Suicide Severity Rating Scale (C-SSRS).
 - Allergies or known hypersensitivity to materials in the Blackrock NeuroPort Array pedestal or Blackrock 256-channel pedestal (i.e. silicone, titanium) or the PMT Subdural Cortical Electrode (i.e. silicone, platinum iridium, nichrome).
4. Addition of PMT Corporation 253-channel 3-mm-pitch electrocorticography array and the Blackrock Microsystems 256-channel connector pedestal and digital headstage to the clinical protocol.

5. Addition of the assistive robotic arm device to the clinical protocol to supplement the existing arm exoskeleton device.
6. Removal of “History of seizures” from the exclusion criteria.
7. Minor correction to wording in the surgical plan to specify laterality of device placement to the dominant (usually left) hemisphere.
8. Changes to the responsibilities of the Data Safety and Monitoring Board, including addition of an independent Medical Monitor and a Neuroethics expert who will assist in monitoring this study and additional adverse-event reporting requirements.
9. Minor correction to the software plan to specify that Python will be used to present the virtual communication effector and as the interface with the Digital NeuroPort system.

Note about the exploratory nature of the clinical trial

The following note is taken verbatim from a supplementary clinical-protocol file included in our prior publication. The reference for this publication is given at the end of the note.

This clinical trial is a Phase I single-center early feasibility study to evaluate the potential of ECoG-based neural interfaces for controlling advanced neuroprostheses that restore motor and communicative functions. Due to the exploratory nature of the trial and the limited number of trial participants, we did not pre-define specific methods and algorithms to evaluate using specific metrics. This is reflected in the primary endpoints for the efficacy assessments of the clinical trial, which are stated in the protocol as “Feasibility of control of a wearable exoskeleton device and a communication interface.”

As a result, a variety of analysis methods will be applied to the datasets collected with the trial participants throughout the trial. Additionally, we did not formalize a statistical analysis plan alongside the protocol. In any reports (publications, presentations, etc.) of analyses that involve data collected as part of this clinical trial, the selection, measurement, statistical testing, and interpretation of outcome metrics will be informed by the relevant literature and performed to the highest standard of analytic and statistical rigor. This includes the present work, which describes a proof-of-concept spelling system controlled by silent attempts to speak and an ECoG-based neural interface with a single participant.

Metzger, S. L., J. R. Liu, D. A. Moses, M. E. Dougherty, M. P. Seaton, K. T. Littlejohn, J. Chartier, G. K. Anumanchipalli, A. Tu-Chan, K. Ganguly & and E. F. Chang (2022) Generalizable Spelling Using a Speech Neuroprosthesis in an Individual with Severe Limb and Vocal Paralysis. *Nature Communications*, 13(1), 6510.

Table 1 CENT 2015 checklist*; CONSORT 2010 checklist items with modifications or additions for individual or series of N-of-1 trials; empty items in the CENT 2015 column indicate no modification from the CONSORT 2010 item

Section/ Topic	CONSORT 2010		CENT 2015	
	No	Item	No	Item
Title and abstract				
	1a	<p>Identification as a randomised trial in the title</p> <p>This is a single-center early feasibility study of the use of an ECoG-based neural interface to test the feasibility of ECoG signals to control devices for motor and speech control in adults affected by neurological disorders of movement. Each participant receives the same intervention. As such, this is not a randomized trial.</p>	1a	<p>Identify as an “N-of-1 trial” in the title</p> <p>For series: Identify as “a series of N-of-1 trials” in the title</p>
	1b	<p>Structured summary of trial design, methods, results, and conclusions (for specific guidance see CONSORT for abstracts)</p> <p>The PMT Subdural Cortical Electrode array, bonded to the Blackrock Microsystems NeuroPort array pedestal or Blackrock Microsystems 253-channel array pedestal will be surgically placed directly on the surface of the brain in regions responsible for speech production and language perception in participants with disorders of motor control. Following surgical implantation of the array and pedestal, the NeuroPort Biopotential Processing System will be connected to the Blackrock Microsystems Neuroport array pedestal or 253ch pedestal to monitor cortical signals. With this ECoG-based neural interface, study participants will take part in recording sessions with researchers to train and assess their ability to control assistive robotic arms and communication outputs. This will be performed in two phases with clinical trial participants.</p> <p><u>Phase 1: Optimize BCI system</u></p> <p>In Phase 1, we will start with preliminary testing to optimize the system to reliably detect neural activity to ensure that the recorded signals are stable and free of artifacts. During this phase, we will work to ensure that we can control both the motor and speech control parts of the study. Based on patient preferences, this phase will be conducted in the outpatient office setting and/or the patient’s home environment, based on patient preference and needs. This phase will likely take around one month, however, this may be longer or shorter for each subject depending on level of subject control.</p>	1b	<p><i>For specific guidance, see CENT guidance for abstracts (table 2)</i></p>

Phase 2: Testing of BCI Control

In Phase 2, we will test feasibility for both neuroprosthetic control and for decoding speech from neural activity. We will begin this phase with testing to improve neuroprosthetic control with the robotic arm. As outlined in the sections below, we have multiple safety features to ensure that there is minimal risk for injury during use of the robotic arms, including subject contact during object interaction and the embodiment phase (i.e. the subjects arm is interacting with the exoskeleton). Throughout this period, neural signals will be recorded and analyzed, and tasks will be performed toward the development, assessment, and improvement of the neural interface system. We will assess quality of performance using kinematic parameters while performing required tasks. We will analyze stability of neural recordings and performance. To measure stability of the neural representation we will analyze the neural correlates of imagined movements. We will also assess changes in spatial correlation scales and other redundancy measures during learning and stable performance. We anticipate that testing will continue to be conducted in the outpatient office or home setting based on the patient's preference and needs.

In phase II, we will also continue to perform experimental testing for control of the virtual communication interface. Throughout this period, neural signals will continue to be recorded and analyzed, and tasks will be performed toward the development, assessment, and improvement of the communication interface.

Introduction

Background
and objectives

2a

Scientific background and explanation of rationale

2a.1

Restoration of function with assistive robotic arms and a communication interface are important goals of BCIs. Multiple neurological disorders can result in severe bilateral upper limb weakness or paralysis. Surveys of patients with quadriplegia provide important guidance about specific rehabilitation needs and preferences as well as targets for intervention. A survey of patients with tetraplegia resulting from SCI found that restoration of arm and hand function was of highest priority (Anderson 2004). Similarly, patients with ALS reported that direct neural control of a robotic arm would be of great importance (Huggins, Wren and Gruis 2011). While there has been extensive research into each disease process, little has been proven to be clinically effective for the rehabilitation of this chronic disability (Wolpaw et al. 2002).

In patients with conditions such as high cervical SCI, basilar strokes or advanced ALS, the effects can be particularly devastating as tetraplegia may be accompanied by paralysis of oral structures, leading to the loss of voluntary vocal function. Individuals with severe traumatic brain injury or high cervical injuries who require mechanical ventilation may also have limited capacity to communicate (Kennedy 1994,

Kubler et al. 2001, Monti et al. 2010). Standard augmentative and alternative communication (AAC) devices are widely available but may not be suitable for individuals with severe or complete paralysis of the voluntary motor system (Selzer et al. 2014). For example, the most commonly used devices are gaze trackers that allow computer cursor control through eye movements (Spataro et al. 2014). However, eye tracking may have a limited role in advanced cases of ALS and after brainstem strokes, where eye movements are frequently affected (Birbaumer et al. 1999, Kennedy and Bakay 1998). They also require sustained visual attention and may create a high cognitive burden. Thus, it remains critical to develop novel technologies to help restore communication as well as upper limb function.

Brain-Computer Interfaces (BCIs) are a very promising method to significantly improve quality of life by restoring upper extremity function and communication ability in patients with motor and speech disabilities. Over the past decade, the rate and sophistication of research involving invasive BCIs have rapidly increased. BMIs have the potential to seamlessly integrate the computational power of artificial electronic systems with that of the nervous system. Multiple neural signals can be used in a BCI, including non-invasive EEG signals and other neural signals such as spikes and electrocorticography (ECoG) that require invasive placement of electrodes. Non-invasive BCIs have been studied for at least two decades. Known limitations of surface EEG recordings are a low 'signal-to-noise' and contamination by muscle activity (Wolpaw et al. 2002). Recent studies suggest that BMIs using invasive recording of neural signals (spikes or ECoG) can allow more rapid intuitive control over complex devices (Carmena et al. 2003, Leuthardt et al. 2009, Leuthardt et al. 2004, Schwartz et al. 2006, Taylor, Tillery and Schwartz 2002). A large basic science and clinical effort is currently devoted to BMIs based on invasive recordings of action potentials. However, it is increasingly clear that there are significant limits on possible translation of spikes based recordings. It does not readily permit reliable long-term recordings (Chestek et al. 2009, Ganguly and Carmena 2009, Gilja et al. 2011, Hochberg et al. 2006).

Electrocorticography (ECoG) offers a promising alternative for BMIs (Pasley et al. 2012, Bouchard et al. 2013, Slutzky et al. 2011, Leuthardt et al. 2006, Ganguly et al. 2009). ECoG has the potential to serve as a robust source of neural signals that can be integrated into a clinically viable device. Specifically, it can be: (1) stably recorded over long-periods of time, (2) possesses sufficient 'signal-to-noise' and (3) is known to be rich in information about neural processes, (4) can allow long-term rapid control of multiple degrees of freedom (DOF). Because ECoG arrays lie on the brain surface, they can be stably monitored for very long periods of time (Nadkarni, Ohno-Machado and Chapman 2011a, Thompson et al. 2014b). This approach has been demonstrated clinically in tens of thousands of patients that have had arrays or stimulating electrodes made of the same materials implanted for years (for indications such as pain, movement disorders, or newer closed loop devices for epilepsy) (Nadkarni et al. 2011a).

			2a.2	Rationale for using N-of-1 approach
	2b	Specific objectives or hypotheses	2b	
		<p>In eight patients with severe disorders of movement control, we will surgically implant PMT Subdural Cortical Electrodes on the brain surface over the motor and language cortices. The electrode will be bonded to a Blackrock NeuroPort Array pedestal or Blackrock 253ch pedestal which can be connected to the Digital NeuroPort system to process and record neural activity in real time. Using this neural interface, we will condition the patient to be able to control assistive robotic arms, communicate with a computer system for typing and perform speech output tasks. We will utilize optimal neural plasticity mechanisms, a novel framework, and advanced language modeling during BCI conditioning.</p> <p>The underlying hypothesis is that ECoG recordings will allow severely paralyzed individuals to control complex neuroprosthetic devices for movement and communication. A closely related hypothesis is that the well-known stability of ECoG signals will allow us to maximally engage neural mechanism of plasticity and thereby optimize long-term skilled acquisition.</p>		
Methods				
Trial design	3a	Description of trial design (such as parallel, factorial) including allocation ratio	3a	Describe trial design, planned number of periods, and duration of each period (including run-in and wash out, if applicable)
		This is an early-feasibility, single-arm clinical trial. We will enroll a cohort of 8 subjects where we propose to record and monitor neural signals using subdural cortical electrodes.		<i>In addition for series:</i> Whether and how the design was individualized to each participant, and explain the series design
	3b	Important changes to methods after trial start (such as eligibility criteria), with reasons	3b	

Participant(s)	4a	<p>Since the trial start, we have made a few changes to eligibility criteria to ensure we capture a representative patient population.</p> <ol style="list-style-type: none"> 1. Added upper age limit of 75 to reduce the risk of enrolling patients with higher change of age-related cognitive decline 2. Included patients with spastic quadriplegic cerebral palsy (with no significant cognitive deficits based on formal neuropsychological testing) to ensure we include patients with disability due to a variety of neurological disorders 3. Added exclusion criteria to exclude patients with uncontrolled hypertension from the protocol, and to ensure patients taking anticoagulation medications can safely stop them during the perioperative period. Both of these modifications were done to ensure that surgical risk is minimized. 4. Removed history of seizures from inclusion criteria, as several participants may have had seizures which are now well controlled or absent, as well as the fact that our study device is used clinically for treatment of seizures. 5. Updated study device to include the 253ch electrocorticography array with 3mm spacing and the Blackrock Microsystems 253ch pedestal to the study protocol. This change was made to increase cortical coverage and increase density. <p>Eligibility criteria for participants</p> <p><u>Inclusion Criteria</u></p> <ul style="list-style-type: none"> ● Age 21-75 years old ● Limited ability to use upper limbs and limited ability to use speech, based on neurological examination by a board-certified neurological specialist, due to stroke, spastic quadriplegic cerebral palsy (with no significant cognitive deficits based on formal neuropsychological testing), amyotrophic lateral sclerosis (ALS), multiple sclerosis, cervical spinal cord injury, brainstem stroke, muscular dystrophy, myopathy or severe neuropathy ● Disability, defined by a 4 or greater score on the Modified Rankin Scale, must be severe enough to cause loss of independence and inability to perform activities of daily living. ● If stroke or spinal cord injury, at least 1 year has passed since onset of symptoms ● Must live within a two-hour drive of UCSF <p><u>Exclusion Criteria</u></p> <ul style="list-style-type: none"> ● Pregnancy or breastfeeding ● Inability to understand and/or read English ● Inability to give consent ● Dementia, based on history, physical exam, and MMSE 	4a†	<p>Diagnosis or disorder, diagnostic criteria, comorbid conditions, and concurrent therapies.</p> <p>For series: Same as CONSORT item 4a</p>
----------------	----	--	-----	---

-
- Active depression (BDI > 20) or other psychiatric illness (active general anxiety disorder, schizophrenia, bipolar disorder, obsessive-compulsive disorder (OCD), or personality disorders (e.g. multiple personality disorder, borderline personality disorder, etc.)
 - History of suicide attempt or suicidal ideation within one's lifetime prior to enrollment, confirmed by a baseline negative Columbia Suicide Severity Rating Scale (C-SSRS)
 - Comorbidities including uncontrolled hypertension, cancer, or major organ system failure.
 - History of intracranial surgery
 - History of substance abuse within the last year
 - Ongoing anticoagulation which cannot be stopped in the peri-procedural period.
 - Inability to comply with study follow-up visits
 - Immunocompromised
 - Has an active infection
 - Has a CSF drainage system or an active CSF leak
 - Requires diathermy, electroconvulsive therapy (ECT), or transcranial magnetic stimulation (TMS) to treat a chronic condition
 - Has an implanted electronic device such as a neurostimulator, cardiac pacemaker/defibrillator or medication pump

4b Settings and locations where the data were collected

4b†

- University of California, San Francisco Medical Center
505 Parnassus Ave
San Francisco, CA 94143
- UCSF Sandler Neuroscience Center
675 Nelson Rising Lane
San Francisco, CA 94143
- UCSF Joan and Sanford I. Weill Neurosciences Building
1651 4th Street
San Francisco, CA 94158
- St. Mary's Medical Center
450 Stanyan St, San Francisco, CA 94117
- The home of each participant.
- Medical office at 181 Andrieux St, Sonoma, CA 95476

4c Whether the trial(s) represents a research study

			and if so, whether institutional ethics approval was obtained	
Interventions	5	<p>The interventions for each group with sufficient details to allow replication, including how and when they were actually administered</p> <p>As mentioned above, this is an early-feasibility, phase I, pilot clinical trial with only one group. Each participant undergoes surgical implantation of intracranial electrodes for the purpose of testing the feasibility of using ECoG signals to control complex devices for motor and speech control in adults affected by neurological disorders of movement.</p> <p>Following implantation of the electrode and pedestal, the NeuroPort Biopotential Processing System will be connected to the NeuroPort Array pedestal or Blackrock Microsystem 253ch pedestal to monitor and record neural signals. With this ECoG-based neural interface, study patients will undergo training and assessment of their ability to control assistive robotic arms and to determine if ECoG brain signals can be decoded for communication and motor control.</p>	5	The interventions for each period with sufficient details to allow replication, including how and when they were actually administered
Outcomes	6a	<p>Completely defined pre-specified primary and secondary outcome measures, including how and when they were assessed</p> <p><u>Primary Endpoints:</u> Feasibility of control of assistive robotic arms and a communication interface.</p> <p>Safety Assessments:</p> <ul style="list-style-type: none"> • Physical examination at all study visits • Perform functional test of the PMT/Blackrock combined neural interface system prior to implantation • Surgical/ or nonsurgical protocol-defined adverse events recorded on adverse events case report forms and use of protocol-defined procedures for adverse event management • Assessment of suicidality using Columbia Suicide Severity Rating Scale, and assessment of changes using the Beck Depression and Anxiety Inventories, at monthly intervals. 	6a.1	
			6a.2	Description and measurement properties

		(validity and reliability) of outcome assessment tools
	6b Any changes to trial outcomes after the trial commenced, with reasons	6b
	N/A	
Sample size	7a How sample size was determined	7a
	<p>Sample size calculation: This is a pilot study to assess the feasibility of an ECoG based implantable BCI device in patients with motor control disorders using intracranial recordings, a communication interface and assistive robotic arms. The collected pilot data will aid in determining the feasibility, reliability and future directions of the brain machine interface for communication and motor control. In addition, the pilot data will be used to formulate more detailed hypothesis on neural plasticity and BMI control in humans. As such, there is no formal sample size requirement for this pilot study.</p>	
	7b When applicable, explanation of any interim analyses and stopping guidelines	7b
	<p>As this is an early feasibility, phase I, pilot clinical trial, there are no interim planned analyses.</p> <p>Stopping guidelines:</p> <p>Surgical and/or non-Surgical protocol defined adverse events will be recorded on adverse event case report forms. Any serious or unanticipated adverse events will be promptly reported to the DSMB, NIDCD, IRB and FDA in line with regulatory policies.</p> <p>Throughout the clinical trial, should a serious adverse event occur that is assessed to be related to the presence or surgical implantation of the electrode system, such as infection, the device will be removed and the study halted for the patient. Removal will be accomplished by re-opening the original incisions, temporary removal of the bone, and removal of the PMT Subdural Cortical Electrodes from the brain and NeuroPort Array pedestal from the skull. The dura will be re-sewn together and the bone fixed again with titanium screws</p> <p>Furthermore, if there is a serious surgical or non-surgical adverse event, or with the onset of suicidality, the study will be halted for the patient.</p>	

If two patients meet one or more of these criteria (i. serious surgical or nonsurgery-related adverse event, or ii. onset of suicidality), the study will be halted until information is reviewed by the DSMB and FDA.

Randomisation:

Sequence generation	8a	Method used to generate the random allocation sequence N/A, not a randomized trial.	8a	Whether the order of treatment periods was randomised, with rationale, and method used to generate allocation sequence
	8b	Type of randomisation; details of any restriction (such as blocking and block size) N/A, not a randomized trial	8b	When applicable, type of randomisation; details of any restrictions (such as pairs, blocking)
			8c	Full, intended sequence of periods
Allocation concealment mechanism	9	Mechanism used to implement the random allocation sequence (such as sequentially numbered containers), describing any steps taken to conceal the sequence until interventions were assigned N/A	9	
Implementation	10	Who generated the random allocation sequence, who enrolled participants, and who assigned participants to interventions	10	
		As mentioned above, this study is an early feasibility, phase I, pilot clinical trial. As such, there is no random allocation sequence applied. Participants are enrolled by the study PI with assistance from IRB approved study clinicians and research coordinators.		
Blinding	11a	If done, who was blinded after assignment to interventions (for example, participants, care providers, those assessing outcomes) and how	11a	

	N/A		
	11b	If relevant, description of the similarity of interventions	11b
	N/A		
Statistical methods	12a	Statistical methods used to compare groups for primary and secondary outcomes As mentioned above, this is an early feasibility, phase I, pilot clinical trial. As such, there are no separate groups for comparison. To work towards our primary objective of feasibility of an ECoG-based neuroprosthesis for motor and communication restoration, we perform analyses to assess the overall performance overtime. The statistical reliability of the decoder will be assessed by non-parametric data permutation wherein the learned mapping between neural activity and the effector position will be artificially broken down and shuffled. Field potential data will be analyzed using wide spectrum power-spectral analysis as well as using specific frequency domain for mean log power (i.e. in the delta, theta, alpha, beta, gamma bands).	12a Methods used to summarize data and compare interventions for primary and secondary outcomes
	12b	Methods for additional analyses, such as subgroup analyses and adjusted analyses	12b
	N/A		<i>For series:</i> If done, methods of quantitative synthesis of individual trial data, including subgroup analyses, adjusted analyses, and how heterogeneity between participants was assessed, (for specific guidance on reporting syntheses of multiple trials, please consult the PRISMA Statement)

			12c	Statistical methods used to account for carryover effect, period effects, and intra-subject correlation
Results				
Participant flow (a diagram is strongly recommended)	13a	For each group, the numbers of participants who were randomly assigned, received intended treatment, and were analysed for the primary outcome As this is an early feasibility, phase I, pilot clinical trial, each patient receives the same treatment, and are assessed as described above for the primary outcome. We have enrolled three participants in total, with two active participants. Both received the same intervention and were assessed for the same primary outcome.	13a.1	Number and sequence of periods completed, and any changes from original plan with reasons
			13a.2	For series: The number of participants who were enrolled, assigned to interventions, and analysed for the primary outcome
	13b	For each group, losses and exclusions after randomisation, together with reasons N/A	13c	For series: losses or exclusions of participants after treatment assignment, with reasons, and period in which this occurred, if applicable
Recruitment	14a	Dates defining the periods of recruitment and follow-up	14a†	

Recruitment began during October of 2018, with enrollment of the participant included in these analyses in September 2022. The current participant will be offered the option to continue in the trial for a maximum length of five years.

General Recruitment Protocol:

Patients with motor impairments secondary to neurological disorders will be recruited from clinics specializing in the treatment of stroke, ALS, and general neurological disorders at UCSF.

For each enrolled subject, if there have been no serious adverse events, we will present the option to continue with the study at the end of a 1-year period. If the subject chooses, we will continue with testing for another year. We will formally present this option every year for a period of 5 years. Notably, the subject will be reminded that he/she will have the option for surgical removal of the device at any point.

	14b	Why the trial ended or was stopped N/A	14b	Whether any periods were stopped early and/or whether trial was stopped early, with reason(s).
Baseline data	15	A table showing baseline demographic and clinical characteristics for each group One participant is included in our one group. Participant was 47 years old at enrollment who suffered a brainstem stroke at the age of 30 years old after which she was diagnosed with quadriplegia and anarthria.	15†	
Numbers analysed	16	For each group, number of participants (denominator) included in each analysis and whether the analysis was by original assigned groups One participant is included in the analyses.	16	For each intervention, number of periods analysed. <i>In addition for series:</i> if quantitative synthesis was performed,

Outcomes and estimation	17a	For each primary and secondary outcome, results for each group, and the estimated effect size and its precision (such as 95% confidence interval) N/A. Primary outcome is feasibility of ECoG-based system.	17a.1	number of trials for which data were synthesized For each primary and secondary outcome, results for each period; an accompanying figure displaying the trial data is recommended.
			17a.2	For each primary and secondary outcome, the estimated effect size and its precision (such as 95% confidence interval) <i>In addition for series:</i> if quantitative synthesis was performed, group estimates of effect and precision for each primary and secondary outcome
	17b	For binary outcomes, presentation of both absolute and relative effect sizes is recommended N/A	17b	
Ancillary analyses	18	Results of any other analyses performed, including subgroup analyses and adjusted analyses, distinguishing pre-specified from exploratory	18	Results of any other analyses performed,

		N/A		including assessment of carryover effects, period effects, intra-subject correlation <i>In addition for series:</i> If done, results of subgroup or sensitivity analyses
Harms	19	All important harms or unintended effects in each group (for specific guidance see CONSORT for harms) N/A, no participants have been withdrawn due to any adverse events.	19	All harms or unintended effects for each intervention. <i>(for specific guidance see CONSORT for harms)</i>
Discussion				
Limitations	20	Trial limitations, addressing sources of potential bias, imprecision, and, if relevant, multiplicity of analyses As this is an early feasibility, phase I, pilot clinical trial, there are limitations of generalizability due to the sample size of the study. However, such limitations are mitigated by the fact that the collected pilot data will aid in the feasibility, reliability, and future directions of brain computer interfaces for communication and motor control, as well as future larger clinical trials which could better generalize.	20	
Generalisability	21	Generalisability (external validity, applicability) of the trial findings Any findings in this early feasibility trial will be applied to future investigations into the use of an ECoG-based neuroprosthesis for motor and speech restoration. As this is a low-enrollment trial, there will not be a large enough number of participants to ensure generalizability. However, this is an early feasibility trial with no aims to generalize.	21	

Interpretation	22	Interpretation consistent with results, balancing benefits and harms, and considering other relevant evidence	22
		Informed by the existing literature on the long-term viability of ECoG interfaces (Nadkarni, Ohno-Machado and Chapman 2011a, Thompson et al. 2014b, Nadkarni et al. 2011a), we expect that the benefit of gaining key knowledge and insights from this early feasibility trial concerning the suitability of an ECoG-based neuroprosthesis for motor and speech restoration are well justified given the known potential risks. Participants are informed of known potential risks and mitigation strategies, which are covered in the informed consent form and the clinical protocol. The findings of the current study, and of our prior work (Metzger, Liu, Moses et al 2022, Moses, Metzger, Liu, et al. 2021), within this clinical trial support the interpretation that ECoG interfaces are clinically viable for communication restoration, although continued development of the approach and further validation with other participants are necessary to affirm this.	
Other information			
Registration	23	Registration number and name of trial registry	23
		The study was registered at ClinicalTrials.gov under the identifier NCT03698149.	
Protocol	24	Where the full trial protocol can be accessed, if available	24
		The full clinical-trial protocol can be found as an attachment alongside the manuscript.	
Funding	25	Sources of funding and other support (such as supply of drugs), role of funders	25
		The following sources of funding supported our prior work (Moses, Metzger, Liu et al. 2021) and/or the current study: A research contract under Facebook's Sponsored Academic Research Agreement; the National Institutes of Health (grant NIH U01 DC018671-01A1); Joan and Sandy Weill and the Weill Family Foundation; the Bill and Susan Oberndorf Foundation; the William K. Bowes, Jr. Foundation; and the Shurl and Kay Curci Foundation.	

*It is strongly recommended that this checklist be read in conjunction with the CENT 2015 Explanation and Elaboration²⁴ for important clarification on the items. The copyright for CENT (including checklist) is held by the CENT Group and is distributed under a Creative Commons Attribution (CC-BY 4.0) license.

†Caution should be taken when reporting potentially identifying information pertaining to CENT items 4a, 4b, 14a, and 15.

References

- Anderson, K. D. (2004) Targeting recovery: priorities of the spinal cord-injured population. *J Neurotrauma*, 21, 1371-83.
- Huggins, J. E., P. A. Wren & K. L. Gruis (2011) What would brain-computer interface users want? Opinions and priorities of potential users with amyotrophic lateral sclerosis. *Amyotroph Lateral Scler*, 12, 318-24.
- Wolpaw, J. R., N. Birbaumer, D. J. McFarland, G. Pfurtscheller & T. M. Vaughan (2002) Brain-computer interfaces for communication and control. *Clin Neurophysiol*, 113, 767-91.
- Kubler, A., B. Kotchoubey, J. Kaiser, J. R. Wolpaw & N. Birbaumer (2001) Brain-computer communication: unlocking the locked in. *Psychol Bull*, 127, 358-75.
- Kennedy, P. R. (1994) 'Locked-in' patients. *Neurology*, 44, 366-7.
- Kennedy, P. R. & R. A. Bakay (1998) Restoration of neural output from a paralyzed patient by a direct brain connection. *Neuroreport*, 9, 1707-11.
- Selzer, M. E., S. Clarke, L. G. Cohen, G. Kwakkel & R. H. Miller. 2014. *Textbook of neural repair and rehabilitation*. Cambridge: Cambridge University Press.
- Spataro, R., M. Ciriaco, C. Manno & V. La Bella (2014) The eye-tracking computer device for communication in amyotrophic lateral sclerosis. *Acta Neurol Scand*, 130, 40-5.
- Birbaumer, N., N. Ghanayim, T. Hinterberger, I. Iversen, B. Kotchoubey, A. Kubler, J. Perelmouter, E. Taub & H. Flor (1999) A spelling device for the paralysed. *Nature*, 398, 297-8.

- Carmena, J. M., M. A. Lebedev, R. E. Crist, J. E. O'Doherty, D. M. Santucci, D. F. Dimitrov, P. G. Patil, C. S. Henriquez & M. A. Nicolelis (2003) Learning to control a brain-machine interface for reaching and grasping by primates. *PLoS Biol*, 1, E42.
- Leuthardt, E. C., G. Schalk, J. Roland, A. Rouse & D. W. Moran (2009) Evolution of brain-computer interfaces: going beyond classic motor physiology. *Neurosurg Focus*, 27, E4.
- Leuthardt, E. C., G. Schalk, J. R. Wolpaw, J. G. Ojemann & D. W. Moran (2004) A brain-computer interface using electrocorticographic signals in humans. *J Neural Eng*, 1, 63-71.
- Taylor, D. M., S. I. Tillery & A. B. Schwartz (2002) Direct cortical control of 3D neuroprosthetic devices. *Science*, 296, 1829-32.
- Schwartz, A. B., X. T. Cui, D. J. Weber & D. W. Moran (2006) Brain-controlled interfaces: movement restoration with neural prosthetics. *Neuron*, 52, 205-20.
- Chestek, C. A., V. Gilja, P. Nuyujukian, R. J. Kier, F. Solzbacher, S. I. Ryu, R. R. Harrison & K. V. Shenoy (2009) HermesC: Low-Power Wireless Neural Recording System for Freely Moving Primates. *Ieee Transactions on Neural Systems and Rehabilitation Engineering*, 17, 330-338.
- Ganguly, K., D. F. Dimitrov, J. D. Wallis & J. M. Carmena (2011) Reversible large-scale modification of cortical networks during neuroprosthetic control. *Nat Neurosci*, 14, 662-7.
- Gilja, V., C. A. Chestek, I. Diester, J. M. Henderson, K. Deisseroth & K. V. Shenoy (2011) Challenges and opportunities for next-generation intracortically based neural prostheses. *IEEE Trans Biomed Eng*, 58, 1891-9.
- Hochberg, L. R., M. D. Serruya, G. M. Friehs, J. A. Mukand, M. Saleh, A. H. Caplan, A. Branner, D. Chen, R. D. Penn & J. P. Donoghue (2006) Neuronal ensemble control of prosthetic devices by a human with tetraplegia. *Nature*, 442, 164-71.
- Nadkarni, P. M., L. Ohno-Machado & W. W. Chapman (2011a) Natural language processing: an introduction. *J Am Med Inform Assoc*, 18, 544-51.
- Thompson, D. E., L. R. Quitadamo, L. Mainardi, K. U. Laghari, S. Gao, P. J. Kindermans, J. D. Simeral, R. Fazel-Rezai, M. Matteucci, T. H. Falk, L. Bianchi, C. A. Chestek & J. E. Huggins (2014b) Performance measurement for brain-computer or brain-machine interfaces: a tutorial. *J Neural Eng*, 11, 035001.
- Nadkarni, P. M., L. Ohno-Machado & W. W. Chapman (2011a) Natural language processing: an introduction. *J Am Med Inform Assoc*, 18, 544-51.
- Moses, D.A., Metzger, S.L., Liu, J.R., et al., (2021) Neuroprosthesis for Decoding Speech in a Paralyzed Person with Anarthria. *N Engl J Med*, 385, 217-227.